Discover novel therapies for human Uveal Melanoma

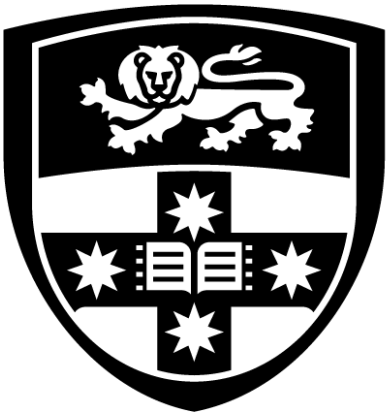

THE UNIVERSITY OF SYDNEY

Janney Z Wang

Sydney Pharmacy School

Faculty of Medicine and Health

The University of Sydney

This thesis is submitted for the degree of

Doctor of Philosophy

2025

Declaration

I hereby declare that this thesis is the result of my own original work conducted after registration for the degree of Doctor of Philosophy at the University of Sydney.

I verify the content of this thesis is my work, it contains no material previously published or written by another person. Proper citation and acknowledgment have been provided for all sources, ideas, and works of others referenced in this research.

I declare that this thesis has not been previously submitted, in whole or in part, as a thesis or dissertation to this or any other institution for the purpose of obtaining a degree, diploma, or any other qualification.

Janney Z Wang

14/03/2025

Authorship contribution statement

Chapter 2 of this thesis is published as “Shu W, Wang JZ, Zhu X, Wang K, Cherepanoff S, Conway RM, et al. Lapatinib dysregulates HER2 signalling and impairs the viability of human uveal melanoma cells. Journal of Cancer. 2023;14(18):3477-95.”

Chapter 3 of this thesis is published as “Wang JZ, Paulus P, Niu Y, Zhu L, Morisseau C, Rawling T, et al. The Role of Autophagy in Human Uveal Melanoma and the Development of Potential Disease Biomarkers and Novel Therapeutic Paradigms. Biomedicines. 2024;12(2).”

I J.W. confirm I am the primary author of this thesis. Specifically, I conceived the research idea, designed the methodology, analysed, and interpreted the data and prepared the manuscript with the assistance of F.Z. I set up and performed the experiments and collected necessary data with the assistance of Y.N, H.D, S.G and F.Z. Y.N, K.W, S.G, M.M, M.M and F.Z participated in editing and reviewing of the manuscript.

Student name: Janney Z Wang

Date: 14/03/25

As the supervisor overseeing the candidature on which this thesis is based, I verify that the authorship attribution statement presented above is accurate and correctly reflects the contributions made.

Supervisor name: A/Prof. Fanfan Zhou

Date: 14/03/25

Thesis Acknowledgement

Before anything, I would like to express my heartfelt appreciation to my supervisor, A/Prof. Fanfan Zhou, for her unwavering academic guidance not only throughout the three years of my PhD journey but also for seeing the potential in me as a student and a researcher during my undergrad and Honours degree. Beyond guiding my research, she has consistently shown concern for my health and well-being, making sure I prioritise my health and safety. Her kindness, intellect, and deep dedication to science has not only inspired but motivated me to become independent, critical thinking, and problem solving making me a well-rounded researcher and a member of society.

I would also like to express my deepest gratitude to those who generously supported me throughout my candidature. Miss Yihe Niu and Miss Sophie Gerstlauer, whose unwavering assistance in both experimental work and idea generation helped me navigate moments of stagnation, played an invaluable role in my research journey. I am deeply appreciative of Professor Michael Murray, A/Prof Michelle Madigan and, Dr Bruce Hammock for sharing their invaluable expertise in writing and research, which greatly enriched my work. My sincere thanks also go to Dr. Kaiser Hamid, Mr James Foster, Mr Wilson Tran and members of COS-TSS team for their professional assistance in lab training and assistance with procuring experimental equipment. I am grateful to Dr. Ling Zhu for lab equipment and expertise. And lastly, I wish to thank all the members of our research group - Yining Luo, Yipeng Lin, Hiep Dang, Inho Choi, Kimberly Co, Alex Jin, Sebastian Kang, Mingwei Liu and Lachlan Ashby - who has stood by my side through moments of joy and challenge, supporting me throughout my candidature.

Lastly, and most importantly, I wish to express my deepest gratitude for the unwavering support and trust from my mother, Min Wang. Her steadfast encouragement has kept me grounded, both in my research and in maintaining my health and well-being. I am also profoundly thankful to my extended family and friends whose love and encouragement have been the foundation upon which my achievements stand.

List of abbreviations

2DG	2 deoxyl glucose	LDH	Lactate dehydrogenase
ACC	Acetyl-CoA carboxylase	LIR	LC3-interacting region
AIM	Atg8-interacting motif	lncRNA	Long non-coding RNA
AKT	Protein kinase B	MALAT1	Metastasis Associated Lung Adenocarcinoma Transcript 1
ARGs	autophagy-related genes	MAM	Mitochondria associated membrane
ATG	Autophagy related	MAPK	Mitogen-Activated Protein Kinase
ATP	Adenosine triphosphate	MEK	Mitogen-activated extracellular signal-regulated kinase
BAP1	BRCA1 associated protein 1	mHTT	Mutant Huntingtin protein
BARD1	BRCA1-associated RING domain protein 1	miRNA	MicroRNA
BAX	Bcl-2-associated X Protein	mRNA	Messenger RNA
Bcl-2	B-cell lymphoma 2	mTOR	Mammalian target of rapamycin
Bcl-XL	B-cell lymphoma-extra large	MTT	Thiazolyl blue tetrazolium bromide
BECN1	Beclin 1 gene	NADH	Nicotinamide adenine dinucleotide
BH3	BCL-2 homology 3	NADPH	nicotinamide adenine dinucleotide phosphate
BNIP3	BCL2 Interacting Protein 3	ncRNA	Non-coding RNAs
BRAF	v-raf murine sarcoma viral oncogene homolog B1	NF1	Proto-oncogene neurofibromin 1
BRCA1	Breast cancer type 1 susceptibility protein	NFκB	Nuclear factor kappa-light-chain-enhancer of activated B cells
CMA	Chaperone-mediated autophagy	NRAS	Neuroblastoma RAS viral oncogene homolog
CTLA-4	Cytotoxic T-lymphocyte-associated protein 4	OCR	Oxygen consumption rate
DFS	disease free survival	OS	Overall survival
DMEM	Dulbecco's Modified Eagle Medium	OXPHOS	Oxidative phosphorylation
ECAR	Extracellular acidification rate	P/S	Penicillin-Streptomycin
ECM	Extracellular matrix	p53	tumour protein p53
EGFR	Epidermal Growth Factor Receptor	PBS	Phosphate-buffered saline

EIF1AX	Eukaryotic Translation Initiation Factor 1A X-Linked	PD-1	Programmed cell death protein 1
EMT	Epithelial-to-mesenchymal transition	PD-L1	Programmed death-ligand 1
ER	Endoplasmic reticulum	PFS	Progression free survival
EV	Extracellular vesicle	PI	Propidium iodide
ERK	Extracellular-signal-regulated kinase	PI	Phosphatidylinositol
FA	Fatty acid	PI3K	Phosphatidylinositol 3-Kinase
FASN	Fatty acid synthase	PKC	Protein kinase C
FBS	Foetal Bovine Serum	PLCγ	Phospholipase C Gamma
FIP200	Focal adhesion kinase family interacting protein of 200 kDa	RAS	Rat sarcoma virus
GCT	Giant cell tumour	ROS	Reactive oxygen species
GNA11	Guanine nucleotide-binding protein subunit alpha-11	rRNA	Ribosomal RNA
GNAQ	Guanine nucleotide-binding protein G(q) subunit alpha	sEH	Soluble epoxide hydrolase
HER	Human Epidermal Growth Factor Receptor	SF3B1	Splicing factor 3B subunit 1
HIF-1α	Hypoxia-inducible factor 1-alpha	SREBP1	Sterol regulatory element-binding protein 1
HOXC4	Homeobox C4	STAT	Signal transducer and activator of transcription
Hsc-70	Heat shock cognate 71 kDa protein	TCA	Tricarboxylic acid
IFN	Type I interferons	TME	Tumour microenvironment
IGF-1	Insulin growth factor-1	tRNA	Transfer RNA
ITS	Insulin-Transferrin-Selenium	UM	Uveal melanoma
JAK	Janus kinase	UPR	Unfolded protein response
KIT	Tyrosine-protein kinase	VEGF	Vascular endothelial growth factor
LAMP-2A	Lysosome-associated membrane protein type 2a	VEGFRs	Vascular endothelial growth factor receptors
LC3	Microtubule-associated protein 1A/1B-light chain 3		

Table of Contents

Thesis abstract

Uveal melanoma (UM) is the most common intraocular malignancy in adults, with a high propensity for metastasis, particularly to the liver. As reviewed in Chapter 1, non-pharmacological approaches remain the gold standard for treating the primary tumour. While these treatments have improved tumour control and may preserve the eye and vision, they are still largely ineffective in preventing or managing UM metastasis, which occurs in over 50% of patients. Consequently, the prognosis for metastatic UM remains poor. Chapter 1 reviews current pharmacological treatments, highlighting the recent introduction of tebentafusp as a novel therapy for patients with metastatic UM. However, its use is restricted to individuals with specific genetic mutations, and patients experience only modest improvements in overall survival. Other molecules currently on clinical trials has yielded disappointing results. As current therapeutic options are limited and effective targets for UM has yet to be found. This thesis explores novel therapeutic strategies to improve UM treatment outcomes by investigating receptor-targeted therapies, autophagy modulation, and metabolic interventions.

Common cancer receptor targets such as EGFR, VEGF and HDAC as well as UM specific targets such as GNAQ/11 and BAP1 have all been extensively studied and trialled in UM both in *in vitro* and *in vivo* studies. However, their effects have not been proven to significantly improve patient outcomes causing concern for patient prognosis. In this thesis, I challenge such finding by re-examine the well-known EGFR receptor family – specifically the HER2 isoform to shed light on its effect in UM. I use HER2 receptor inhibitor lapatinib to see the effects of HER2 receptor inhibition on cell viability, cell metastasis and reproductive potential, and *in vivo* xenograft mouse model. After confirming the positive effects of HER2 inhibition, I further explore the mode of death using flow cytometry and western blot to confirm the overall signalling effect of HER2 inhibition. HER2 inhibition through lapatinib has been shown to effectively reduce UM cell viability in both *in vitro* and *in vivo* models, while also decreasing metastatic potential, suggesting HER2 as a prospective receptor target for UM treatment. This chapter re-imagines a classic paradigm by re-examine receptors that was once thought to be ineffective in UM.

Different modes of cell death can offer valuable insights into potential treatment strategies for UM. Chapter 3 presents an in-depth review of one such recently characterised mechanism — autophagy. Chapter 3 offers a comprehensive literature review to further explore the relationship between autophagy and key cellular components, such as mitochondria and the endoplasmic reticulum (ER), focusing on processes like ER stress and the unfolded protein response (UPR), and their potential impact on cancer treatment strategies.

The dwindling pipeline of novel drugs poses a significant barrier to discovering effective treatment strategies, and UM is no exception. In Chapter 4 the novel compound UC2288 is tested in UM primary, metastatic as well as patient tumour derived *ex vivo* cell lines to assess its anti-cancer effect. UC2288 was proven to cause potent cell viability reduction, ROS production, mitochondria health disruption and ER stress production in a tumour specific manner as healthy retinal cell lines MIO-M1 and ARPE19 was minimally affected. UC2288 also extend its effect to prevent cell invasion and disrupt reproduction to prevent metastatic tumour formation. It is hypothesised UC2288 induces anti-UM effect partly through inducing significant amount of ER stress resulting in the unfolded protein response and causing autophagic cell death.

The effect of UC2288 is expanded in chapter 5 through co-treatment with glucose depletion. UM is shown in chapter 5 to be significantly glucose dependent when compared to other macronutrients. The reduction in cell viability under glucose-depleted conditions prompted the co-treatment of UM cells with small molecules. Among them, glucose depletion exhibited an synergistic anti-UM effect with UC2288 but no other small molecules that have been found to be potent in the treatment of UM. When UC2288 is treated in glucose free medium, UM cells exhibited a significant increase in cytotoxicity and ROS production. Surprisingly, the IC_{50} values and mitochondrial health did not show proportional changes relative to the observed level of cell death. This indicates other possible additive effects that does not directly link to increase in UC2288 potency. Through this the metabolic profile was explored in post UC2288 treatment and a further increase in glucose dependence as depicted in the increase in basal glycolysis is seen in UM cell lines suggesting UC2288 to potentially disrupt UM metabolic profiles.

In conclusion, this thesis explores UM treatment multifacetedly through receptor targeting, novel compounds, and co-treatment strategies. Given UM's therapeutic challenges due to its location and metastatic potential, this research highlights the benefits of HER2 inhibition and UC2288 in

enhancing cytotoxicity and reducing metastasis. These findings provide valuable insights for potential clinical applications and contribute to the ongoing efforts to develop more effective UM therapies, offering promising directions for future preclinical and clinical investigations aimed at improving patient outcomes.

Chapter 1: Introduction

Uveal melanoma (UM) is the most common form of intraocular malignancy in adults with an average occurrence rate of 5-8 cases per million. Tumours were most reported within the choroid at 85 - 90% followed by the ciliary body with ~6% and then iris at ~5% (1, 2). Numerous epidemiology studies have been conducted for UM, yet no consistent results have been achieved. Its occurrence is irrespective of gender; however, the likelihood of occurrence increases with age peaking at 70-74 years old and arises more commonly within the Caucasian population. Among this population, a south to north latitude shift appears to correspond to an increased risk of UM (3). Although rare, UM has a high mortality rate of 31% by 5 years, 45% by 15 years, and 52% by 35 years (4). Up to 80% of UM related mortality occurs within the first 10 years of diagnosis irrespective of the treatment types (4).

The occurrence of metastasis is partly due to delays in symptoms and tumour detection. UM patients are often asymptomatic or with minor symptoms such as blurred vision, photopsia and floaters. Tumours have been documented to be undetected by the initial consultation regardless of health professionals. Treatment delays were often observed irrespective of the referring healthcare professionals. Patients whose tumours were initially missed experiencing delays twice as long as those whose tumours were correctly diagnosed at the first consultation (1). Patients also waited longer to attend follow-up consultations if the referral was not made as urgent or if tumours were undetected and the symptoms were mild. When diagnosed, majority of the patients had tumours below 15mm and a thickness of below 6mm (1). Patients with tumours categorised as American Joint Committee on Cancer (AJCC) stages II and III exhibited higher mortality rates when treatment was delayed beyond one month after diagnosis. In contrast, patients with stage I tumours demonstrated lower mortality rates within the first 10 years; however, a significant increase in mortality was observed starting from the 11th year onwards (5). Up to 50% of patients develop distant metastasis. Metastasis has a hematogenous origin with the liver being the most common site of metastasis (94%) followed by the lung, bone, and skin (6). The median survival rate of patients with metastasis is around 4 months with an estimated 1-year survival rate of approximately 13% (6). The diameter and thickness of the primary tumours are directly correlated with survival rates. Tumours with a basal diameter under 11 mm and a thickness less

than 3 mm showed a mortality rate of 16%. Those with a basal diameter under 16 mm and a thickness between 3–8 mm had a mortality rate of 32%, while tumours with a basal diameter over 15 mm and a thickness greater than 8 mm exhibited a mortality rate of 53% (7). Evaluation of tumour size indicated that an increase in size by a millimetre increases the risk for metastasis by 5% (8).

1.1 UM Pathogenesis

UM pathogenesis involves complex genetic and molecular alterations that drive tumour development, progression, and metastatic potentials within the unique ocular environment. In contrary to its cutaneous counterparts that is primarily driven by the mutations in the B-Raf proto-oncogene, serine/threonine kinase (BRAF), the neuroblastoma RAS viral oncogene homolog (NRAS) and the proto-oncogene neurofibromin 1 (NF1) (9, 10), UM is most commonly seen to have the mutations detected in the guanine nucleotide-binding protein G(q) subunit-α (GNAQ) or guanine nucleotide-binding protein subunit-α11 (GNA11) genes. The disruption in GTPase activity results in the constitutive activation of the downstream signalling pathways such as the mitogenic activated protein kinase pathway (MAPK) and the phosphatidylinositol-3-kinase (PI3K)/AKT pathway, causing an increase in cellular growth and proliferation with elevated the metastatic potentials (11, 12). The loss of somatic mutations of the BRCA-1 associated protein (BAP1) is highly associated with an increase in the aggressiveness of UM tumours. This loss of function has been found in 84% of metastatic tumours. BAP1 encodes one of several classes of deubiquitinating enzymes. Additionally, BAP1 contains several domains for binding of Breast cancer type 1 susceptibility protein (BRCA1) and BRCA1-associated RING domain protein 1 (BARD1), to form a tumour suppressor complex. BAP1 is also found to have a regulatory role in stem cell pluripotency and other developmental processes. BAP1 acts as a tumour suppressor gene in cancer cells, and its loss of function is a pivotal event that impacts on tumour progression and is closely linked to a higher risk of metastasis (13).

Contrarily, mutations within the splicing factor 3B subunit 1 gene (SF3B1) and eukaryotic translation initiation factor 1A X-linked gene (EIF1AX) are associated with favourable prognosis. SF3B1 is a component of a complex responsible for splicing pre-mRNAs. However, no consistent links between SF3B1 mutation and splicing abnormalities have been detected (14).

SF3B1 is associated with favourable prognostic features such as younger diagnosis age and fewer undifferentiated epithelioid cells. Patients with SF3B1-mutant tumours may have a lower rate of metastasis compared to its wild type counterparts. Similarly, EIF1AX mutation is associated with amino acid substitution and better metastatic free survival rate (15, 16). As EIF1AX and SF3B1 are mutually exclusive from BAP1 mutations, these two marker genes may have protective prognostic features.

Tumour metastatic rate and patient mortality have been shown to be heavily associated with chromosome 3, specifically monosomy 3 (17). Such increase in poor prognosis may be due to the loss of specific tumour suppressor genes. To note, BAP1 is located on chromosome 3p21.1 showing an association between monosomy 3 and poor prognosis. Likewise, chromosome 8 abnormality was also associated with poor prognosis with patients experiencing more aggressive tumour presentation, when both monosomy 3 and chromosome 8 gain are present. Interestingly, chromosome 6 abnormality was shown to have protective effects with optimal patient prognosis. This effect is seen even when combined with monosomy 3 or chromosome 8 gain (17, 18).

1.2 UM Treatment

At present, the clinical guidelines for UM treatment are mainly relying on non-pharmacological regimens. The current three main treatment options for UM are radiotherapy, laser therapy and surgical therapy (19). Tumour size, condition of the eyes and tumour location are considered when choosing the treatment type with the preferences to preserve the eyes and vision. Thus, radiotherapy is one of the most used local treatment options.

1.2.1 non-pharmacological treatments for UM

Radiotherapy is classified into two main types: brachytherapy (plaque radiotherapy) and teletherapy (charged particle or stereotactic radiotherapy). In the case of brachytherapy, radioactive seeds are placed within a specially made dish-shaped applicator and is sutured externally at the site of the tumours. The most used radioisotopes are iodine-125, ruthenium-106, and palladium-103 (20). The plate is removed when cumulative dose of 80-100 Gy is attained at the tumour apex. Overall, this treatment method does not differ from mortality rate when compared to enucleation, while offering adequate local control and preserving eye function (21-

23). Side effects attained within treatments include macular oedema, retinal detachment and neovascular glaucoma that are primarily managed and prevented with intravitreal injection of steroids (23, 24). Charged particle therapy is another form of radiotherapy that involves charged particles such as proteins, helium ions or carbon ions with specific kinetic energy. This form of treatment offers the advantage of homogeneous dose of radiation at tumour sites minimising a damage to the surrounding tissues. This form of treatment may have kinetic energy adjusted depending on the tumour depth allowing for effective control of smaller tumours. Similar to brachytherapy, charged particle therapy offers greater eye and vision retention, while maintaining local tumour control (25-27). Likewise, in the case of charged particle therapy, stereotactic therapy is conducted with multiple beams of protons focused onto the tumours at different directions. This offers a high dose of radiation at the tumour site, while preserving surrounding tissues and allowing local treatment of larger tumours (28, 29).

Laser therapy is achieved through delivering high intensity light to the tumour sites. However, this form of treatment has fallen out of favour where radiation is available, due to its potential side effects such as retinal traction, gliosis and tumour recurrence (30). Laser therapy such as transpupillary thermotherapy, may be opted in as an adjuvant therapy to decrease tumour size when combined with radiation therapy. This combination offered better tumour control, when brachytherapy alone was insufficient to reduce tumour sizes (30). When using transpupillary thermotherapy alone, tumour selection is key to treatment success. Limitation of this treatment includes smaller pigmented tumours are away from the optic disk. Although tumour recurrence is low, permanent damage can be caused to the retina leading to visual loss shortly after treatments (31). Nonetheless, more recent analysis has concluded transpupillary thermotherapy had little effect when combined with brachytherapy in comparison to brachytherapy alone. This limits its need in the current therapeutic paradigm (32). Another form of laser therapy is the photodynamic therapy that utilizes a non-thermal laser to activate photosensitive dyes resulting in blood vessel closure and tumour death. However, as pigmentation within the tumours can interfere with the laser, this treatment should only be used on amelanotic or lightly pigmented tumours (33-35),

Surgical removing part of or all the eyeballs is considered, if the tumour is unsuitable for the local therapies mentioned above. Of which, endoresection and exoresection are first considered owning to that they may preserve partial visual function. Endoresection or transretinal resection

is performed with vitreous cutters passed through the retina. Patients are then referred to phototherapy or brachytherapy to eliminate any tumour remnants (36). Although less invasive, it was considered as a controversial option with fears of intraocular seeding of tumour remnants and incomplete removal of the tumours. Regardless, long term follow-up of post operative patients showed tumour recurrence similar to that of brachytherapy (37, 38). Exoresection is considered more invasive, as a 'trapdoor' is opened on the scleral for improved operation clarity. Patients are kept hypotensive and under general anaesthesia to minimise complications such as haemorrhage, brain under perfusion and scleral flap complications. Tumour recurrence is higher when compared to that of radiotherapy and therefore, post operative plaque therapy is often required to minimise tumour recurrence (39, 40).

When the tumour is too large (involves more than 40% of intraocular volume) or if the tumour has progressed into orbital tissues, enucleation or orbital exenteration will be considered, respectively. Enucleation involves a removal of the globe while retaining the remaining tissues such as eyelids and eye muscles. This procedure results in numerous issues including poor patient outcomes and increased tumour dissemination likely caused by fluctuations in intraocular pressure during the procedure (41, 42). Enucleation is now used as a secondary resort, when vision preserving managements have failed (43). Similarly, orbital exenteration involves the removal of the globe as well as surrounding tissues, when UM has advanced out of the eyes. This is often followed by adjuvant radiation therapy to control the tumours. This procedure is rarely necessary but can be performed with curative intent (44). Due to the advancement of the tumours, disease free survival (DFS) and overall survival (OS) are significantly lower (44, 45).

1.2.2 Pharmacological therapies of UM

There are few pharmacological therapies clinically approved for UM, although a lot of attempts have been made to discover drugs for UM. The outcome of UM drug discovery is in general unsatisfied. Recent advancements have been made for metastatic tumour treatment with the introduction of immunotherapeutic drug tebentafusp (trade name of "Kimtrack"). Unlike conventional immunotherapy, it is a T-cell receptor–bispecific molecule that redirects T cells to kill gp100-positive melanoma cells (46). Tebentafusp is only effective to patients with the HLA-A*02:01 positive mutation in unresectable metastatic UM. HLA-A*02:01 mutations are notably more common within the Caucasian population (47). Noteworthy, tebentafusp treatment is

associated with severe adverse effects, with 47% of patients experiencing grade 3 or 4 treatment related adverse effects. Tebentafusp only moderately improves patient survival for 5 months and increases 3-year patient survival by 9% when compared to the investigator's choice of therapy (i.e. pembrolizumab, ipilimumab, or dacarbazine) (46). Many other candidate drugs tested for UM treatment in pre-clinical and clinical phases have yielded disappointing outcomes (48).

1.2.2 a Cytotoxic drugs

Tumour recurrence and metastasis have been the leading issues for UM with a poor patient prognosis. There is an urgent need for effective drug therapies that can target both primary and metastatic UM. Conventional cytotoxic therapies has been proven to be ineffective in both primary and metastatic UM with varying adverse effects (49).

1.2.2.b Targeted therapies

With GNAQ and GNA11 being the most common mutations in UM, drug candidates involved in these genes and their downstream pathways have been painstakingly explored (50). The MEK enzymes MEK1 and MEK2 have been identified as the key components within the RAS/MAPK signally pathway. The MEK inhibitor selumetinib has undergone numerous studies evaluating its efficacy in UM patients carrying the GNAQ/GNA11 mutation. A randomised phase II study was conducted with 101 UM patients to compare selumetinib with either temozolomide or dacarbazine (51). Although patients had an increase in progression free survival of around 8 weeks, the median OS was not different in the treatment and control groups (51). Subsequent phase III trial with 129 metastatic UM patients randomly assigned to selumetinib and dacarbazine or dacarbazine alone, showed a similar result (52). The patient free survival (PFS) was only increased by 1 month in the combination treatment group and the overall survival (OS) did not show any statistical difference between these groups (52). Similarly, another MEK1/2 inhibitor trametinib also underwent several trials. A phase I trial included 16 UM patients demonstrated a limited treatment response (53), with a median PFS of 1.8 months, although two patients had a 24% tumour reduction (53). Overall, the limited benefits of the MEK inhibitors suggested that these targeted therapies are not proven in treating UM patients.

The PI3K/Akt/mTOR signalling pathway has been identified to be dysregulated in up to 55% of UM patients, as it is linked to the GNAQ/GNA11 mutations (50). As such, several agents have been tested with UM patients to verify its efficacy. The mTOR inhibitor everolimus was

combined with pasireotide in a phase II trial in patients with metastatic UM (54). Patients had a median PFS of 16 weeks and OS of 11 months. However, there were no documented complete or partial response to this combination (54). Some other targeted therapies have only been tested in non-clinical models. For instance, the AKT inhibitor MK2206 showed synergistic effect when combined with selumetinib in a preclinical study in UM cell lines and xenograft mouse models (55). Furthermore, the interplay of PI3K, Akt and mTOR has been extensively studied by Babchia et. al. (56) through PI3K pathway inhibition. PI3K inhibitor LY294002 greatly reduced cell viability. However, the same extend of cell death was not observed in downstream rapamycin-induced mTOR inhibition alone. It is recognised that the negative feedback loop of mTOR inhibition paradoxically activated PI3K/Akt pathway as well as increased cyclin D1 expression leading to cell growth. When all these pathways were downregulated, the paradoxical effect was attenuated and cell viability was further decreased (56). Although many agents were shown to be beneficial in treating UM, these agents are still at the early stages of pre-clinical trials and further research is required to ascertain their role in UM.

Protein kinase C (PKC) refers to a family of closely related protein kinase isoforms. These closely linked proteins have crucial roles in both MAPK and PI3K signalling pathways (57). As GNAQ mutant UM tumours undergo proliferation from PKC activation, PKC inhibitor enzastaurin have showed more potent anti-cancer effect in GNAQ mutant tumours. UM cells were found to undergo G1 cell cycle arrest and apoptosis in the GNAQ/11 mutant cells when compared to the wild type cells (58). PKC inhibitor AEB071 showed superior results when combined with MEK inhibitors but did not show complete cell suppression when treated alone (59, 60). As there are numerous isoforms of PKC, completely inhibition of its pathways with single drug alone has been proven difficult.

Apart from GNAQ/11 based pathways, several studies have explored the therapeutic potentials of other chemical modulators against surface receptors. Of which, well known oncogenic receptors such as epidermal growth factors receptors (EGFR), insulin-like growth factor receptors (IGFR) and vascular endothelial growth factor receptors (VEGFR) are under the spotlight as potential treatment targets.

EGFR regulates cell growth and proliferation through the MAPK and PI3K pathway similar to MEK1/2. EGFR is a group of four receptors (HER1, HER2 HER3 and HER4) that dimerise

when activated. Mutations in EGFR may alter the signalling pathway causing tumour formation. EGFR has also been linked to metastatic potentials (61). Various forms of targeted therapies such as monoclonal antibodies and small molecule kinase inhibitors have been identified to target this group of receptors. The monoclonal antibody cetuximab and kinase inhibitor gefitinib were tested against high or low EGFR expressing UM cells showing cytotoxicity with a release of tumour necrosis factor α in high expressing UM cell lines (62). Yet, a phase II trial of gefitinib in 52 patients with metastatic choroidal and non-choroidal melanoma demonstrated a limited response with 1.4 months for PFS and 10.9 months for OS (63).

Insulin like growth factor receptors namely insulin growth factor-1 (IGF-1) receptors have been shown to have an association with the increased risk of death in UM (64). This discovery may be explained by the fact that IGF-1 is mainly produced at the liver, a preferential metastatic site of UM (64). The IGF-1 effects were reversed by PI3K inhibitor LY294002 in UM cell lines (65). The monoclonal antibody AVE1642 against IGF-1R have been evaluated in trials of patients with advanced solid tumours (66), but nothing has been done for UM.

Vascular endothelial growth factor receptors (VEGFRs) are responsible for the generation of new vascular structure from pre-existing vessels. This process is critical to tumour growth and proliferation (67). Drugs designed to target this process such as bevacizumab, have been tested pre-clinically but a paradoxical increase in tumour growth was documented (68). Clinical trials with 101 UM patients also showed no significant improvement with bevacizumab treatment, questioning the effectiveness of VEGFR inhibitors in the treatment of UM (69).

Although treatment options have been advanced with tebentafusp, the eye is wildly recognised as an immune-privileged organ. Inflammatory markers are supressed within the eye to prevent inflammation related tissue damage. With this, both the innate as well as the adaptive immune response are supressed in the eye (70). Such factor also contributes to drug development involved with immune checkpoint inhibitors. CTLA-4 inhibitor ipilimumab was tested against unresectable or metastatic cutaneous, uveal and mucosal melanoma (71). The median PFS was similar in all groups at 3 months, while the OS was longer in cutaneous melanoma patients and remained similar in non-cutaneous melanoma patients (71). A phase II trial of ipilimumab in pre-treated and treatment-naïve patients with metastatic UM patients demonstrated similar PFS and OS and no patient experienced partial or complete response (72). Another option for immune

therapy is the utilisation of PD-1/PD-L1 inhibitors. The efficacy of nivolumab was evaluated in patients with metastatic UM but similar results to ipilimumab was documented (73). In addition, PD-1 inhibitor pembrolizumab showed unsatisfactory outcomes (74). The limiting results of immune checkpoint inhibitors in UM solidified the eye to be an immune privileged area, in which immunotherapy may not be effective.

1.3 UM therapeutic targets

Recent advancement in the molecular and genetic understanding of cancer biology drives the development of innovative therapies, providing a hope and new possibilities for improved outcomes in lethal cancers like UM. As targeting commonly known factors such as GNAQ/11 and BAP1 have limited anti-UM effect, attempts are highly desired to explore potential therapeutic targets for UM. UM is considered an atypical adult tumour due to its unusually low mutational burden compared to other cancers such as cutaneous melanoma (75). This suggests that factors beyond exonic DNA mutations play a significant role in shaping UM's genetic landscape and influencing its metastatic potential. However, limited changes within the genome and related protein expression drastically increase the difficulty of identifying novel targets for targeted therapeutics (76). Here we explore unconventional approaches and propose alternative methods in identifying potential tumour specific drug targets.

1.3.1 Non-coding RNAs

RNA therapies have been debated as a possible treatment method because there are many components yet to be analysed. It is well known that that the three basic form of RNAs are the messenger RNA (mRNA), transfer RNA (tRNA) and ribosomal RNA (rRNA), therapies against which are well documented and proven useful in treating various diseases (77). A less known component is that the introns once thought to be a non-coding region that is removed to form the functional RNA, was recently brought back to the spotlight as containing fundamental functions in gene regulation and cell development (78). Non-coding RNAs (ncRNA) can be classified into two groups: short ncRNAs and long ncRNAs. Recent studies have shown both types to play an oncogenic and tumour suppressive roles as well as prognostic role in tumours (77).

Targeting ncRNA may also pose as a potential option for cancer treatment with studies demonstrated effective tumour control through modulating the expression of target genes involved in tumour growth and survival (79). Exploration of ncRNA may also benefit current drug therapies as a potential steppingstone to overcome therapy resistance (78). Non-coding RNA is currently being under investigation in UM as a potential prognostic and diagnostic marker, as well as a possible druggable target. Its function has been explored genetically but also epigenetically for its prognostic value (80). Earlier cancer diagnosis may also be made possible with ncRNA. NcRNA such as SAMMON has been confirmed to have consistent expression in UM tumours. Such information may promote UM diagnosis and the prevention of tumour progression (81). NcRNA, particularly long ncRNA (lncRNA) are ideal molecules with therapeutic potentials, because they are tissue specific, have fast turnover and ambient binding sites allowing for increased chances of treatment success. The upregulation or downregulation of ncRNA can be achieved through methods such as small interfering RNA, anti-lncRNA oligonucleotides, CRISPR technology, or by disrupting the interactions between lncRNA and target molecules (82). Non-coding RNAs represent a promising frontier in cancer prognosis, diagnosis and therapy, shedding light on UM drug development.

1.3.2 HER receptors

Despite that previously EGFR (HER1, ErbB1) has been proven to show limited effects in UM, the HER receptors have three other isoforms: HER2 (ErbB2), HER3 (ErbB3) and HER4 (ErbB4). Their receptor activity is also regulated by extracellular ligands and activation of the receptor can be achieved through dimerization of two HER receptors to form a homo- or heterodimers (83). Of which, HER1 and HER2 are the most extensively studied, which have the most common mutations in glioblastoma and breast cancer, respectively. HER3 is currently regarded as a non-proto-oncogenic receptor as it is inherently inactive with no catalytic kinase function. However, it is hypothesised to play an activating role in a kinase dimer. HER4 receptor is the least characterised isoform as its signalling has been implied in cell death and tumorigenicity (83). Compared to HER1, HER2 HER3 and HER4 are relatively less studied in UM and may pose as possible therapeutic targets for UM. Recent research has found the expression of HER2 in UM (84). Although less than that of breast cancer, HER2 expression is consistent and restricted to tumour sites. Preliminary trials including pre-clinical, and phase I trials have been conducted and

showed targeting HER2 may be an effective therapeutic option (84, 85). Notably, novel therapies such as HER2 CAR-T cells has also been employed in mouse models and showed efficacy in UM (86). Little research has been done for HER3 in UM due to its inherent inactivity. Nonetheless, studies have found HER3 to be solely localised in the nucleus of UM tumours and is associated with favourable patient outcomes (87). Currently no research has been conducted on HER4 regarding its association with UM. Overall, HER receptors may play a role in the prognosis and treatment of UM, despite the ineffectiveness of EGFR inhibitors in UM. This poses a possibility to future directions for therapeutic development.

1.3.3 Mitochondrial and endoplasmic reticulum stress

Mitochondrial and endoplasmic reticulum (ER) stress play a key role in cancers by regulating tumour growth, survival, and therapy resistance (88). Through adaptation, cancer cells can mitigate various stress factors, including hypoxia, nutrient shortage, metabolic and oxidative stress through signalling that alleviate mitochondrial or ER stress. As the powerhouse of cells, the mitochondria are responsible for key cellular processes that directly affect cell viability and function (88). Similarly, the ER is a central biosynthesis organelle responsible for protein synthesis and processing (89). It play roles in protein modification and folding as well as has a supervisory role in identifying incorrections that may lead to cell destruction (89). These key cellular organelles have been highly recognised for maintaining homeostasis of cells. They have been identified to be tethered by mitochondrial-associated membrane proteins (MAMs) forming an inter-organellar network. This network is responsible for multiple cellular processes regulating the mitochondria and ER, calcium regulation and lipid metabolism (90). As lipids influx into the mitochondria through vesicles is not possible, the MAM proteins function as a trafficking system to regulate the movement of lipids into the mitochondria. Oxidative stress through the accumulation of reactive oxygen species (ROS) generated by the mitochondria, is also promptly detected by MAM proteins, and shuttled to the ER for processing. Protein folding and modification are regulated in the ER through the unfolded protein response (UPR). UPR proteins also functions as MAM components, while MAM proteins can also affect the UPR pathways and actively intensify their intertwined relationship (91).

1.3.4 Cell autophagy

The mitochondria ER complex is responsible for regulating numerous processes that are hallmarks in cancer formation and invasion (92). The regulation of calcium ions is essential in cancers as it is deeply involved in cancer progression (91). The epithelial-to-mesenchymal transition leads to tumour invasion and resistance to apoptosis. BAP1 is the tumour suppressor protein involved in the MAM. It facilitates calcium influx into the mitochondria and its abnormalities as seen in UM may induce inappropriate influx of calcium disrupting cell homeostasis leading to tumorigenesis (93). Although cancer cells experience a change in glycolysis through the Warburg effect (94), lipid metabolism remains relatively consistent with only documented increases in lipid usage and metabolism to facilitate energy and signalling factor production. Enzymes utilised in lipid and cholesterol synthesis are also upregulated in various cancers (95). Lipids as a signalling factor also play a complex role in tumorigenesis, in which, the MAMs are involved in the regulation of lipids within both the mitochondria and ER (91). A specialised cell death mechanism – autophagy has also been reported as a response to ER stress (96). Autophagy has been linked to cell survival mechanism as a form of rescue, under cellular stress such as hypoxia and nutrient deprivation. On the other hand, once the accumulation of stress factors can no longer be controlled, autophagy is activated, and cell death occurs. Autophagic processes have been shown to be both tumour protective and tumour-lytic based on the amount and type of stresses in presence (97, 98). This may present as a novel strategy in cancer treatments.

Mitochondrial and ER stress have been briefly explored in UM. Discoveries such as novel drug therapies and ER stress related drug resistance forms the basis of utilising mitochondria, ER and related proteins as druggable targets (97, 99, 100). Future research in these aspects is highly desired to validate the effectiveness of targeting these pathways/organelles/processes.

1.4 Conclusion

Overall, UM is a rare but deadly cancer with poor prognosis and limited treatment options. UM and its metastasis have been proven fatal in majority of patients, putting them on a countdown to death once diagnosed. Although efforts have been made to identify novel therapies against

commonly formed mutations in UM, there are few proven therapies available at present. Considering the only approved drug, tebentafusp can benefit a sub-population of patients and only extend PFS for a limited period, there remains an urgent need to develop novel and effective therapies to target the unique molecular and metabolic vulnerabilities of this fatal cancer.

1.5 Objective of this thesis

Given the grim nature of UM. It is imperative for novel targets and compounds to be identified for its treatment. This thesis aims to re-examine a foundational principle in UM drug targets through examining both registered and novel small molecules in both primary UM cell line 92.1 and metastatic UM cell line OMM2.5 in terms of anti-cancer effect and tumour specific targeting. Specifically

To reassess the role of HER family receptors with a focus on HER2 in UM through the use of the HER2 inhibitor lapatinib and explore their potential anti-cancer effects in UM therapy by investigating the underlying mechanisms of their action. (Chapter 2)

To explore the recently revisited cell death mechanism—autophagy—and its paradoxical role in cancer survival and therapy. Additionally, to assess its potential impact on UM through a comprehensive literature review. (Chapter 3)

To investigate the anti-cancer effects of novel small-molecule inhibitors targeting p21 and sEH in UM, this study will assess their anti-cancer properties, tumour specificity and elucidate the underlying mechanisms of action, particularly evaluating the potential role of p21 inhibition in cancer treatment. (Chapter 4)

To assess the metabolic impact on UM by restricting macronutrients in vitro and to explore the potential additive effects of nutrient depletion combined with small-molecule UC2288 co-treatment in UM therapy. (Chapter 5)

Chapter 2: Lapatinib dysregulates HER2 signalling and impairs the viability of human uveal melanoma cells

Abstract

Purpose

Uveal melanoma (UM) is the principal type of intraocular malignancy in adults. Up to 50% of UM patients develop metastatic disease with very poor survival. There are few drugs available to treat the primary or metastatic UM. This study was undertaken to evaluate the anti-cancer effect of lapatinib and corroborate the potential of HER2 inhibition in the treatment of UM.

Methods

The anti-UM activity of lapatinib was assessed using cell viability, cell death and cell cycle analysis, and its anti-metastatic actions were evaluated using would healing, invasion and colony formation assays. Immunoblotting was used to substantiate the actions of lapatinib on apoptotic and HER2 signalling. The anti-UM activity of lapatinib was further evaluated in a UM xenograft mouse model.

Results

Lapatinib decreased the viability of four UM cell lines (IC50: 3.67-6.53 μM). The antiproliferative activity of lapatinib was corroborated in three primary cell lines isolated from UM patient tumours. In UM cell lines, lapatinib promoted apoptosis and cell cycle arrest, and strongly inhibited cell migration, invasion and reproductive cell growth. Lapatinib dysregulated HER2-AKT/ERK/PI3K signalling leading to the altered expression of apoptotic factors and cell cycle mediators in UM cell lines. Importantly, lapatinib suppressed tumorigenesis in mice carrying UM cell xenografts.

Conclusion

Together the present findings are consistent with the assertion that HER2 is a viable therapeutic target in UM. Lapatinib is active in primary and metastatic UM as a clinically approved HER2 inhibitor. The activity of lapatinib in UM patients could be evaluated in future clinical trials.

2.1 Introduction

Uveal melanoma (UM) is a rare cancer that is very different from its cutaneous counterpart (101). As the primary intraocular malignancy, UM accounts for over 85% of ocular tumours and is also the second most common type of melanoma (~5% of all cases) (102, 103). The incidence of UM is similar in males and females and affects both eyes equally; however, it is more frequently identified in Caucasians and in adults aged over 40 (103, 104).

Although the survival rate is around 84% for early-stage UM (AJCC stages I and II), patients often experience treatment delays due to the difficulty in distinguishing tumours from benign tissues. UM tumours are often asymptomatic until they reach a significant size (1, 105, 106). Not surprisingly, the mortality rate increases dramatically in late stage UM (102). Up to 50% of patients develop metastases, particularly in the liver, prior to diagnosis (4, 107). The median survival rate of UM patients with liver metastases is 4-6 months and those whose disease is more advanced may survive <3 months (108-110).

Clinically, enucleation has been widely used in the treatment of primary UM tumours, but this may lead to irreversible eye damage. More recently, other treatment options such as brachytherapy, proton beam therapy and phototherapy, have been used to treat primary UM tumours with the aim of preserving vision (43, 101, 111). Although the current clinical guidelines state that laser- and radiotherapy are the primary treatment for UM primary tumours, the effectiveness of these regimen in patients is limited to early diagnoses and small sized tumours. Nevertheless, such non-pharmacological approaches are unable to prevent metastatic lesions developing in distant tissues. Even though hepatic chemoembolization, isolated hepatic perfusion, intra-arterial chemotherapy, radiotherapy, and surgical resection are effective in the treatment of patients with liver cancer, these approaches are generally ineffective in UM tumours that have metastasized to the liver (110, 112, 113). Therefore, the identification of drugs that can effectively treat primary tumours and prevent metastasis in UM patients would be highly significant.

Both cutaneous melanoma and UM are derived from melanocytes. However, unlike cutaneous melanoma, environmental factors, such as UV radiation and latitude, are not associated with the development of UM. Furthermore, cutaneous melanoma is characterised by mutations that

activate the v-raf murine sarcoma viral oncogene homolog B1 (BRAF), neuroblastoma RAS viral oncogene homolog (NRAS), tyrosine-protein kinase (KIT) and phosphatidylinositol 3-Kinase (PI3K) pathways, whereas UM is unrelated to these mutations. UM is characterised by low tumour mutational burden compared to cutaneous melanoma where mutagenic effect of UV light is apparent (114, 115). However, UM displays a distinct genetic profile that may be associated with its development and prognosis (116). Notably, the most common mutations in UM occur in the tumour suppressor gene and the guanine nucleotide binding protein Gαq/Gα11 (GNAQ/11) gene, which accounts for over 40% of genetic mutations in UM, followed by BRCA1 associated protein 1 (BAP1). Mutations within these two regulatory genes result in increased cell growth, proliferation and metastasis leading to poor prognosis in UM (117, 118). Other molecular changes including monosomy of chromosome 3, amplification or gain of chromosome 8q all appear to contribute to the grim prognosis of UM patients (17, 119). Drugs that are used clinically for the treatment of cutaneous melanoma are ineffective in the treatment of UM (48, 101, 120-124).

The epithelial growth factor receptor (EGFR) family consists of 4 members: ErbB1–4. ErbB receptors are transmembrane proteins that have a cytoplasmic binding domain, a transmembrane domain and an intracellular domain that interacts with downstream signalling pathways. Receptor activation causes hetero- or homo-dimerization, followed by autophosphorylation on tyrosine residues in the intracellular kinase domain. Activation of downstream pathways, such as the PI3K/protein kinase B (AKT), Ras/mitogen-activated protein kinase (MEK)/extracellular-signal-regulated kinase (ERK), phospholipase C Gamma (PLCγ)/protein kinase C (PKC), and Janus kinase (JAK)/signal transducer and activator of transcription (STAT) cascades, regulates cell survival, proliferation, differentiation, motility, apoptosis, survival, invasion, migration, adhesion, and angiogenesis (125, 126). Therefore, ErbB isoforms have been widely studied as cancer drug targets (127). Among the 4 ErbBs, HER2 has an established role in breast cancer. It has also been shown to have an important role in the prognosis of various other cancers such as gastric, biliary tract, colorectal and non-small cell lung cancer. The overexpression/amplification of HER2 in these cancers may contribute to the poor prognosis and more aggressive tumours (128). Hence, it is important that the role of HER2 is evaluated in UM.

With advances in gene profiling, multi-kinase inhibitors have been suggested to have potential value in the development of new treatment strategies in UM (129-131). We recently tested several multi-kinase inhibitors in UM cell lines (84). We found that afatinib, which is a potent inhibitor of multiple ErbB receptors, including EGFR, HER2 and HER4, induced cell death and prevented cell migration in UM cell lines. It is noteworthy that EGFR and HER4 are not commonly expressed in UM tumours (63, 84, 121, 129-134). Therefore, neither of these receptors is likely to be a primary molecular target for UM drug development. The finding that afatinib dysregulated HER2 signalling to exert its anti-UM activity suggests that HER2 could be a novel therapeutic target in UM (84). To substantiate the potential clinical significance of HER2 in UM, we investigated the anti-UM activity of the HER2 inhibitor lapatinib in the present study. Lapatinib was selected because it is clinically approved for use in patients with HER2-positive breast cancers that are resistant to the front-line agent trastuzumab (135). Thus, lapatinib has the potential advantage that it may be more rapidly translated to clinical application in UM.

Indeed, we have demonstrated some of specific applications of Lapatinib on UM in Research Square, which is not a recognized publisher. The purpose of the preprint to receive comments from peers in the field that could further improve the study for subsequent formal publication by an appropriate journal. Indeed, we have improved the present study by including additional data based on the feedback we received on the preprint (e.g., Fig 6E).

2.2 Material and Methods

2.2.1 Reagents and biochemicals

Dulbecco's Modified Eagle Medium (DMEM), Foetal Bovine Serum (FBS), Insulin-Transferrin-Selenium (ITS), L-Glutamine, Penicillin-Streptomycin (P/S) and Roswell Park Memorial Institute Medium (RPMI-1640) were purchased from Thermo Scientific (Lidcombe, NSW, Australia). Giant cell tumour (GCT) conditioned medium was obtained from United Biosciences (Carindale, QLD, Australia). The β-actin antibody, dimethyl sulfoxide (DMSO) and thiazolyl blue tetrazolium bromide (MTT) were purchased from Sigma-Aldrich (Castle Hill, NSW, Australia). Lapatinib was from Selleck Chemicals (Houston, Texas, USA), dissolved in DMSO and stored at -20ºC. Antibodies were purchased from Cell Signalling Technology (Danvers, MA,

USA): Akt (pan, Cat. #: 4685), Bcl2-associated X protein (Bax; D2E11, Cat. #: 5023), Bcl-XL (54H6, Cat. #: 2764), cyclin D1 (Cat. #: 55506), GAPDH (D16H11, Cat. #: 5174), HER2/ErbB2 (Cat. #: 4290), ERK (Erk, Cat. #: 4695), PI3K p85 (19H8, Cat. #: 4257), phospho-Akt (Ser473, Cat. #: 4060), phospho-HER2/ErbB2 (Tyr1196, Cat. #: 6942), phospho-PI3K p85 (Tyr458)/p55 (Tyr199) (E3U1H, Cat. #: 17366), phospho-ERK (Thr202/Tyr204, Cat. #: 4370) and STAT1 (D1K9Y, Cat. #: 14994). The FITC Annexin V Apoptosis Detection Kit II was purchased from BD Bioscience (North Ryde, NSW, Australia). Goat anti-mouse and anti-rabbit IgGs that were conjugated with horseradish peroxidase were obtained from Bio-strategy delivery technology (Tullamarine, VIC, Australia). PVDF membranes were from Merck Millipore (Bayswater, VIC, Australia).

2.2.2 UM cell lines

UM cell lines used in this study were obtained as indicated previously (84). All cell lines were regularly checked for mycoplasma with MycoAlert Mycoplasma Detection kit (Lonza, Mount Waverley, VIC Australia) to ensure optimal viability. RPMI-1640 was used to culture C918, Mel202, MP46 and 92.1 cells and DMEM was used to maintain OMM-1 and OCM-1 cells. All culture media was supplemented with 10% heat-inactivated FBS (v/v), 1% L-Glutamine and 1% P/S (Thermo Scientific, Lidcombe, NSW, Australia). Cells were incubated in a humidified incubator (5% CO2) at 37 °C.

The early literature indicated that the C918 cell line was derived from primary UM (136). According to the previous report (137), the STR profile of the C918 cell line seemed identical to that of the cutaneous melanoma C8161 cell line (138). However, the reference to the STR profile of C8161 cells could not be verified – either on the journal website or through other resources e.g., PubMed, Medline. Therefore, the authenticity of the information contained within Yu et al. still remains to be fully substantiated. We compared the STR profiles of the C918 cell line obtained from the Swiss Institute of Bioinformatics and the C8161 cell line provided by Lonza. We found that these two STR profiles were quite different. In addition, we undertook a proteomics analysis to compare C918 cells with the malignant human melanoma cell line A375. We found that that p75NTR and S100 were down-regulated in C918 while MITF was up-regulated. This is consistent with a previous report that immunophenotyping for proteins such as HMB-45, HMB-50, p75NTR, S100 and MITF could be used to distinguish uveal and cutaneous

melanomas (139). Based on the evidence from genotyping and immunophenotyping studies described above, we consider that C918 and C8161 appear to be different cell lines. Thus, our study is consistent with a number of other recent reports that C918 is an in vitro model of UM (140-142).

2.2.3 Cell viability assay

Assays of MTT reduction were used to determine cell viability after lapatinib treatment. UM cells were cultured in 96 well plates (2x104cell/well). Cells were treated with various concentrations of lapatinib in RPMI-1640 or DMEM containing 1% FBS. MTT (0.5 mg/mL) was added 24 h later and, after incubation in the dark for 2 h, cells were washed with phosphate-buffered saline (PBS; 0.154 M NaCl, 0.001 M KH_2PO_4, 0.003 M Na_2HPO_4; pH 7.4), DMSO was added, and plates were shaken for 10 min at room temperature. Absorbance was measured at 550 nm in a microplate reader (Model 680, Bio-Rad, Gladesville, NSW, Australia). IC50 values were calculated by non-linear regression of MTT inhibition as a function of drug concentration (GraphPad Prism 7.0; San Diego, CA).

2.2.4 Annexin V/propidium iodide flow cytometry assay

UM cells were seeded and treated with lapatinib (5 µM) in medium containing 1% FBS. Cells were collected 24 h after treatment, washed with PBS, suspended, and stained with annexin V and propidium iodide (PI) for 20 min at room temperature. Samples were subjected to flow cytometry (Guava easycyte; Merck Millipore, Bayswater, VIC, Australia) and apoptotic and necrotic cells were quantified as described previously (84).

2.2.5 Cell cycle analysis

Cells were seeded and treated with lapatinib (5 µM) for 24 h, then harvested and washed twice in PBS before fixing overnight in cold 70% ethanol at -20 °C. The ethanol was removed, samples were washed with PBS and then stained in the dark with PI for 30 min at 37 °C, after which they were analysed by flow cytometry (Guava easycyte).

2.2.6 Scratch-wound cell migration assays

Cells were cultured on 24-well microplates (5 × 104 cells/well). After 24 h scratches were made with a Wound Maker instrument (Sartorius, Dandenong South, VIC, Australia). Cells were washed with PBS and incubated in medium containing 1% FBS (v/v) and lapatinib (5 μM) for 24 h. Cells were incubated at 37°C and photos were taken at 2 h intervals with an Essen IncuCyte S3 instrument (10X magnification; Sartorius). Cell migration rates were determined using Image J software (National Institutes of Health, USA). Migration rate was calculated as:

$$Migration\ Rate\ \% = [\frac{\text{Area(initial)} - \text{Area(final)}}{\text{Area(initial)}}] \times 100$$

Area (initial) is the area of the scratch measured immediately after wounding (t = 0 h).

Area (final) is the area of the wound measured 24 h after the scratch was applied.

2.2.7 Matrigel invasion assay

UM cells were seeded into 96-well plates (3-4 × 104/well). After 24 h, scratches were made as described above. Cell debris was removed by washing with PBS. Matrigel Matrix (BD Falcon, Chatswood, NSW, Australia) diluted in culture medium (200 – 800 μg/mL) was added to each well and allowed to solidify for 1 h at 37 °C. Following this, cells were treated with lapatinib (5 μM), and treatments were replenished at 24h intervals. The plates were imaged over 24 to 72 h with an Essen IncuCyte S3 instrument. Cell invasion rates were determined using Image J software and the invasion rate was calculated as:

$$Invasion\ Rate\ \% = [\frac{\text{Area(initial)} - \text{Area(final)}}{\text{Area(initial)}}] \times 100$$

2.2.8 Colony formation assay

Cells were treated with lapatinib (5 μM) in 12 well plates and then aliquoted into 24-well plates (200 cells/well) for 6-8 days. Methanol (100%) was used to fix cells before staining with crystal violet. Colony growth was defined microscopically as a cluster of at least 50 cells. Photos were taken in an Essen IncuCyte S3, using whole-well scan mode at 4 X magnification. Image J software was used to identify the leading edge of the cell population.

2.2.9 Western blot

Cells were treated with lapatinib and incubated for 24 h before they were harvested with lysis buffer containing NP-40 (1% IGEPAL, 150 mM NaCl and 50 mM Tris, pH 7.8) containing protease inhibitors. Lysates were then centrifuged at 15,000 rpm (10 min, 4 °C) to separate protein-containing supernatants and cell remnants; supernatant fractions were denatured on a heat block.

Proteins in supernatant fractions were separated by electrophoresis, transferred to a PVDF membrane and incubated in 5% non-fat milk dissolved in PBS containing Triton 0.05% X-100 (PBST) at room temperature for 30 min. The membranes were cut prior to hybridisation with different antibodies. The membranes were incubated overnight with a primary antibody at 4 °C. Membranes were washed three times with PBST and were then incubated at room temperature with a secondary antibody for 1h. Signals were detected using chemiluminescence (SuperSignal West Pico, Thermo Scientific, Lidcombe, NSW, Australia) and were visualized with ImageQuant LAS500 (GE Health Care, Silverwater, NSW, Australia) or Chemidoc image machine (Bio-Rad, Gladesville, NSW, Australia).

2.2.10 Primary UM tumour derived cell lines

Human UM tumour samples were obtained with approval from St. Vincent's Hospital Sydney Human Ethics Committee (HREC/17/SVH/346) and experiments were strictly conducted as per the relevant guidelines and regulations. All the informed consent for the patient samples used in this study have been obtained. Tumour tissues were surgically removed, cut into segments, treated with trypsin-EDTA and then washed three times with PBS (pH 7.4). Individual cells were collected and incubated at 37°C in RPMI-1640 medium containing 20% FBS (v/v), 1% L-glutamine, 1% P/S, 1% ITS and 2% GCT under a 5% CO2 atmosphere. All experiments were conducted in cells at passage 2 to 5.

2.2.11 UM xenograft mouse model

Animal ethics approval was obtained from the Laboratory Animal Ethics Committee of Jiangsu Institute of Nuclear Medicine (Wuxi, China).

Animal experiments were conducted in accordance with approved protocols and regulations. The study Results were reported according to ARRIVE guidelines (143). C918 cells were mixed in a 2:1 ratio with Matrigel and injected subcutaneously in BALB/c nude mice (5 weeks old; male; Chang Zhou Cavens Laboratory Animal Co., Ltd, Changzhou, China). Tumour volume was measured with callipers every 3 d until they reached ~100 mm3 in size. Tumour volumes were calculated as (a × b2)/2, where a and b are the length and width of the tumours, respectively. Once tumours reached the desired volume (around day 10), mice were randomly assigned to two groups to receive either lapatinib (25 mg/kg; n=7) or vehicle (n=7) once daily by intraperitoneal injection. Body weights and tumour sizes were measured every 2 days for 14 days. Drug administration was continued for 24 days. When treatments were complete, the mice were anesthetised with pentobarbital sodium (50 mg/kg) by intraperitoneal injection. Tumours were excised, weighed, photographed, and fixed in 4% paraformaldehyde for subsequent analysis.

2.2.12 Positron emission tomography (PET) scanning

68Ga Activity was eluted from a 68Ge/68Ga generator and used to prepare [68Ga] Ga-NOTA-PRGD2 tracer, as described previously (25). On the day of scanning, the mice received ~3.7MBq of 68Ga NOTA-PRGD2 under anaesthesia via tail vein injection. Dynamic imaging acquisition was conducted for 60 min after tracer administration using an Inveon microPET scanner (Siemens Medical Solutions, Erlangen, Germany). Vendor software (ASI Pro 5.2.4.0) was used to detect regions of interest using decay-corrected whole-body coronal images.

2.2.13 Histology and immunohistochemistry

Tumour tissues fixed in paraffin blocks were cut into 8 μm sections and were stained with hematoxylin and eosin (Beyotime Institute of Biotechnology, Jiangsu, China). Sections were incubated (4ºC) with an anti-Ki67 antibody (Cat. #: ab15580, Abcam, Shanghai, China), followed by incubation with a horseradish peroxidase-conjugated secondary antibody. Immunohistochemical staining was conducted with a DAB substrate kit (Shanghai Bio-Platform Technology Company, Shanghai, China) and light microscopy (Olympus; Tokyo, Japan).

2.2.14 TUNEL assay

TUNEL assay was used to detect cell death in paraffin-embedded tumour sections. Briefly, sections were placed on slides and stained with the TUNEL assay kit (Beyotime Institute of Biotechnology, Jiangsu, China), as described previously (97); nuclei were counter-stained with hematoxylin. Images were analysed using a KF-PRO-120 slide scanner (Konfoong Bioinformation Tech, Ningbo, China).

2.2 15 Statistics

Data are presented as mean ± standard deviation (SD) with significance defined as $p < 0.05$. Observers were blinded in in vivo studies. Statistical analysis was conducted using one-way ANOVA and Dunnett's post-hoc test to compare multiple independent groups in GraphPad Prism 9.0.

2.3 Results

2.3.1 Lapatinib decreased the viability of UM cells

The anti-UM activity of lapatinib were evaluated in C918, 92.1 and Mel202 cells that were derived from primary UM tumours and in OMM-1 cells that were isolated from a subcutaneous metastasis. All four cell lines were treated with lapatinib over the concentration range of 0 to 50 μM. Cell viability was then estimated using MTT reduction assays. As shown in Fig. 1, the IC50 values of lapatinib ranged from 3.67 μM to 6.53 μM across the four UM cell lines. It is noteworthy that the above-mentioned cell lines have BAP1 mutations. Therefore, we also investigated the effect of lapatinib in OCM-1 and MP46 cells in which BAP1 was mutated or absent. Similar IC50s were observed in these two cell lines (Suppl Fig. 1), which suggested that the effect of lapatinib is independent of BAP1 status.

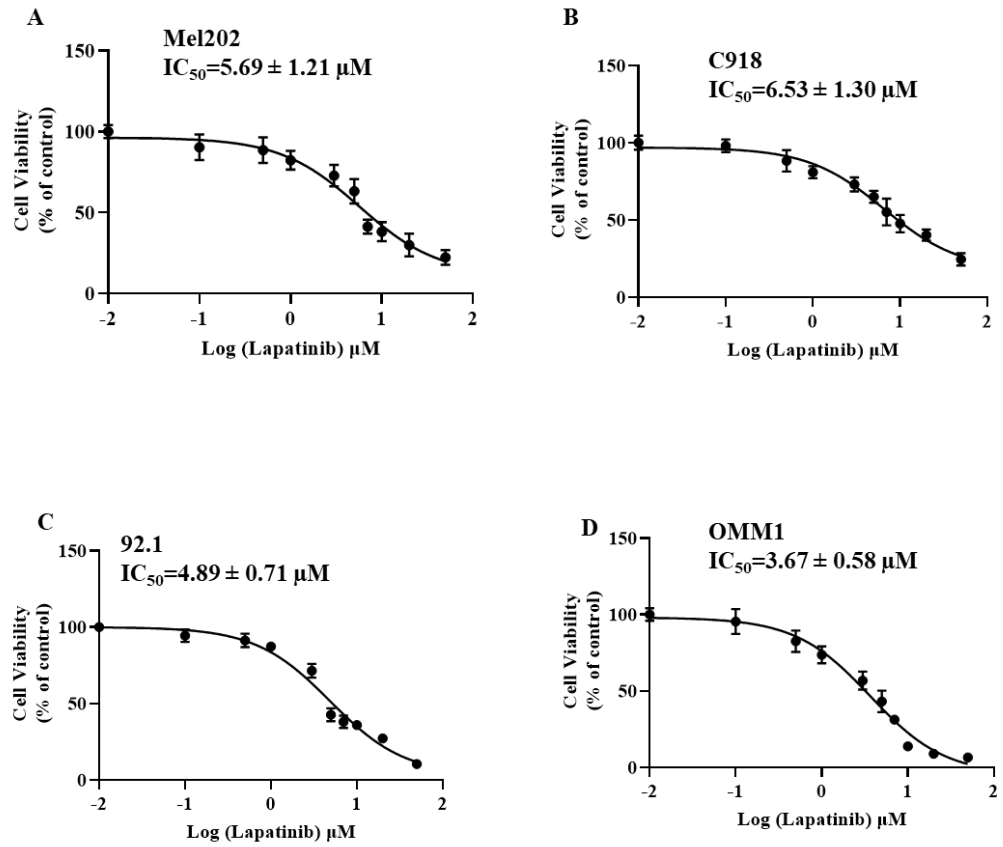

Figure 1. Lapatinib decreases the viability of UM cell lines. Mel202 (A), C918 (B), 92.1 (C) and OMM1 (D) cells were treated with lapatinib (0-50 µM) at 37°C for 24 h. Cell viability was assessed in MTT reduction assays. IC50s of lapatinib in UM cell lines were estimated by non-linear regression (GraphPad Prism 7.0; San Diego, CA).

2.3.2 Lapatinib induced apoptosis and cell cycle arrest in UM cell lines

The capacity of lapatinib to promote UM cell death was evaluated using Annexin-V/PI staining and flow cytometry. Apoptosis was found to be the principal cell death mechanism in all four UM cell lines after treatment with lapatinib (5 µM, 24 h; Fig. 2). Thus, lapatinib increased the proportion of apoptotic cells to 2.73-6.40-fold compared to control ($p<0.001$, Fig. 2B, 2D, 2F, 2H). In accord with these findings, lapatinib (5 µM) also decreased viability and activated apoptosis in three tumour-derived cell lines from UM patients (Fig. 3).

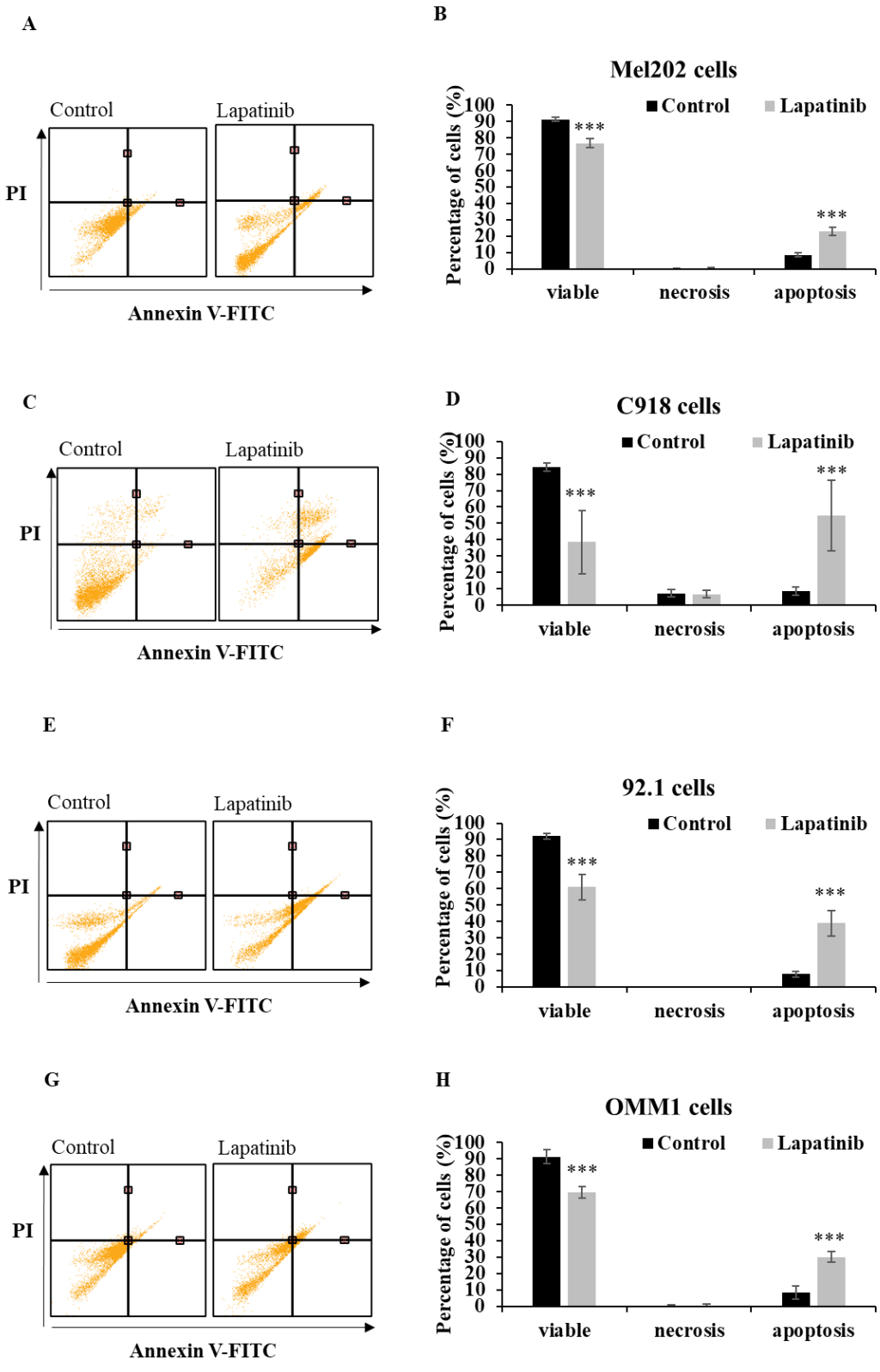
A
Control
Lapatinib
PI
Annexin V-FITC
B
Mel202 cells
Control
Lapatinib
Percentage of cells (%)
100
90
80
70
60
50
40
30
20
10
0
***
***
viable
necrosis
apoptosis
C
Control
Lapatinib
PI
Annexin V-FITC
D
C918 cells
Control
Lapatinib
Percentage of cells (%)
***
***
viable
necrosis
apoptosis
E
Control
Lapatinib
PI
Annexin V-FITC
F
92.1 cells
Control
Lapatinib
Percentage of cells (%)
***
***
viable
necrosis
apoptosis
G
Control
Lapatinib
PI
Annexin V-FITC
H
OMM1 cells
Control
Lapatinib
Percentage of cells (%)
***
***
viable
necrosis
apoptosis

*Figure 2. Lapatinib activates apoptosis in UM cell lines. Mel202 (A & B), C918 (C & D), 92.1 (E & F) and OMM1 (G & H) cells were treated with lapatinib (5 µM) at 37°C for 24 h, stained with Annexin V-FITC/PI and subjected to flow cytometry. Representative cell death profiles are shown for Mel202 (A), C918 (C), 92.1 (E) and OMM1 (G) cells. The percentages of viable, necrotic and apoptotic cells are indicated as mean ± SD for Mel202 (B), C918 (D), 92.1 (F) and OMM1 (H) cells. Experiments were performed on 3 independent occasions and each experiment included three repeats. Control treatments consisted of vehicle (DMSO) alone. ***p < 0.001 vs. control by One-way ANOVA and Dunnett's post-hoc test.*

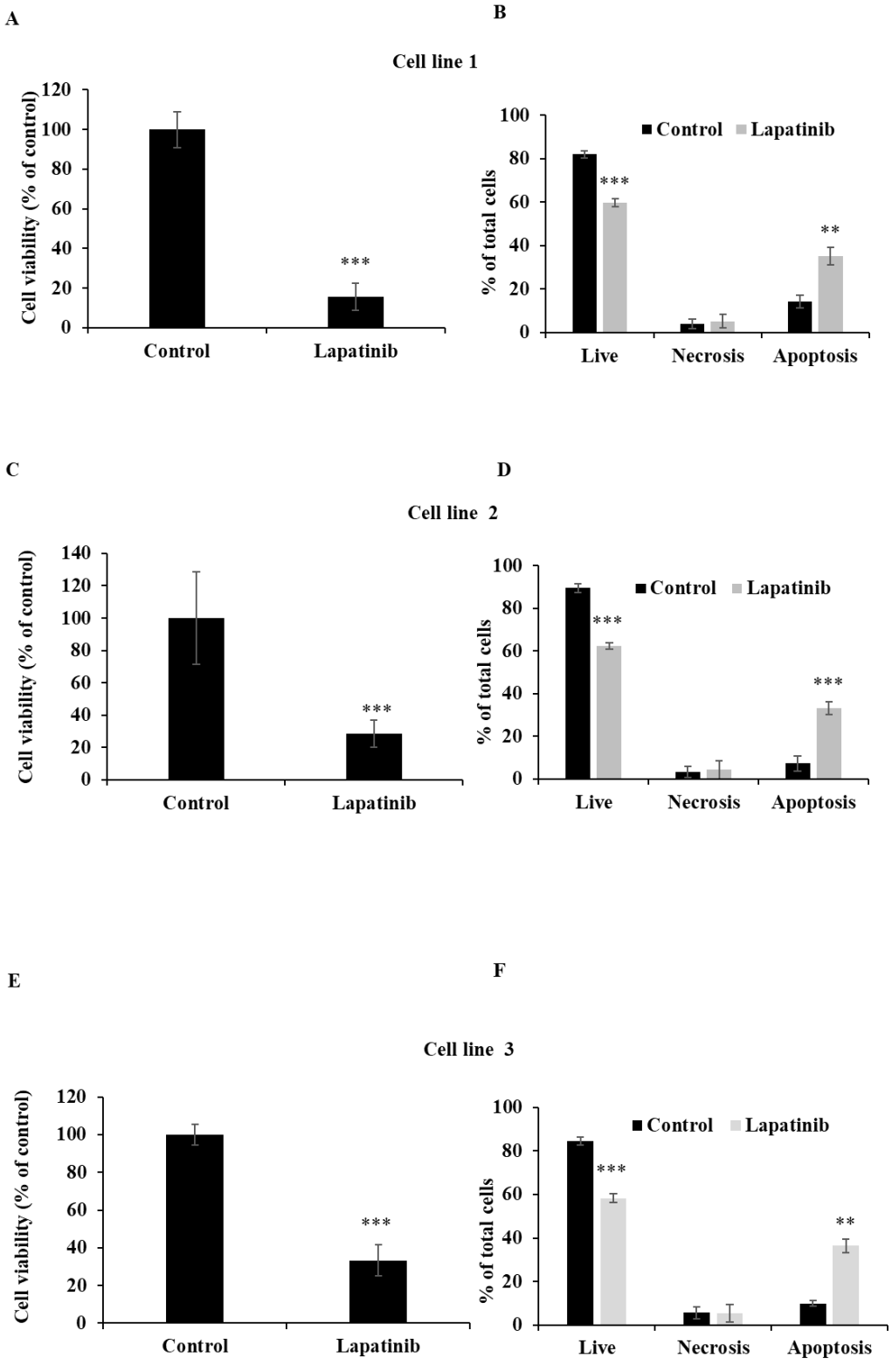
A
B
Cell line 1
Cell viability (% of control)
120
100
80
60
40
20
0
***
Control
Lapatinib
% of total cells
100
80
60
40
20
0
Control
Lapatinib
***
**
Live
Necrosis
Apoptosis
C
D
Cell line 2
Cell viability (% of control)
140
120
100
80
60
40
20
0
***
Control
Lapatinib
% of total cells
100
80
60
40
20
0
Control
Lapatinib
***
***
Live
Necrosis
Apoptosis
E
F
Cell line 3
Cell viability (% of control)
120
100
80
60
40
20
0
***
Control
Lapatinib
% of total cells
100
80
60
40
20
0
Control
Lapatinib
***
**
Live
Necrosis
Apoptosis

*Figure 3. Lapatinib decreases viability and activates apoptosis in primary UM-tumour derived cell lines. UM tumour-derived cell lines were treated with lapatinib 5 µM for 24 h at 37°C. The viability of each primary cell line was assessed using MTT reduction (A, C and E). After treatment, cells were stained with Annexin V-FITC/PI and subjected to flow cytometry. The percentages of viable, necrotic, and apoptotic cells are indicated as mean ± SD for each primary cell line in B, D and F. Experiments were performed on 3 independent occasions and each experiment included three repeats; control treatments consisted of vehicle (DMSO) alone. **p < 0.01; ***p < 0.001 vs. control by One-way ANOVA and Dunnett's post-hoc test.*

The cell cycle arrest assay is to indicate the influence of treatment on cell cycle progression, which is relevant to cell death. The inhibitory effect (IC50) is an overall outcome from lapatinib-induced cell death and cell cycle arrest, so it is a functional read-out of the composite anti-cancer effects of lapatinib in UM cell lines. To further evaluate the impact of lapatinib on viability, UM cells were stained with PI and subjected to cell cycle analysis by flow cytometry. The proportion of cells in G0/G1 phase was increased by lapatinib (5 µM, 24 h; $P<0.001$), while the proportion of cells in G2/M phase was decreased ($P<0.001$) and cells in S phase were unchanged (Fig. 4). Taken together, these findings indicate that lapatinib is highly effective in inducing apoptosis and cell cycle arrest in UM cell lines.

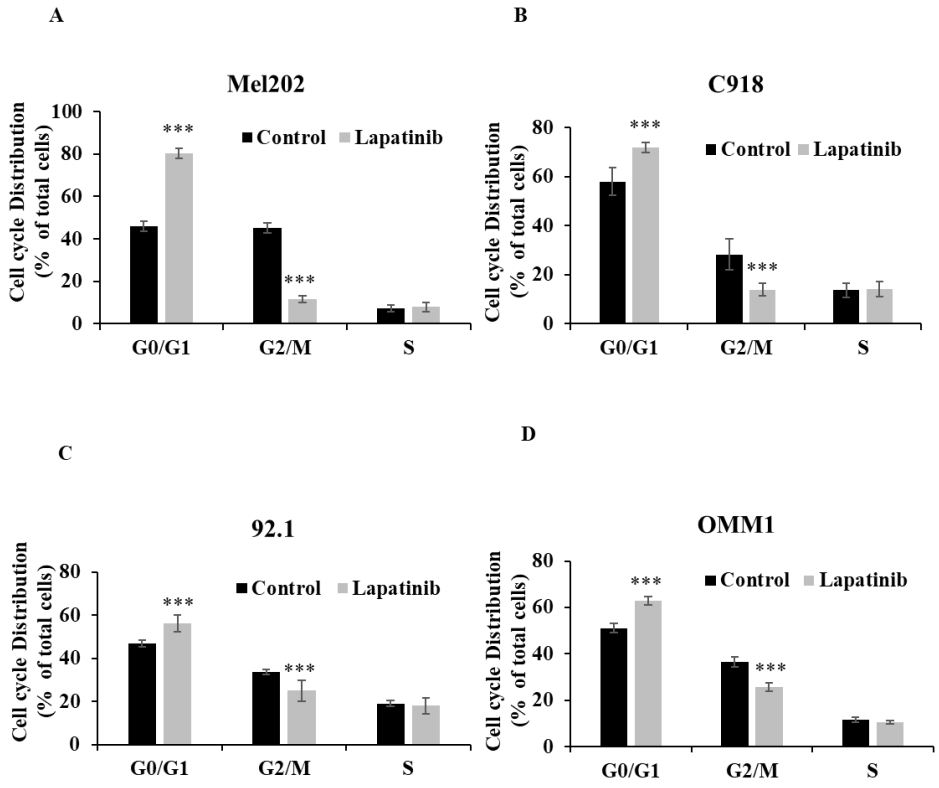

*Figure 4. Lapatinib induces cell cycle arrest in UM cell lines. Mel202 (A), C918 (B), 92.1 (C) and OMM1 (D) cells were treated with lapatinib (5 µM) for 24 h at 37°C. Cells were stained with PI and subjected to flow cytometry. The percentages of cells in G_0/G_1, G_2/M and S phases are shown as mean ± SD. Experiments were performed on 3 independent occasions and each experiment included three repeats; control treatments consisted of vehicle (DMSO) alone. ***$p < 0.001$ vs. control by One-way ANOVA and Dunnett's post-hoc test.*

2.3.3 Lapatinib modulates STAT1 and apoptotic signalling in UM cells

STAT1 is an important regulator of apoptosis (144, 145). In the present study, the capacity of lapatinib to modulate the expression of STAT1 and its downstream signalling was examined. Treatment with lapatinib substantially increased STAT1 expression to 1.4 - 4.9-fold compared to control across all four UM cell lines (Fig. 5A, 5C, 5D, 5F, 5G, 5I, 5J, 5L). Further, lapatinib decreased the expression of the anti-apoptotic Bcl-XL and increased the pro-apoptotic BAX in

all four UM cell lines (Fig. 5). Consistent with the activation of apoptosis Bcl-XL:BAX ratios were markedly decreased by lapatinib (5 μM, 24 h), as shown in Fig. 5B, 5E, 5H and 5K.

Because lapatinib induced cell cycle arrest in UM cell lines (Fig. 4) we assessed the expression of cyclin D1- a key cell cycle mediator that is also downstream from STAT1. Treatment with lapatinib (5 μM, 24 h) decreased cyclin D1 expression in UM cells to 0.24–0.47 fold compared to control (Fig. 5C, 5F, 5I and 5L).

In summary, lapatinib induced cell death was associated with dysregulated expression of STAT1 and its downstream targets cyclin D1, BAX and Bcl-XL.

Fig. 5

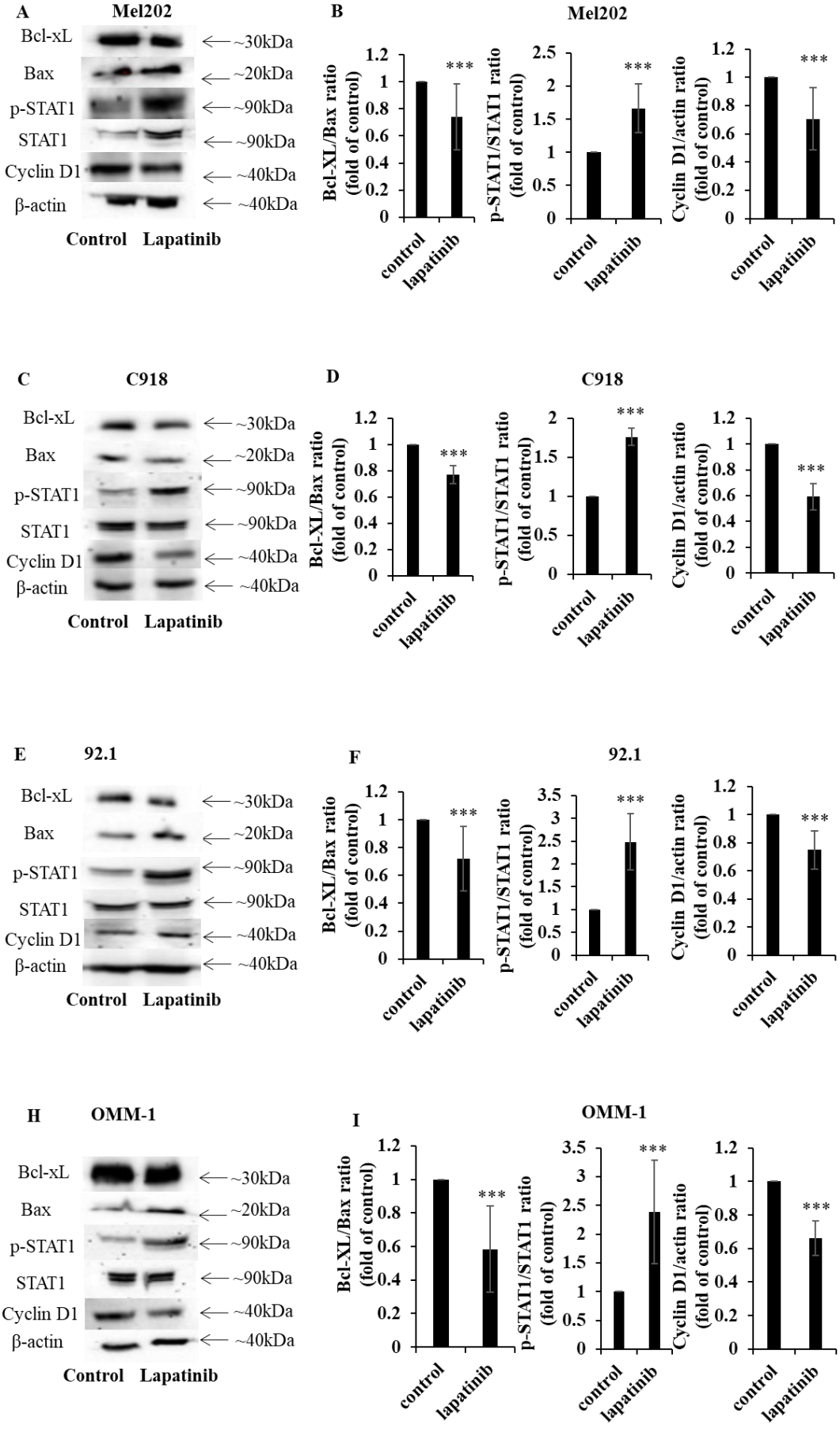
A
Mel202
Bcl-xL
Bax
p-STAT1
STAT1
Cyclin D1
β-actin
~30kDa
~20kDa
~90kDa
~90kDa
~40kDa
~40kDa
Control
Lapatinib
B
Mel202
Bcl-XL/Bax ratio (fold of control)
p-STAT1/STAT1 ratio (fold of control)
Cyclin D1/actin ratio (fold of control)
***
control
lapatinib
C
C918
D
C918
E
92.1
F
92.1
H
OMM-1
I
OMM-1

*Figure 5. The lapatinib-mediated activation of apoptosis is associated with the modulation of STAT1, Bcl-XL and cyclin D1 expression in UM cell lines. Expression of Bcl-XL, BAX, p-STAT1, STAT1 and cyclin D1 was determined by Western blotting with β-actin as the loading control. Cells were treated with lapatinib (5 μM) at 37°C for 24 h, then harvested, lysed, denatured and subjected to sodium dodecylsulfate-polyacrylamide gel electrophoresis. Representative images of proteins of interest are shown for Mel202 (A), 92.1 (C), C918 (E) and OMM-1 (H) cells. Densitometry analysis for protein quantification was conducted using Image J. Bcl-XL: BAX and p-STAT1: STAT1 expression ratios as well as the expression of cyclin D1 relative to β-actin are shown for Mel202 (B), C918 (D), 92.1 (F) and OMM1 (I) cells as fold of control (mean ± SD); control treatments consisted of vehicle (DMSO) alone. Experiments were performed on three separate occasions. ***p < 0.001 vs. control by unpaired t-test.*

2.3.4 Lapatinib inhibited UM cell migration, invasion and suppressed reproductive growth

The migration, invasion and colony formation assay (tumour reproductive growth analysis) are well established methods to evaluate the anti-metastatic effect of drugs. The impact of lapatinib on UM cell migration was examined in scratch-wound healing assays. As shown in Fig 6A, 6C and 6E, lapatinib decreased rates of migration in the Mel202, C918 and 92.1 cell lines that were derived from primary UM tumours to 26% – 36% of control ($P < 0.001$).

Lapatinib also potently inhibited the invasion of UM cells in the Matrigel invasion assay. As shown in Fig. 6B, 6D and 6F, treatment with lapatinib reduced cell invasion rates of Mel202, C918 and 92.1 cell lines to 13% - 67% of control ($P<0.001$).

Colony formation assays were also performed to assess reproductive cell growth upon lapatinib treatment (5 μM, 24 h). As shown in Fig. 6G, lapatinib significantly decreased the number of viable colonies post treatment in all three cell lines ($P<0.001$).

These findings suggest that lapatinib has anti-metastatic actions in UM.

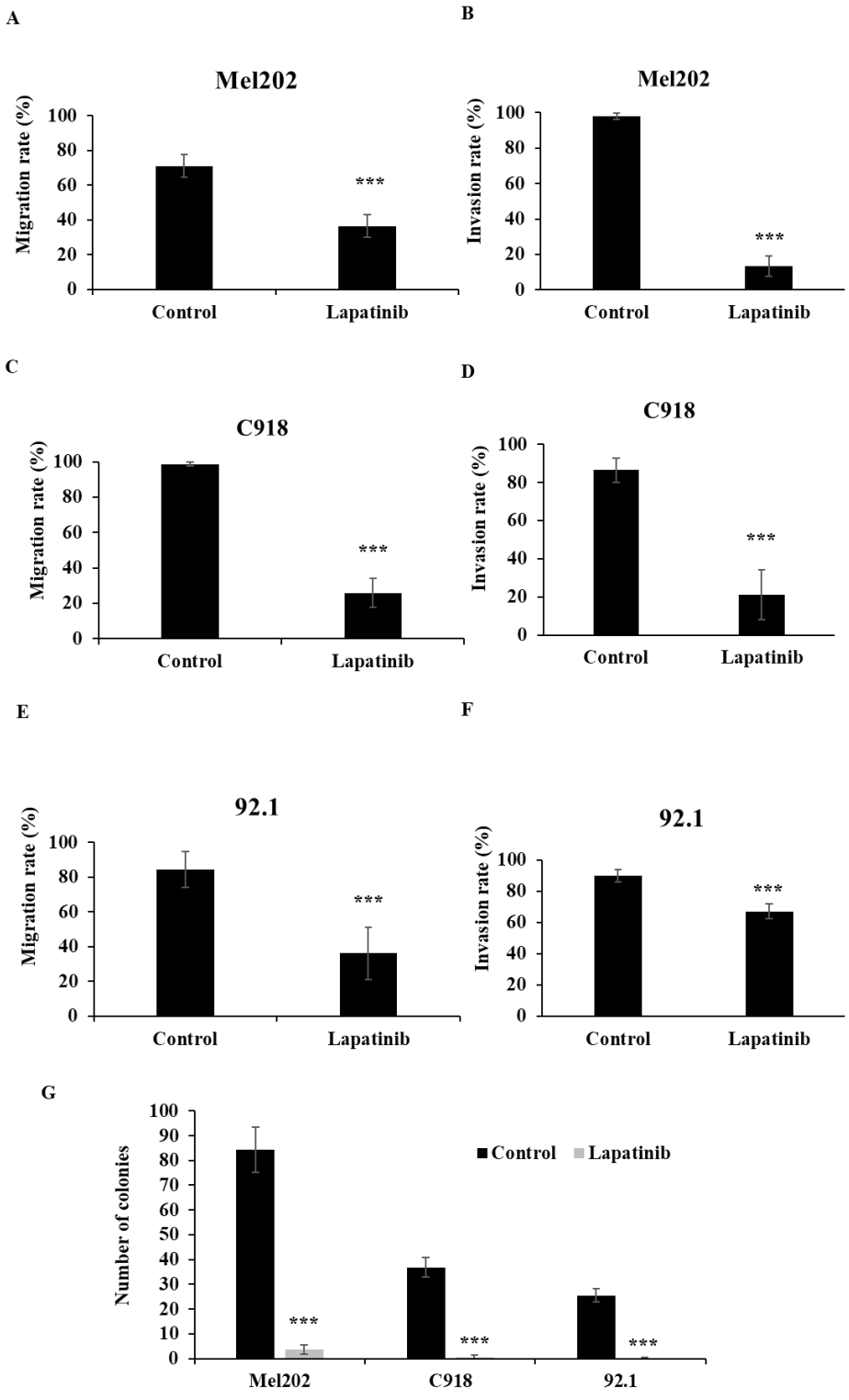

Figure 6. Lapatinib is anti-metastatic in primary tumour-derived UM cell lines. The anti-migratory actions of lapatinib were assessed in scratch-wound assays. UM cell lines were

*treated with lapatinib (5 µM) at 37°C for 24 h. Cell images were captured at 0 and 24 h. The rate of cell migration was estimated as the means of each repeat and are indicated as percentage of control (means ± SD) for Mel202 (A), C918 (C) and 92.1 (E). Cell invasion upon lapatinib treatment was studied in Matrigel invasion assays. UM cell lines were treated with lapatinib (5 µM) at 37°C for 24 h to 72 hr. Cell images were captured at 0 and 24 to 72 h. The rate of cell invasion was estimated as the means of each repeat and are indicated as percentage of control (means ± SD) for Mel202 (B), C918 (D) and 92.1 (F). Reproductive cell growth after lapatinib treatment was evaluated in colony formation assays. (G) Colony number is indicated as the percentage of control (mean ± SD). Experiments were performed on 3 independent occasions and each experiment included four repeats; control treatments consisted of vehicle (DMSO) alone. ***p < 0.001 vs. control by One-way ANOVA and Dunnett's post-hoc test*

2.3.5 Lapatinib exerts its anti-UM activity by inhibiting HER2 signalling

Lapatinib is an established inhibitor of HER2 and is used clinically in the treatment of HER2-positive cancers, including breast cancers that are resistant to the first-choice agent trastuzumab (146-148). Unlike other ErbB receptor isoforms, it has been found previously that HER2 is uniformly expressed in UM cells (84, 149, 150).

We assessed the impact of lapatinib on the expression of HER2 and its phosphorylated isoform in the four UM cell lines. In these experiments, cells were initially cultured in serum-free medium and were then treated with 20% FBS for 10 min immediately prior to treatment with lapatinib (L+; Fig. 7) or vehicle (C+; Fig. 7). This rapidly activated HER2 phosphorylation that was attenuated by lapatinib (Fig. 7; compare the values for lapatinib and control in the Tables at right). Important downstream targets of HER2 include ERK, PI3K and AKT. Inclusion of lapatinib also prevented the activation of these pathways after serum addition (Fig. 7; compare L+ *versus* L- relative to C+ *versus* C-). Noteworthy, the comparison of protein expression in Fig. 7 is the ratio of phosphorylated and total forms of HER2, PI3K, AKT and ERK in each treatment. The samples for estimation of each pair of proteins were obtained in parallel analyses from the same experimental treatment. Thus, loading controls in each panel are not required.

To our knowledge, the expression of HER2 has not been reported in population or similar studies of UM patients. Based on our own observation, the expression of HER2 varies widely across multiple UM cell lines. We also qualitatively confirmed the expression of HER2 protein in the three primary tumour-derived cell lines used in the present study (Suppl Fig. 2). Importantly, we also explored the Cancer Genome Atlas Program (TCGA) database (https://portal.gdc.cancer.gov/). In a cohort of 80 UM patients, ErbB2 (HER2) was expressed in all tumour samples and its expression was significantly higher than EGFR and ErbB4 ($p<0.001$) (Suppl Fig. 3). In addition, we demonstrated the effectiveness of HER2 inhibitors, especially afatinib, lapatinib and neratinib, in UM cells in the present study and in our previous paper (84). In the literature, Forsberg et. al has also investigated HER2 as a possible target and reported HER2 to be expressed in UM (149). Overall, these findings indicate that lapatinib inhibits HER2 and its downstream signalling and suggests that these may be early events in its anti-UM activity.

A

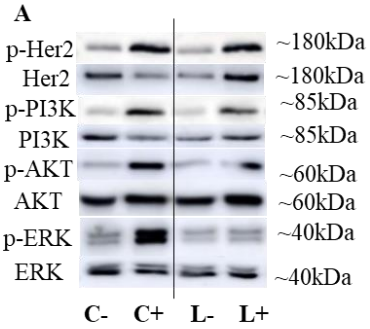

Mel202	Control	Lapatinib
p-HER2/HER2	2.68 ± 0.72	1.26 ±0.21 #
p-PI3K/PI3K	3.00 ±0.74	1.12 ± 0.18 #
p-AKT/AKT	2.65 ± 0.49	1.52 ±0 .31 ##
p-ERK/ERK	2.67 ±0.52	1.59 ± 0.27 #

B

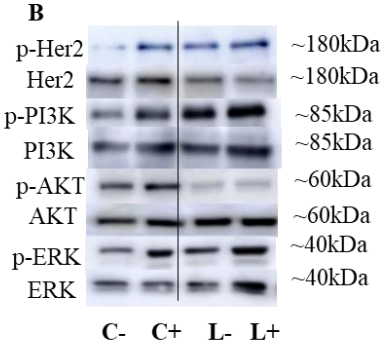

92.1	Control	Lapatinib
p-HER2/HER2	2.77 ± 0.47	1.66 ± 0.49 ##
p-PI3K/PI3K	1.72 ± 0.14	1.00 ± 0.03 ###
p-AKT/AKT	1.74 ± 0.29	1.07 ± 0.02 #
p-ERK/ERK	1.70 ± 0.14	1.01 ± 0.12 #

C

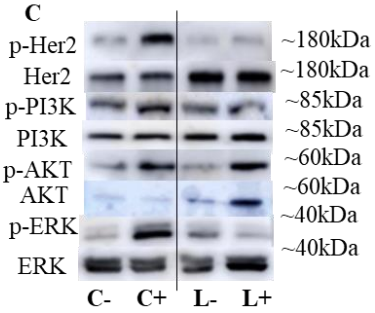

C918	Control	Lapatinib
p-HER2/HER2	2.66 ± 0.46	1.18 ± 0.17 #
p-PI3K/PI3K	1.71 ± 0.18	0.84 ± 0.08 ##
p-AKT/AKT	2.57 ± 0.35	1.25 ± 0.27 ##
p-ERK/ERK	2.20 ± 0.48	0.87 ± 0.14 #

D

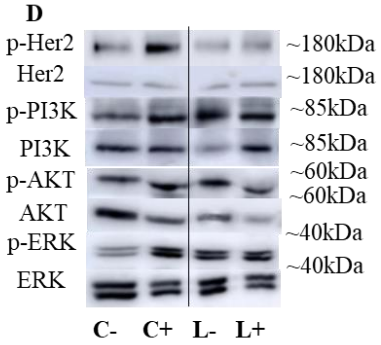

OMM.1	Control	Lapatinib
p-HER2/HER2	1.98 ± 0.11	1.00 ± 0.22 ##
p-PI3K/PI3K	1.32 ± 0.03	0.65 ± 0.17 ##
p-AKT/AKT	2.19 ± 0.15	1.10± 0.22 ###
p-ERK/ERK	2.74 ± 0.20	1.09± 0.06 ###

Figure 7. The lapatinib-mediated activation of cell death is associated with inhibition of HER2 and its downstream signalling cascades in UM cell lines. In each experiment, four sets of cells were cultured in serum-free medium for 24 h. Two of the four sets of cells were then treated for 10 min with medium containing 20% FBS while the other two sets of cells remained serum-free. In the next step, one each of the sets of serum-treated and serum-free cells was treated with lapatinib (5 μM) at 37°C for 1 h, while the others were treated with vehicle alone (DMSO), and lysates were prepared. This produced a four-way design that evaluated the effect of serum addition and lapatinib addition on the signalling pathways (Key: C-: vehicle control without serum stimulation; C+: vehicle control with serum stimulation; L-: lapatinib treatment without serum stimulation; L+: lapatinib treatment with serum stimulation). Expression of HER2, AKT, ERK and PI3K and their phosphorylated isoforms was evaluated by Western blotting and densitometry analysis. Representative images of p-HER2, HER2, p-AKT, AKT, p-PI3K, PI3K, p-ERK and ERK are shown for Mel202 (A), 92.1 (B), C918 (C) and OMM-1 (D) cells. Densitometry analysis was conducted using ImageJ and the ratios (L+/L-) and (C+/C-) were calculated for the effects on lapatinib and DMSO respectively on the expression of phosphorylated and total forms of the proteins. These data, as fold of corresponding control (mean ± SD; no serum stimulation), are shown in the Tables to the right of panels A-D. Experiments were repeated on three occasions. #p < 0.05; ##p < 0.01; ###p < 0.001 vs. control by Two-way ANOVA.

2.3.6 Lapatinib has potent anti-tumour activity in a UM xenograft mouse model

The anti-UM activity of lapatinib was examined further in a xenograft model.(97) Lapatinib (25mg/kg for 14 d) was administered to nude mice that carried UM cell xenografts: tumour growth was suppressed (Fig. 8A and 8B). From PET scan analysis, the final tumour sizes in the lapatinib-treated mice were smaller than those in controls (Fig. 8C).

Confirmatory immunohistochemical staining was undertaken in tumour samples that were collected at the end of the experimental treatments. From H&E staining the tumour architecture was improved by lapatinib treatment (Fig. 8D). Staining of the cell proliferation marker Ki67

was decreased by lapatinib and apoptosis as reflected by TUNEL staining, was increased (Fig. 8D).

Overall, these data indicate that lapatinib inhibits tumour growth, suppresses cell proliferation, and activates tumour cell apoptosis *in vivo* in mice carrying UM-cell xenografts.

A

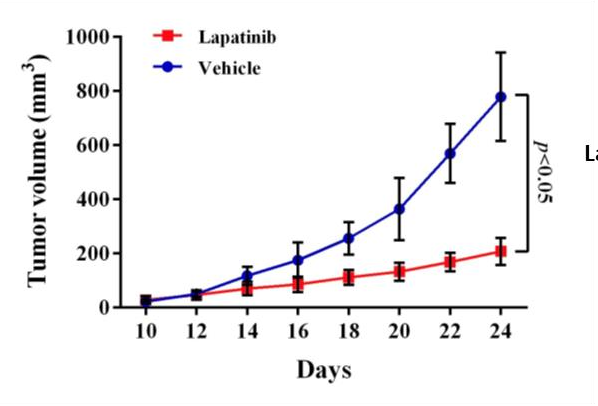
Lapatinib
Vehicle
Tumor volume (mm3)
1000
800
600
400
200
0
10
12
14
16
18
20
22
24
Days
p<0.05

B

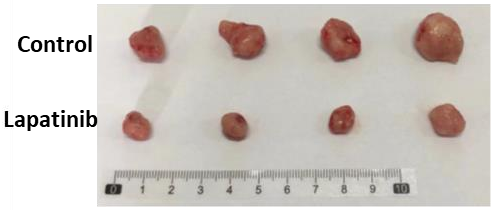
Control
Lapatinib

C

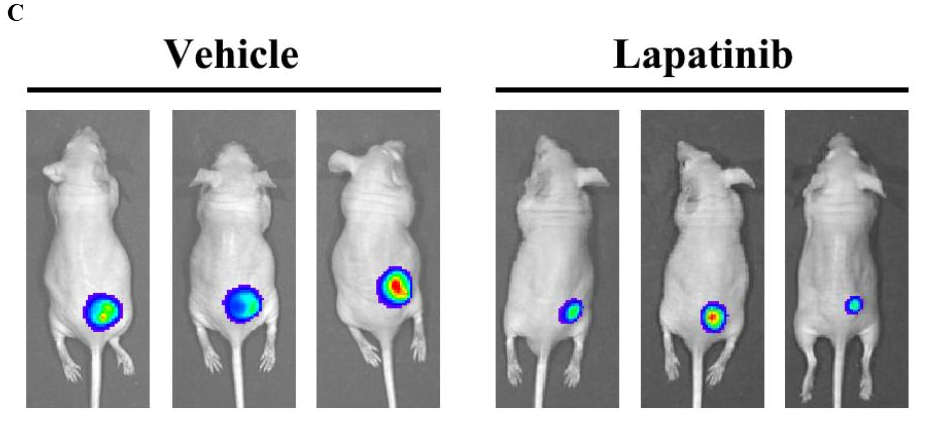
Vehicle
Lapatinib

D

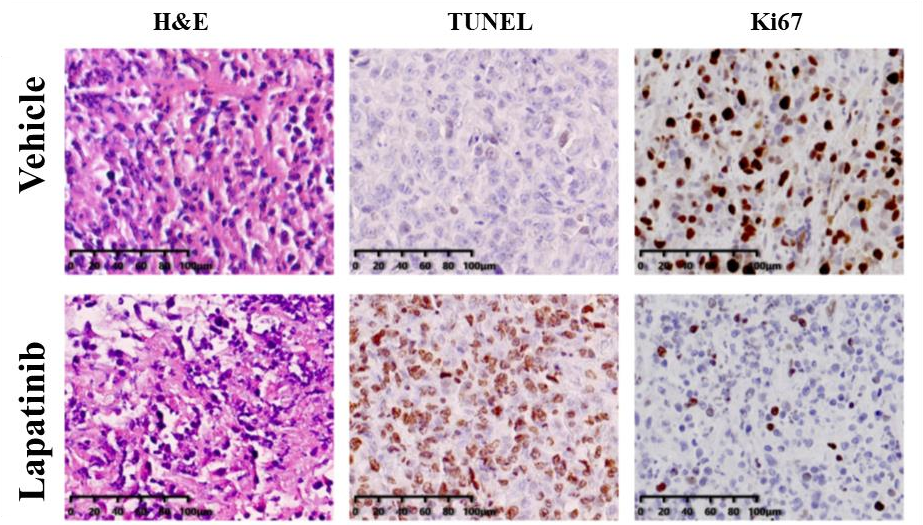
H&E
TUNEL
Ki67
Vehicle
Lapatinib

Figure 8. Lapatinib inhibited tumour growth in UM xenografted mice. BALB/c nude mice were inoculated with C918 cells. After 14 d, mice received either lapatinib (25 mg/kg per day, n = 10) or vehicle (n = 12) on day 10 by intraperitoneal injection; treatments were continued for a further 14 d. Tumour volumes and body weight of mice were measured every 2 d. At the end of the experiment, mice were either sacrificed to harvest tumour samples or were subjected to whole body PET scan (n = 5 for lapatinib and 6 for vehicle). Tumour size vs treatment time is indicated in (A) and representative tumour images at the end of experiment are shown in (B). Data are presented as tumour volumes at each time point (mean ± SD; n = 5 for lapatinib and 6 for vehicle); $p < 0.05$ vs. control by unpaired t-test. Representative PET scans are shown in (C). Harvested tumours were embedded in paraffin and sections were prepared for staining. Representative images of hematoxylin and eosin (H&E) staining of tumour sections are shown in the panels at left, TUNEL staining is indicated in the central panels and Ki67 staining is shown in the right panels (D).

2.4 Discussion

ErbB receptors regulate cellular homeostasis. Dysregulation of the receptors leads to impairment of proliferative and pro-survival mechanisms in cells and may contribute to disease progression (151-153). Intracellular signalling cascades downstream from ErbB receptors are regulated by phosphorylation events that are mediated by kinase intermediates. The development of small molecule inhibitors of ErbB receptor-linked kinases has revolutionised the treatment of a number of cancers (154). The ErbB receptor member EGFR was initially suggested to be a potential drug target in UM. However, EGFR inhibitors like gefitinib have been disappointing in clinical trials that have been conducted in UM patients (48, 63, 132, 155). Despite these outcomes, small molecules that target other members of the ErbB family have not been widely considered as alternative agents for use in patients with UM.

We found previously that the EGFR, HER2 and HER4 inhibitor afatinib, was an effective anti-cancer and anti-metastatic agent in UM (84). EGFR inhibition appears to be of limited value in UM (84, 133, 156). None of the UM cell lines included in the previous and current study express

EGFR; and two of the four UM cell lines do not express HER4 (84). Therefore, these receptors are unlikely to be the primary targets for afatinib. In contrast, HER2 is expressed in UM tumours as well as the four UM cell lines included in this study (Fig. 7 and Suppl. Fig. 2) (84, 149, 157). Moreover, we also explored the Cancer Genome Atlas Program (TCGA) database (https://portal.gdc.cancer.gov/). In a cohort of 80 UM patients, HER2 was expressed in all tumour samples and its expression was significantly higher than EGFR and HER4 ($p<0.001$) (Suppl Fig. 3). Thus, it is now appropriate to evaluate in greater detail the potential clinical value of HER2 targeting in the treatment of UM.

Lapatinib is a high affinity HER2 inhibitor (Table 1) (158), and is currently approved in combination with cytotoxic agents such as capecitabine for HER2-positive breast cancers (159-161). Lapatinib is a reversible inhibitor of the kinase binding site of HER2, and blocks downstream proliferative and pro-survival signalling (159). Lapatinib has advantages of receptor targeting specificity over afatinib. Afatinib is 28-fold more potent against EGFR than HER2, and is also effective against common mutant EGFRs, whereas the relative activity of lapatinib against HER2 is greater (Table 1) (162). Thus, off-target effects at EGFR in multiple tissues are expected to be less likely with lapatinib. The previous studies have demonstrated the cytotoxic effect of lapatinib in melanoma cell lines (163, 164), but its influence on UM cell lines remains unclear. In the present study, we investigated the anti-cancer and anti-metastatic actions of lapatinib in a range of UM models for the first time. Lapatinib decreased UM cell viability by inhibiting cell proliferation and by promoting apoptosis and cell cycle arrest. Lapatinib also decreased tumorigenesis *in vivo* in mice that carried UM cell xenografts. Afatinib and lapatinib have different efficacies against other cancer types (165). Compared to afatinib (84), lapatinib was more effective in inhibiting UM cell migration and reproductive cell growth, which suggests that it may have utility in the suppression of UM metastasis. In contrast, afatinib was slightly more effective in the induction of cell apoptosis and cell cycle arrest (Table 1). Taken together, these findings suggest that afatinib may be considered for the treatment of primary UM tumours. And lapatinib may be used as an adjuvant therapy in the prevention of UM metastasis following the non-pharmacological treatment of primary UM tumours or be applied to UM patients together with agents like tebentafusp (an FDA approved immunotherapeutic drug of UM) in the future.

Table 1. The comparison of the anti-UM effects of afatinib and lapatinib

		Afatinib	Lapatinib
Molecular target		Irreversible inhibitor of EGFR, HER2 and HER4 (162)	Reversible inhibitor of EGFR and HER2 (158)
IC_{50} in inhibiting HER2 (nM)		14 (162)	9.2 (158)
IC_{50} in reducing cell viability in UM cell lines (μM)	Mel202	5.29 ± 1.21 (84)	5.69 ± 1.21
	92.1	4.52 ± 1.41 (84)	4.89 ± 0.71
	C918	3.43 ± 0.82 (84)	6.53 ± 1.30
	OMM-1	4.47 ± 1.16 (84)	3.67 ± 0.58
Cell death mechanism in UM cell lines (5 μM treatment for 18 and 24 h, respectively)		Apoptosis (5.79-10.20-fold of control) (84)	Apoptosis (2.73-6.40-fold of control)
Inhibition of UM cell migration (5 μM treatment for 24 h)		0.23–0.73-fold of control (84)	0.26–0.36-fold of control
Inhibition of UM reproductive cell growth (5 μM inhibitor for 24 h)		0.02–0.29-fold of control (84)	0.01–0.04-fold of control
UM cell cycle arrest (5 μM treatment for 18 and 24 h, respectively)	G0/G1	1.33–1.53-fold of control (84)	1.19–1.75-fold of control
	G2/M	0.34–0.46-fold of control (84)	0.26–0.74-fold of control
Tumour growth inhibition in xenograft model		0.30-fold of control group (15 mg/kg per day for 16 days) (84)	0.23-fold of control (25 mg/kg per day for 14 days)

HER2 is not activated by ligand binding but is instead a signal transducer that heterodimerises with other ErbB receptors that are ligand activated (84, 166). Because EGFR was not detected in

any of the four UM cell lines tested in this study (84), and HER4 is only expressed in two of the four cell lines (data not shown), these receptors are unlikely to be required for the anti-UM activity of lapatinib or afatinib.

HER2 is an important driver of tumorigenesis in several cancers, including HER2-positive breast cancers where its expression is amplified (167). HER2 overexpression or activation in breast cancer is often accompanied by poor prognosis due to more aggressive and invasive behaviour (168, 169). HER2 expression was inversely correlated with outcomes from breast cancer treatment (170-172). HER2 activation is also associated with increased tumour size and invasiveness (173, 174). In a large study (n=1,012), ~37% of patients with HER2 positive breast cancer reportedly had brain metastases (175).

HER2 is linked to the activation of multiple downstream signalling pathways that regulate tumorigenesis, including STAT1-regulated cascades (176-178). STAT1 regulates an array of complex cellular processes, notably in tumour cells and in the immune system, as an anti-proliferative and pro-apoptotic gene (179). STAT1 regulates cell cycle progression and the inhibition of HER2 was found to increase STAT1 expression and promote cell cycle arrest by downregulation of cyclin D1 (176, 180) which suppresses tumorigenesis (181, 182). STAT1 physically interacts with cyclin D and forms a complex with G_1 CDK to mediate IFN-γ-dependent G_1 cell cycle arrest (176). STAT1 also regulates the transcription of Bcl-2 genes that modulate apoptosis. Thus, the activation of STAT1 upregulates pro-apoptotic BAX and downregulates the anti-apoptotic Bcl-2 and Bcl-XL (183). In the present study, lapatinib promoted cell cycle arrest and apoptosis by decreasing the expression of cyclin D1 and the anti-apoptotic Bcl-XL.

HER2 also regulates the AKT, ERK and PI3K-linked signalling pathways that modulate cell proliferation, migration, and death (184) and that contribute to tumorigenesis in multiple cancer types (56, 185). The overarching consensus is that the activation of HER2-AKT/ERK/PI3K cascades increases cell proliferation, survival and migration (186-188). The present findings that lapatinib impairs PI3K, Akt and ERK signalling downstream from HER2 are consistent with its antiproliferative and antimigratory actions in UM cells.

Lapatinib has additional advantages that could facilitate its clinical translation. The anti-cancer activity of lapatinib due to HER2 inhibition has been established in studies of HER2-positive

breast cancer, including advanced metastatic disease (189-191). Lapatinib is currently administered orally in a once daily dosage regimen (dose range 100 to 1,500 mg per day) and produces C_{min} values in the range 0.29–0.77 μM and C_{max} values in the range 0.70–5.63 μM (192, 193). These plasma concentrations likely fall within the range of those required for effective anti-UM activity (Fig. 1). Lapatinib also crosses the blood brain barrier, because it has been shown that brain metastases were decreased to 50%-53% of control in xenografted mice with metastatic breast cancer (189). Noteworthy, lapatinib is also under clinical investigations for several other solid tumours with high EGFR and/or HER2 expression (194).

The present study found that lapatinib decreased tumour cell migration, invasion and reproductive growth, which suggests that the drug may be developed as an adjuvant therapy in the prevention of UM metastases. The finding that the anti-cancer actions of lapatinib are consistent with inhibition of HER2 and its downstream targets supports the potential utility of lapatinib in UM (Fig. 9). And this finding is aligned with the report of Ma *et al*. that UM patients with higher risk and lower overall survival rates are more susceptible to drugs including lapartinib (195). Clinical trials to test this directly in UM patients may now be warranted.

It has been recognised that the usual systemic administration route may not be optimally effective in delivering lapatinib to UM patients. However, with the development of drug delivery technology, novel drug carriers may be used to facilitate the localised delivery of agents. For example, nanoparticles can enhance drug permeability, increase stability and control release rate; these are ideal carriers for targeted drug delivery. Specific nanoparticles, including albumin, chitosan and other natural polymer nanoparticles, have been shown to effectively penetrate the eye allowing for improved ocular drug delivery (196). Future studies are warranted to investigate the suitability of this drug delivery route for lapatinib in the treatment of UM; however, this is beyond the scope of the current study.

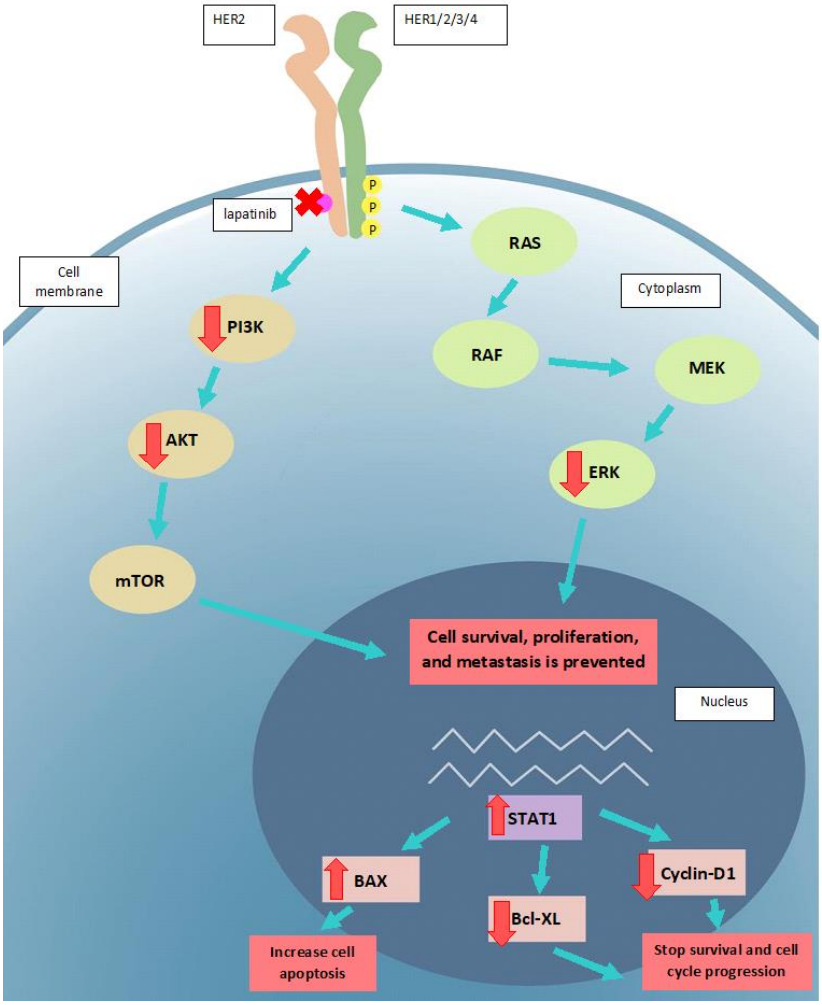

Figure 9. The proposed mode of action of lapatinib in UM cell lines. Lapatinib inhibits HER2 and its downstream signalling along PI3K/AKT and Ras/MEK/ERK pathways. UM apoptosis is activated by upregulation of BAX and STAT1 as well as a downregulation of Bcl-XL and cyclin D1.

Key: intracellular p, phosphorylated residues in receptors; AKT: Protein kinase B; BAX: Bcl-2-associated X Protein; Bcl-XL: B-cell lymphoma-extra-large; ERK: extracellular-signal-regulated kinase; MEK: Mitogen-activated protein kinase kinase; mTOR: mammalian target of rapamycin; RAS: RAS viral oncogene homolog; PI3K: Phosphatidylinositol 3-Kinase; RAF: rapidly activated fibrosarcoma; STAT1, signal transducer and activator of transcription-1.

This principal findings from the present study are that lapatinib is a potential candidate for the treatment of UM, based on its anti-cancer and anti-metastatic activities in in vitro, ex vivo and in vivo models. Importantly, the present study supports the assertion that HER2 is a promising therapeutic target in UM. Taken together, lapatinib is a model HER2 inhibitor that is already approved for the treatment of HER2-positive breast cancer that could now be evaluated further in clinical trials in UM patients.

Chapter 3: The Role of Autophagy in Human Uveal Melanoma and the Development of Potential Disease Biomarkers and Novel Therapeutic Paradigms

Abstract

Autophagy is a form of programmed cell degradation that enables the maintenance of homeostasis in response to extracellular stress stimuli. Autophagy is primarily activated by starvation and mediates the degradation, removal or recycling of cell cytoplasm, organelles and intracellular components in eukaryotic cells. Autophagy is also involved in the pathogenesis of human diseases, including a number of cancers. Human uveal melanoma (UM) is the primary intraocular malignancy in adults and has an extremely poor prognosis; at present there are no effective therapies. Several studies have suggested that autophagy is important in UM. By understanding the mechanisms of activation of autophagy in UM it may be possible to develop biomarkers to provide more definitive disease prognoses and to identify potential drug targets for the development of new therapeutic strategies. This article reviews the current information regarding autophagy in UM that could facilitate biomarker and drug development.

3.1 Introduction

Cellular homeostasis is controlled in part by the balance between protein synthesis and degradation. The regulation of protein turnover is achieved through mechanisms that sense environmental changes to activate protein synthesis or degradation (197). Autophagy regulates the degradation, removal and recycling of intracellular components of the cytoplasm and other organelles (198). There are three defined forms of autophagy: macroautophagy, microautophagy and chaperone-mediated autophagy (CMA). Macroautophagy is the process in which cytoplasmic cargo is delivered to lysosomes through double membrane-bound vesicles known as autophagosomes. Vesicles fuse with the lysosome where enzymic protein degradation occurs. In contrast, microautophagy is the process in which lysosomes take up cytoplasmic components

directly through invagination of the lysosomal membrane. CMA is a secondary response to starvation and, unlike the aforementioned processes, directly involves the translocation of unwanted proteins to the lysosome under the control of chaperone proteins such as Hsc-70 (198, 199). In most cases macroautophagy is the primary means by which cytoplasm-to-lysosome delivery occurs; therefore, macroautophagy is more commonly referred to as 'autophagy.'

The autophagic program of cell degradation was initially thought to be a response to stimuli like starvation to allow for recycling and regeneration of cellular macromolecules. However, recent studies have shown that autophagy has a significant role in the maintenance of homeostasis, even in non-starved cells (200). As such, autophagy has a greater physiological and pathological role in higher eukaryotic cells, including the regulation of cell death, the elimination of microorganisms, the control of intracellular protein and organelle turnover, adaptation to starvation and ageing and tumour suppression (201, 202). Additionally, autophagy modulates innate and adaptive inflammatory responses, antigen presentation, and pathogen clearance (203). Age-related decreases in autophagic activity have been proposed to contribute to the pathogenesis of ageing diseases (204). Taken together, autophagy plays a vital role in cell homeostasis, and the dysregulation of autophagy is a feature of numerous diseases.

Human uveal melanoma (UM) arises primarily from melanocytes of the iris (accounts for ~6% of UM cases), ciliary body (~4% of UM cases) and choroid of the eye (~90% of UM cases) (205). The symptoms of UM mainly include blurred or distorted vision and visual field loss or photopsia. However, patients may also be asymptomatic resulting in delayed diagnosis and treatment. Furthermore, there is often a delay in treatment as multiple referrals may be required before a diagnosis can be made (206).

UM consists of ~5% of all cases of melanoma and has an incidence that varies across different regions, ranging from ~1 to 9 per million population per year. UM primarily impacts Caucasians, which aligns with the risk factors of fair skin, light-coloured eyes and certain hereditary conditions such as the BAP1-tumour predisposition syndrome. Additionally, most UM patients are between the age of 50 and 70 years, and the incidence in adolescents is very low (<1%) (103, 207, 208). The incidence of UM is increased at higher latitudes (209).

While relatively rare, UM is lethal and has a high mortality rate, of ~30% at 5 years and ~45% at 15 years (210). Moreover, UM has a high metastatic rate of ~50%, with the liver being the most

common target organ; in metastatic disease the median survival is ~4–5 months with a 1-year survival rate of 10–15% (205).

The high mortality rate in UM patients is primarily due to a deficiency of information regarding its pathogenesis and the absence of effective treatments (48). Current approaches to treat primary UM mainly include enucleation and conservative treatments such as brachytherapy and radiotherapy. However, in many cases, tumours may have already metastasised or advanced locally to the point where conservative treatment is no longer effective. At present validated methods to diagnose the early onset of disease are not available (1, 111, 211). Thus, there is an urgent need to develop new prognostic methods and therapeutic approaches in UM. Literature indicates that autophagy is important for developing biomarkers and identifying therapeutic targets in UM. Thus, this review summarises the current information regarding autophagy in UM that may provide insights in its diagnosis and treatment.

3.1.1 Selective and non-selective autophagy

Due to differences in the stimuli for initiation, autophagy is often classified into selective and non-selective autophagy. Non-selective autophagy is essentially a sequestration and bulk degradation system in which cells turn over and intracellular components are recycled (201, 212). Non-selective autophagy is activated in response to starvation to maintain the cellular supply of lipids, amino acids, carbohydrates, and nucleotides. On the other hand, selective autophagy is activated when there is a need to remove or recycle harmful or unwanted cellular components. Thus, autophagy maintains the quality control of organelles and cellular structures, including cytoplasmic aggregates, endoplasmic reticulum, exogenous proteins, lipid droplets, mitochondria, peroxisomes and ribosomes (213).

Although different signals activate the alternate forms of autophagy, selective and non-selective autophagy utilize common machinery (214). The major distinction between non-selective and selective autophagy is the ability to distinguish functional and non-functional organelles or misfolded and correctly folded proteins. The criteria that enable these distinctions to be identified in cells remain largely unknown. However, it has been hypothesised that the cargo itself provides the template that determines the dimensions of the phagophore through specific membrane protein recognition (213-215). This is the “cargo-ligand-receptor-scaffold” model. The

interaction between the receptor and scaffold controls cargo recruitment to the phagophore assembly site, where an autophagosome forms. The cargo-ligand-receptor-scaffold model allows selective autophagy to meet at least three essential criteria that differ from non-selective autophagy: (1) the cargo must be specifically recognized, (2) the cargo must be efficiently transported to a new autophagosome and (3) non-specific material must be excluded from the autophagosome (216). In selective autophagy, the autophagosomes are smaller and are more tightly bound to the cargos.

In yeast, autophagy-related protein (ATG)-11 is the most common scaffold protein that is involved in several types of selective autophagy, e.g., the cytoplasm-to-vacuole targeting pathway, mitophagy (the removal of damaged mitochondria), and pexophagy (the turnover of peroxisomes). However, a functional counterpart of ATG11 is yet to be discovered in mammals. Nevertheless, it is known that in both yeast and mammals, the receptor proteins subsequently bind to ATG8, which is one of the LC3 family proteins, through either the AIM (Atg8-family-interacting motif) or LIR (LC3-interacting region) sequence. AIM and LIR allow for direct binding of cargo to the autophagy machinery (217).

3.1.2 Autophagy pathway

The autophagy pathway can be separated into three main stages: the formation of the phagophore, autophagosome establishment and autolysosome formation/material degradation (Fig. 10) (214). During the first stage, an isolation membrane (or phagophore) is formed using lipids from the endoplasmic reticulum (ER), Golgi apparatus or endosome. The phagophore then elongates and engulfs intracellular components such as protein aggregates, organelles, and ribosomes. Membranes closes and are then fused with lysosomes to form autolysosomes contain the enzymes that degrade autophagic cargos (218).

Autophagy commences with the activation of Unc-51-like kinase 1 (ULK1) and -2 (ULK2) and the formation of complexes with ATG proteins in mammalian cells. For example, ATG9 mediates elongation of the initial sequestering compartment and phagophore formation. The class III PI 3-kinase complex I (PI3KC3-C1) is then activated by ULK1 and phosphorylates phosphatidylinositol (PI) on the endosomal membrane to generate PI-3-monophosphate (PI3P), a key membrane marker for intracellular trafficking and autophagosome formation. Two other

ATG proteins – ATG8 and ATG12 - are the drivers of autophagosome formation (213, 214, 219-221). This process is modulated by the AMP kinase/mammalian target of rapamycin (AMPK/mTOR) pathway that regulates ULK1 (214, 221). Disruption of the autophagy pathway may lead to the development and progression of human diseases, particularly cancers and neurodegenerative diseases (222).

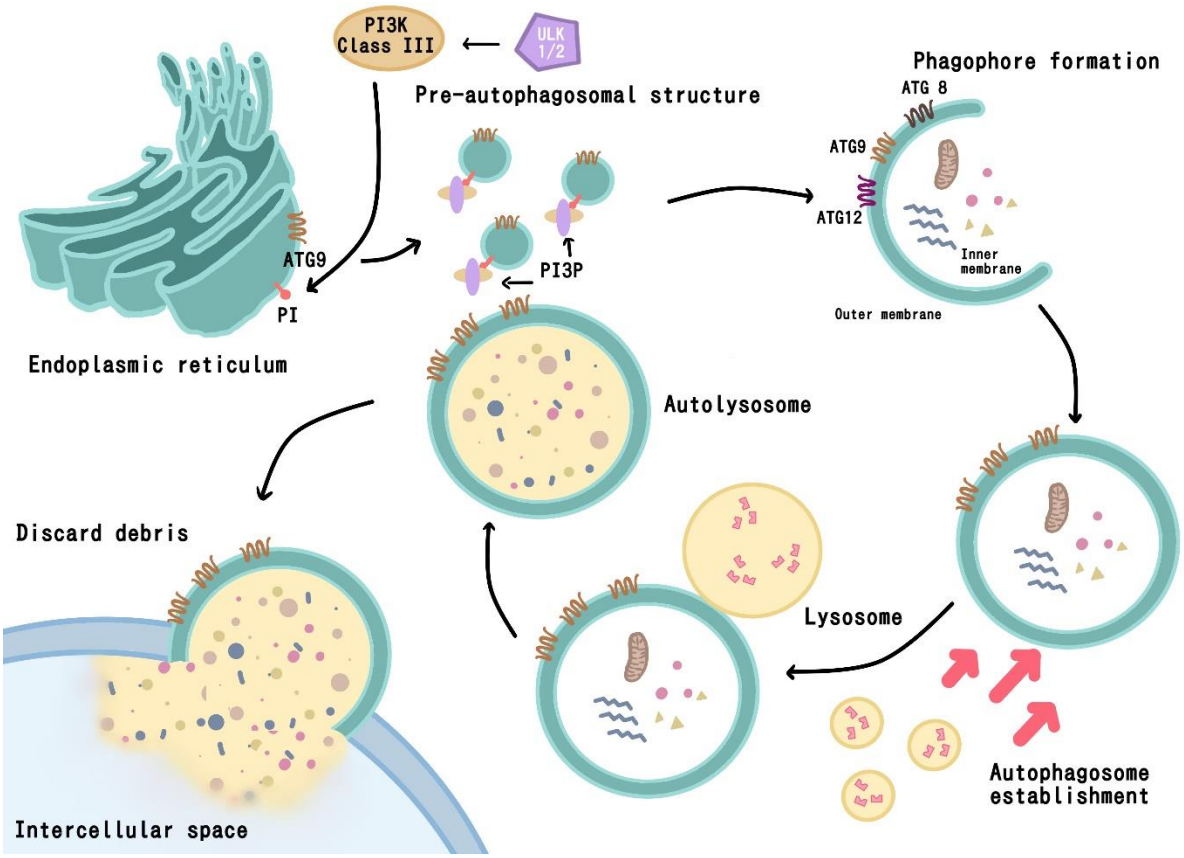

Figure 10. Overview of the autophagy pathway. Unc-51-like kinase 1 (ULK1) and -2 (ULK2) activate autophagy by binding with ATG9, to form pre-autophagosomal structures that separate from the endoplasmic reticulum (shown here), Golgi apparatus, mitochondrion, or recycled endosomes. Pre-autophagosomal structures then assemble to form phagophores that activate ATG12. Lysosomes fuse with an autophagosome to produce an autolysosome so that the enclosed cargo may be lysed and then either recycled or removed.

3.2 Autophagy in human diseases

As a key mechanism in the maintenance of homeostasis, autophagy regulates cellular energy production and macromolecular synthesis through pro-survival pathways. Autophagy is dysregulated in human diseases, including cancer (e.g. prostate, breast, ovarian) and neurodegenerative disease (e.g. Alzheimer's and Parkinson's disease) (223). The evidence that autophagy participates in numerous disease processes underscores its importance as a potential target for disease treatment.

3.2.1 Autophagy in cancers

The role of autophagy in cancer is somewhat controversial. Some studies suggest that autophagy is a pro-tumorigenic mechanism because it enables metabolite recycling and supports tumour metabolism, which increases cancer cell survival. Other studies suggest that autophagy acts as a tumour suppressor that prevents cancer initiation by facilitating the elimination of misfolded or aggregated proteins and damaged organelles (224),

In immortalised mouse kidney cell lines, autophagy is activated in response to long-term starvation, which decreases cell size. This suggests that the clearance of cytosolic proteins and organelles may aid survival under conditions where apoptosis is inhibited (225). Because defects in apoptosis can promote tumorigenesis, the activation of autophagy is required for the removal of defective intracellular molecules that may otherwise promote tumorigenesis (226). The inhibition of autophagy leads to the accumulation of unnecessary cytosolic materials and promotes metabolic stress (227, 228). The BECN1 gene encodes the major autophagic regulator beclin-1 (also known as ATG6), and defective beclin-1 can inactivate autophagy (229). Autophagy may be inactivated either directly - via allelic loss or defective BECN1 or ATG6 - or indirectly - through constitutive activation of the pro-survival phosphatidylinositol 3-kinase (PI3K) pathway (230-232). Bhutia *et al.* found that autophagy was attenuated by oncogenic mutations during tumour initiation (20). Importantly, the BECN1 gene is deleted in around 50% of breast, ovarian and prostate cancer cases (233, 234). Bax-interacting factor-1 (Bif-1) has a role in membrane dynamics and is another important gene that modulates apoptosis and autophagy. Bif-1 production is decreased in gastric and prostate cancer and Bif-1 null mice show increased

susceptibility to tumorigenesis (235). These findings are consistent with an anti-cancer role for autophagy.

On the other hand, there is also evidence that autophagy is pro-tumorigenic. Because autophagy maintains access to nutrients and removes unwanted cellular material, this can increase the resilience of the tumour cell to metabolic stress, such as hypoxia (226, 236). Furthermore, autophagy allows tumour cells to self-digest during prolonged stress, which prevents cell division and promotes dormancy (226). Such cells retain the capacity to resume growth and tumorigenic activity once conditions have normalized (224). In support of this contention, Degenhardt *et al*. (226) reported that the inhibition of autophagy in cells in which apoptosis is defective, promoted tumour cell death, suggesting that autophagy may disrupt tumour suppression. Finally, deletion of the autophagy regulator FIP200 gave rise to multiple defects in autophagy leading to tumour suppression in the MMTV-PyMT mouse model of breast cancer. Gene expression profile of the tumours in mice determined that loss of FIP200 had no effect on apoptosis within the tumour site but increased immune responses through genome-wide alteration of genes encoding proteins involved in response to Type I interferons (IFN) stimulation and other immune responses such as immune cell infiltration and cytokine production and facilitated the removal of malignant cells (237).

Although it remains unclear why autophagy exhibits different actions at different stages of cancers, this information may have prognostic value. For example, different autophagy-related genes (ARGs) have recently been found to correlate with patient survival profile and may be further developed as tumour biomarkers in breast, glioblastoma, and colon cancer (238). The role of calcium in tumour prognostics has also been explored with the focus on autophagy. As BAP1 along with other tumour suppressors regulate calcium release from the ER to drive cell death. Truncating mutations in the tumour suppressor gene BAP1 increased susceptibility to developing malignant pleural mesothelioma (MM). Findings show BAP1 mutations resulted in downregulation of calcium dynamics and as autophagy is regulated by these cellular processes, it is hypothesised BAP1and autophagy may be a regulator of MM development (239, 240). Mutations within oncogenes such as the splicing-factor-3B-subunit-1 (SF3B1) has been studied as a novel treatment target associated with autophagy. Fuentes-Fayos *et al.* demonstrated inhibition of SF3B1 bring about significant alterations within the AKT-mTOR and ß-catenin

signalling pathways which is closely associated with glioblastoma (GBM) progression and initiation while also having direct involvements with autophagy regulations suggestive of changes in SF3B1 can influence GBM through autophagic pathways (241, 242). Autophagic processes has also been widely explored in other melanomas such as cutaneous melanoma (CM). Being the most common type of melanoma, connection between autophagy and CM has comprehensively examined. Although the precise function and effect of autophagy in CM remains controversial with reports of it being both tumorigenic and tumour suppressive (243), further studies have indicated one of the most common mutations occurring in CM – the $BRAF^{V600E}$ mutation is closely related to inhibition of autophagic cell death through transcription factor EB (TFEB). Li et al. demonstrated BRAFi induced autophagy through activation of TFEB via ERK signalling pathway inhibition (244). Furthermore, a key autophagy regulator, AMPK, is inhibited by $BRAF^{V600E}$ activity hereby promoting melanoma cells proliferation (245). Herewith, demonstrating the diversity of autophagy in different cancers.

Autophagic mediators are potential targets for cancer prognosis and the development of new therapeutics in common cancers, but little is known about their role in rare cancers. Human UM is a rare cancer and several studies have explored the potential of ARGs as prognostic biomarkers in UM.

3.3 Autophagy in uveal melanoma

3.3.1 Current treatments affecting autophagy in UM

Although autophagy has been extensively studied in various cancers. Being a rare cancer, the concept of autophagy largely remains unexplored in UM. UM is characterised by genetic mutations to the paralogous guanine nucleotide-binding protein Gq subunits alpha and alpha-11 (GNAQ and GNA11, respectively) which are observed in 80-90% of tumours (11, 246). However, despite the high incidence of GNAQ/GNA11 mutations, overall UM has a relatively low mutational burden so that targeted treatments based on genetic driver mutations have been difficult to identify (247). Recent studies have suggested that GNAQ/GNA11 and autophagic pathways may be linked. Ambrosini *et al.* demonstrated that signalling by mutant GNAQ/GNA11 was impaired by the MEK inhibitor selumetinib and the AKT inhibitor MK2206.

AKT and MEK are different signalling pathways that converge at GNAQ/GNA11. Therefore, when inhibitors of these two pathways are used together, there is a synergistic increase in autophagic cell death through activation of AMPK (55). Furthermore, the combination inhibited tumour growth in xenograft mouse models (55) . These effects were genotype dependent because the autophagic markers beclin1 and LC3 were induced in GNAQ-mutant cells, whereas apoptotic cell death was activated in BRAF-mutant cells, and cells without either mutation underwent cell-cycle arrest (55). Similar findings were noted with the MAPK inhibitor trametinib in combination with the autophagy and lysosomal inhibitor, chloroquine (248). These apparent links between GNAQ/GNA11-driver mutations and autophagy now warrant further research to identify potential new treatments in UM.

In PDX isolates of UM, neratinib caused the internalization and degradation of GNAQ and GNA11 that was enhanced by the histone deacetylase inhibitor entinostat (249). Down-regulation of GNAQ and GNA11 required Beclin1 and ATG5 (249). The combination of neratinib and entinostat engaged multiple pathways to mediate killing, including ROS-dependent activation of the ATM kinase via the AMPK-ULK1-ATG13-Beclin1/ATG5 axis (249). Knock down of ATM, AMPK or ULK-1 prevented ATG13 phosphorylation and the degradation of RAS and Galpha subunits (249). Over-expression of activated mTOR prevented ATG13 phosphorylation and suppressed killing (249). Thus, neratinib and entinostat down-regulates oncogenic RAS and the oncogenic drivers present in most UM tumours and promotes autophagic cell death (249). Indeed, targeting dysregulated AMPK-linked cascades may represent a new strategy in UM treatment. Thus, metformin - an adenosine monophosphate-activated kinase (AMPK) activator – inhibited the proliferation and migration of ocular melanoma cells both in vitro and in vivo and attenuated autophagic influx (250). It would be of potential interest to pursue these observations and assess whether they may be new treatment modalities in UM.

Natural compounds have is also in the spotlight as potential treatment options for UM. The compound (−)-4-O-(4-O-β-D-glucopyranosylcaffeoyl) quinic acid (QA) derived from the endophytic fungus *Penicillium* sp.FJ-1 of *Avicennia marina* has its effects explored on UM. Treatment with QA demonstrated potent anti-proliferative effects in a concentration dependant manner. Cell autophagy was induced through up regulating mRNA expression of Beclin-1 and down regulation in LC-3, P62and PI3K signalling pathway. This effect was further analysed on

in vivo xenograft mouse models where QA not only decreased tumour volume compared to vehicle but also increased pro-apoptotic protein expression causing overall cell death (251).

Nonetheless, the conflicting nature of autophagy on tumour progression, survival and suppression is also present in UM. The protective effect of autophagy was elucidated in UM through Annexin A2 receptor (AXIIR). Zhang et al. validated the dual effect of AXIIR in UM. Although overexpression of AXIIR through plasmid transfection resulted in overall decrease in cell viability through apoptosis, this effect was reduced with the activation of autophagy. The use of autophagy inhibitor on AXIIR overexpressed cells resulted in a greater apoptotic death suggesting autophagy to resume a cellular protective role (252). Similarly, novel drug therapy study using the autophagy inhibitor elaiophylin resulted in induced cell death in UM cell lines C918, OCM-1A and Mel270 but not healthy retinal cell line ARPE-19. Treatment with elaiophylin generated oxidative stress and mitochondrial dysfunction while causing the inhibition of mitochondria autophagy. The resulting oxidative stress caused subsequent accumulation of defective mitochondria and ultimately cell death. The treatment result further translated into *in vivo* xenograft mouse models where treatment with elaiophylin caused reduction in tumour size compared to control as well as displayed an increase in apoptotic TUNEL positive cell indicative of apoptosis (97). Previous studies have linked autophagy with the resistance of tumours to chemotherapy (253). The selamectin and cisplatin combination showed a synergistic effect in inhibiting UM cell growth and in tumour-bearing nude mice *in vivo* (253). Selamectin inhibited the expression of ATG9B, thus decreasing autophagy (253). The cisplatin resistance-associated genes PDGFRB, DUSP1, MAST1 and IL11 were also downregulated in UM cells treated with selamectin (253). These findings provide counter arguments for autophagy in UM. Admittingly autophagy in UM remains disputed, therefore new definitive markers for prognosis and treatment is in need to aid in patient survival. Below this review will examine the novel findings for UM biomarkers.

3.3.2 Protein based UM autophagy biomarkers

There is an urgent need for new prognostic approaches in UM for potential diagnostic and prognostic tool that also serve as treatment markers. Protein mutations as exampled in table 1 are apparent in majority of cancers including UM and can serve as both diagnostic tool as well as

target for novel drug therapies. Ealy intervention could prohibit the development of metastatic disease and improve survival rates.

A promising autophagy-related biomarker is Beclin-1, which is encoded by the BECN1 gene on chromosome 17q21 (Table 1). BECN1 is essential for autophagosome formation because it facilitates the recruitment of other ATG proteins. Deletion of BECN1 has been reported in human breast, ovarian and prostatic cancer cell lines and BECN1+/− mutant mice exhibit a high incidence of spontaneous tumours, which implies a tumour suppressor function for autophagy (254). In UM BECN expression is associated with a lower risk of metastasis and an increase in disease-free survival (254). Giatromanolaki *et al.* explored the potential role of BECN1 as a prognostic marker in cohort of 99 UM tumours following enucleation. Survival analysis showed that both under- and over-expression of BECN1 was associated with metastasis and poor disease survival. However, under-expression of BECN1 was related to a slower rate of initial metastasis rate than with overexpression of BECN1 (255). At present the role of beclin-1 in cancer is not completely clear but it remains a potential biomarker in UM.

The BCL2 19 kD protein-interacting protein 3 (BNIP3) has been assessed as a potential prognostic biomarker for UM (Table 1). BNIP3 is a BH3 containing protein from the BCL-1 family that modulates cell death, autophagy and cytoprotection. BNIP3 possess the BH3 domain (Bcl-2 homology) that is common to both pro- and anti-apoptotic bcl-2 family proteins. However, unlike other Bcl-2 proteins, BNIP3 interacts directly with other BCL-2 family members via its C-terminal transmembrane domain rather than the BH3, which underlies its dual effects on cell survival (256). Apart from activation of apoptotic pathways through Bcl-2, upregulation of BNIP3 also induces mitochondrial depolarisation and autophagy (257). Studies in breast cancer and malignant glioma have reported that increased BNIP3 decreased metastasis and improved outcomes (258, 259). However, conflicting reports in salivary adenoid cystic carcinoma and non-small cell lung cancer have also appeared (260, 261). In these tumours increased BNIP3 led to poor prognosis and decreased metastatic free survival. Similar findings were made in the cohort study of Jiang *et al.* who found that high expression of BNIP3 was associated with hyper-pigmentation, deeper scleral invasion and a poor prognosis in UM (262). BNIP3 detection could help stratify high-risk patients and identify new therapies targeting BNIP3 as a promising approach to treat UM (262).

Autophagy is also modulated by the PI3K/AKT/mTOR, p53, MAPK and NFκB signalling pathways (Table 1) (263-265). Protein tyrosine kinase 6 (PTK6) is an mTOR regulator and promotes breast, colorectal and lung tumorigenesis by activating multiple signalling pathways (266-268). Although PTK6 has been explored in other cancers its involvement in UM is yet to be fully investigated. However, Liu *et al.* reported that increased PTK6 expression in UM cells was associated with a poor prognosis (269). Increased PTK6 activates mTOR and inhibits autophagy which increases tumorigenesis by promoting the proliferation, migration, and invasion of UM cells and inhibiting autophagy (269). PTK6 binds to SOCS3 in UM cells so that targeting the SOCS3-PTK6 signalling axis might be a novel and promising therapeutic strategy for patients with UM (269). Mutations in the BRAF gene are common in cutaneous melanoma but not in UM (270). However, from gene profiling studies this mutation was detected in some cell lines (271-273). Indeed, in BRAF V600E mutant UM cells vemurafenib produced cell death by inhibiting BRAF and mTOR (274). Thus, the mTOR-linked signalling pathway is implicated in UM survival.

Table 2. Summary of key genes/proteins as potential late biomarkers for autophagy.

Gene/protein	Physiological role(s)	Clinical advantage/disadvantages	Reference
BECN1/Beclin-1	- Important in formation of autophagosomes	- A key component of autophagy, a promising prognostic factor - Inconclusive role in tumorigenesis	(254, 255)
BCL2 19 kD protein-interacting protein 3 (BNIP3)	- A BCL-1 family member - Modulates cell death, mitochondrial depolarisation and autophagy	- may enhance tumour killing effect - Hard to be therapeutic target as many Bcl-1 family proteins with similar functions	(256-258, 260, 262)

Mammalian target of rapamycin (mTOR)	- Important for cell survival and cell death	- Well studied with detailed and readily available pathways and pharmacotherapy - May have off-target effects due to versatility	(263-265, 269, 270, 274)

3.3.3 Gene based UM biomarkers

With advancement in technology, patient-based tumour gene sequencing and related therapies have become more mainstream. Early identification of genetic mutation and variation can serve as prognostic and treatment tool to aid in patient recovery and minimise metastasis.

ARGs have been evaluated increasingly as potential cancer biomarkers (226, 228, 229, 236). In recent years, several ATG genes have been identified as potential biomarkers for use in cancers such as breast cancer, colon cancer and glioblastoma (275-277). ATG genes and other ARGs could also be developed as UM biomarkers. Recently, Zheng *et al.* identified a robust 9-ARG signature that was prognostic of survival in a cohort of 230 patients with UM (278). The Cancer Genome Atlas (TCGA) UM cohort was used as a training set to identify the signature that was then validated using four other cohorts of 150 UM patients (278). The 9-ARG signature was distinctively enriched in high-risk UM patients and was associated with several cancer hallmarks, including angiogenesis, IL6-JAK-STAT3 signalling, reactive oxygen species production and oxidative phosphorylation, as well as immune-related functional pathways and immune cell infiltration (278). Moreover, the ARG signature seemed to distinguish between low- and high-risk UMs (278). Although the small sample size in the investigation highlights the need for caution, ARG analysis could well be a promising new approach for further evaluation in UM.

Autophagy-associated long non-coding RNA (lncRNA) may also be potential prognostic indicators in UM (Table 2). lncRNA are RNAs of 200 nucleotides or longer that do not encode protein and that were previously considered to be transcriptional noise (279). However, lncRNA may be important in cellular development, including epigenetics, chromatin remodelling and genetic imprinting (280, 281). Dysregulation of lncRNA is associated with tumorigenesis (282-284). Multiple lncRNA are linked to epigenetic and genomic modifications, and are both tumour

suppressors and oncogenes (285). Detailed analyses, such as that performed by Li *et al.*, have demonstrated that induction of the lncRNA ZNNT1 by rapamycin upregulated ATG12 expression in UM cells and inhibited tumorigenesis by activating autophagic cell death (286). Specific lncRNA might be developed as biomarkers and treatment targets of UM (287, 288). Another novel discovery of LnRNA is LINC01278. This gene is closely related to autophagic genes in UM and acts as a double-edged sword where it can promote tumour metastasis, on the other hand, LINC01278 inhibited the progression cancer progression through MiRNA activation. Liu et al. discovered the inhibitory effects of LINC01278 on UM. resulting data proposed LINC01278 to have inhibitory effects on UM where overexpression caused decrease in proliferation, migration, and invasion levels of UM cell line OCM-1 and MUM-2B. This was done through activating the autophagic pathway with P62 up regulation and decreasing LC3 II/LC3 ratio along with mTOR signalling pathway. This finding was also translated onto xenograft mouse models where upregulation of LINC01278 reduced the volume and weight of tumour compared to control. With these as the basis, more research into the insight of the function and use of LnRNA is encouraged to uncover potential diagnostics and treatment options for UM (289).

Like the lncRNA, micro-RNA (miRNA) may be potential UM biomarkers and anti-cancer drug targets (Table 2). miRNAs are single non-coding strands of 21-23 nucleotides that modulate gene expression by regulating mRNA decay or translation inhibition/activation (290). An individual miRNA can target multiple genes – a property that may be advantageous in the development of new anti-cancer therapies (291). Targeting miRNA has been evaluated in gastric cancer, hepatocellular carcinoma, lung cancer and oesophageal cancer (292-295). Multiple miRNAs appear to be dysregulated in UM (296-298). Certain miRNAs are potential prognostic markers for UM and clustering tumours according to miRNA expression appears to correlate with metastatic risk (299, 300). Wu *et al.* found using cell and mouse models that overexpression of miRNA miR-608 down-regulated the tumour promoting gene HOXC4, that was attenuated by overexpression of metastasis-associated lung adenocarcinoma transcript 1 (MALAT1), which is implicated in cancer as a pivotal regulator of pro-tumorigenic signalling (301). Knockdown of HOXC4 suppressed UM cell migration, proliferation, invasion and cell cycle progression (81). Targeting MALAT1 may be a viable approach in the development of new UM treatments.

MALAT1 was upregulated in UM tissues and its knockdown has been found to suppress UM cell proliferation, colony information, invasion and migration (302).

Drug treatments that modulate miRNA expression have also been explored to some extent and exhibit promising activity. Sun *et al.* evaluated the flavonoid genistein in UM. Inhibition of UM cell growth by genistein was time- and dose-related (303). In *in vivo* studies genistein inhibited xenograft growth (303). Genistein modulated miR-27a expression and, in turn, the Zinc Finger And BTB Domain Containing 10 gene that regulates RNA polymerase related DNA transcription (303). Further study is now warranted to evaluate other miRNAs in UM progression, and whether they may be targeted for therapeutic purposes.

Genetic profiling with the ever-expanding patient database is becoming the frontiers of cancer research. correlation between genetic mutations and patient prognosis has been utilised in many cancers, however, this area of study is still generally lacking in UM (table 2). With increased UM patient data, this field of research will provide imperative information to the diagnostics and treatment paradigm of UM. By using the TCGA-UVM gene database then validating it with gene expression database (GSE84976, GSE 22138) Liu et al. was able to successfully correlate autophagy and immune related genes to reveal four novel genes: PRKCD, MPL, EREG, and JAG2 in UM that has been correlated with prognosis in other malignancies (304). The risk scores generated for the four genes are closely related to chromosome 3 status and was an accurate interpretation of patient prognosis when used in the three patient databases. Further correlation identified immune changes such as fraction of CD4, CD8, regulatory T cell and NK cell activation, monocytes, macrophages M1, and mast cells in the high-risk score group to significantly differ from UM patients in the low-risk score group. Additionally, association between drug resistance of two common drug among the three database and risk score determined significant differences in drug sensitivity where high risk group could be more sensitive to chemotherapy (304).

Overall, multiple potential prognostic biomarkers that regulate autophagy in UM have been found. Greater understanding of the molecular roles of autophagy and its regulation in UM could clarify whether these proteins may be useful in understanding and diagnosis of UM progression and whether they may be potential drug targets.

Table 3. Summary of key genes/RNAs as potential biomarkers for autophagy.

Gene/RNA	Physiological role(s)	Clinical advantages/disadvantages	Reference
Autophagy related genes (ARGs)	- Set of genes required for autophagy. - Mutations of ARGs may result in issues with the autophagy process.	- Multiple targetable genes allow for combination therapy. - Ubiquitous, difficult to differentiate tumour from healthy cells.	(226, 228, 229, 236, 278)
Long non-coding RNA	- Non protein coding RNA. - Effect on cellular regulatory functions.	- Multiple targetable genes allow for combination therapy. - Mutations in the genes allow for targeted therapy. - Involved in cellular development, such as epigenetics, chromatin remodelling and genetic imprinting.	(279-281, 285, 287, 288)
Micro RNA (miRNA)	- Highly conserved non-coding RNA molecules. - Involved in the regulation of gene expression.	- Multiple targetable genes may allow for combination therapy. - Difficult to be considered as a target for pharmacotherapies due to its versatility in the body.	(290, 291, 293, 296, 299, 300)
Genetic profiling	Mutation identification through high output methods. Genetic mutation can result in cancer formation.	Can pinpoint UM based mutation. On different cell lines Can easily verify findings on different databases. May not translate directly into clinical situation.	(304)

3.4 Conclusion

Autophagy is a key process in cellular homeostasis and its activation promotes the degradation and recycling of damaged cells, abnormal cellular material and removal of toxic materials. The activation of autophagy is implicated in a number of cancers, including UM. Although its function in UM remains largely under-defined, autophagy mechanisms and mediators have emerged as promising therapeutic targets that could be used to develop new treatment options for UM where there are no effective drugs at present. As key autophagy-related genes, RNAs and proteins may have distinct roles in tumour and non-tumour cells (e.g., mutations impacting on function), targeting these genes/proteins/RNAs may be a viable way to develop therapeutics for tumour cells. In addition, identifying novel biomarkers based on autophagic mediators may be used to prolong patient survival where currently the prognosis is bleak.

Chapter 4: The novel kinase inhibitor UC2288 as a potential drug for human uveal melanoma

Abstract

Purpose

Uveal melanoma (UM) is the most common intraocular malignancy in adults, characterized by a poor prognosis and a high metastatic rate. While non-pharmacological therapies exist, they are often ineffective in preventing metastasis, the leading cause of mortality in UM patients. Currently, limited drug treatment options are available, and clinical trials have yielded disappointing results, underscoring the urgent need for effective therapeutic agents. In this context, we investigated UC2288, a novel compound, for its potential efficacy in treating UM.

Methods

The anti-cancer effects of UC2288 were evaluated both in vitro and ex vivo using various assays, including assessments of cell viability, cytotoxicity, cell cycle progression, and cell migration/invasion. Key signalling pathways implicated in UC2288's anti-cancer effects were analysed via Western blotting. In vivo efficacy was determined using primary UM tumour xenograft mouse models, with anti-tumour effects assessed through the Xenogen Living Image system and immunohistochemical staining of relevant markers and tissues.

Results

UC2288 rapidly reduced cell viability, induced cytotoxicity, increased reactive oxygen species (ROS) production, directly affected mitochondrial membrane potential in UM cells, and activated endoplasmic reticulum (ER) stress-related signalling proteins. Notably, UC2288 induced S-phase cell cycle arrest, inhibited cell migration and invasion, and suppressed clonogenic growth. These effects were further confirmed by Western blot analysis using pathway-specific markers. Consistent observations were achieved in both patient-derived primary tumour cell samples and xenograft mouse models.

Conclusion

Our data indicate that UC2288 is an effective anti-UM therapeutic agent capable of targeting both primary and metastatic tumours. The induction of ER stress may be a key mechanism underlying UC2288's action in UM. Importantly, UC2288 demonstrated tumour selectivity both in vitro and in vivo, making it a promising candidate for UM therapy.

4.1 Introduction

Uveal melanoma (UM) is the most common intraocular cancer in adults with an incidence rate of 5-8 cases per million (305). Literature indicated that UM occurs more frequently in Caucasians with light pigmented eyes compared to other ethnic groups (305). UM occurs equally in both genders but more in patients with older age (a median presenting age of approximately 59 years old). Approximately 90% of the tumours develop posteriorly in the choroid, 7% in the ciliary body and 3% in the iris (305). UM tumours often develop asymptomatically in its location, resulting in a delay in diagnosis and treatment. It has a poor prognosis with up to 50% of patients ultimately developing metastasis to the distal organs (1). As metastasis spread haematogenouly with the most site being the liver (~93%), followed by the lung (~24%) and bones (~16%) (306). The survival rate of UM patients drastically decreases in the presence of metastasis (4). Thus, metastasis is the leading cause of death in UM patients. A meta-analysis concluded that the median progression free survival (PFS) of UM is 3.3 months, and the median overall survival (OS) is about 10.2 months in metastatic UM patients (307). It has been recognised that delays in diagnosis and treatment significantly contributes to the elevated metastatic chance (a 5% increase of metastatic rate in patients with every 1 millimetre increase in tumour size) (8).

UM pathogenesis remains poorly understood, which largely hinders its therapeutic development. The primary therapeutic options for UM are non-pharmacological. Local treatments such as brachytherapy, laser therapy and surgery have been extensively applied and evaluated for their efficacy and patient outcomes (19). As described in the literature, local treatments are often deemed effective for the primary tumours while preserving the function and structure of the eyes. At present, brachytherapy has been well established with a relatively low chance of recurrence. And the newly developed regimens such as proton beam therapies are advantaged in delivering high doses of radiation to larger tumours without compromising healthy tissue structures (308, 309). Yet the metastasis rate remains high in UM patients despite their primary tumours have

been treated. This may largely be due to the micro-metastasis already present at the time of diagnosis (310).

On the other hand, a lot of attempts have been made to explore drug therapies against UM. Most of drug candidates showed poor clinical outcomes in UM patients (48) and there are very few options showed promises. Studies and trials targeting well recognised UM mutations such as GNAQ/11 and BAP1 has yielded disappointing results and common targeted anti-cancer therapies such as EGFR inhibitors, VEGF inhibitors and small molecules inhibitors failed to show consistent results in improving the overall patient outcomes in UM (52, 63, 67, 71). Moreover, drugs that are effective in treating cutaneous melanoma and other cancers, showed minimal effectiveness in UM, mainly due to the distinct tumour biology and ethology of UM from other cancer types. Till now, tebentafusp has been clinically approved for unresectable metastatic UM (46). However, its clinical outcomes are unsatisfied as it only mildly increases the PFS and OS of UM patients, and is only effective for HLA-A*02:01 positive patients (46). Many other candidate drugs including those targeting various oncogenic receptors, have shown poor results in tumour control and patient outcomes (48, 311). Thus, there is an urgent need to explore new and effective therapeutic agents for primary and metastatic UM.

Our preliminary study evaluated the influence of several chemical compounds on the viability of UM cell lines (Suppl. Fig. 1). We found that UC2288 compound has the relatively more potent effect across all the cell lines tested. Thus, in this study, we further explored the anti-cancer and anti-metastatic effect of UC2288 in *in vitro*, *ex vivo* and *in vivo* UM models.

4.2 Materials and methods

4.2.1 Reagents

6-CHLOROMETHYL-2',7'-DICHLOROD (CM-H2DCFDA), AlamarBlue Cell Viability Reagent, CyQUANT LDH Cytotoxicity Assay, Dimethyl sulfoxide (DMSO), Dulbecco's Modified Eagle Medium (DMEM), eBioscience Annexin V-FITC Apoptosis Detection Kit, L-Glutamine, Penicillin-Streptomycin (P/S) and Roswell Park Memorial Institute Medium (RPMI-1640) were purchased from Thermo Scientific (Lidcombe, NSW, Australia). Foetal bovine serum was purchased from CellSera (Rutherford, NSW, Australia). Thiazolyl blue tetrazolium bromide

(MTT) was purchased from Chem-Supply (Gillman, SA, Australia). PVDF membranes were purchased from Merck Millipore (Bayswater, VIC, Australia). JC-1 was obtained from Sapphire bioscience (Redfern, NSW, NSW).

4.2.2 Cell lines

The 92.1 cell line was obtained from Prof. M.J. Jager (Leiden University Medical Centre, Leiden, Netherlands) and the OMM2.5 cell line was a kind gift from Dr. S Manisha (University of Melbourne, Melbourne, Australia). MIO-M1 and ARPE-19 cell lines were kindly provided by Prof. M Gillies (Save Sight Institute, Sydney, Australia). All cell lines were authenticated by Australian Genome Research Facility, Urrbrae, Australia) every 6 months and routinely checked for mycoplasma every 3 months with MycoAlert Mycoplasma Detection kit (Lonza, Mount Waverley, VIC Australia). 92.1 and OMM2.5 are cultured in RPMI medium supplemented with 10% heat-inactivated FBS (v/v), 1% P/S and 1% L-Glutamine. MIO-M1 and ARPE-19 cell lines are maintained in DMEM medium plus 10% FBS, 1% P/S and 1% L-Glutamine. All cells are incubated at 37°C in a humidified incubator with 5% CO_2. All cells are used within 30 passages to ensure uniformity in DNA sequence.

4.2.3 Cell viability assay

MTT assay was performed as the primary cell viability assay as described previously (312). Cells were seeded onto 96 well plate with confluency of 90% after overnight incubation. Cells were treated with UC2288 dissolved in DMSO and diluted with respective medium supplemented with 1% FBS. MTT (0.5mg/ml) is added after treatment for 24 hours and incubated for 1 to 4hours. Cells are then dissolved with DMSO to release the purple crystalline and shaken for 5 minutes at room temperature. Absorbance is measured at 550nm in the Multiskan SkyHigh Microplate Spectrophotometer (Thermofisher, Lidcombe, NSW, Australia). IC_{50} was obtained using MTT and analysed with non-linear regression of cell viability verses drug concentration (GraphPad Prism 7.0; San Diego, CA).

AlamarBlue assay is another typical cell viability assay, which was also adopted in this study. Cells were seeded and treated as above. AlamarBlue was diluted (1:9) with respective medium without FBS and added to treated cells. Cells were incubated for 30 minutes to 4 hours and

absorbance was read at 550/590nm using the Victor x Multilabel Plate Reader (PerkinElmer, Waltham, Massachusetts, United States).

4.2.4 Lactate dehydrogenase (LDH) cytotoxicity assay

LDH assay was conducted using supernatant from treated cells and was superimposed with MTT assay. Supernatant was first extracted from the treated plate and LDH assay was added and shaken in room temperature for 30 minutes protected from light before stop solution was added and absorbance was measured at 490/655nm using the microplate reader (Model 680, Bio-Rad, Gladesville, NSW, Australia).

4.2.5 Reactive oxygen species (ROS) assay

ROS level was measured using the non-specific ROS indicator CM-H2DCFDA. As mentioned in previous papers (313), the reagent was prepared according to manufacturer protocol and cells were incubated for 1 to 1.5 hours protected from light. Fluorescence was measured at 450/500nm using the Victor x Multilabel Plate Reader (PerkinElmer, Waltham, Massachusetts, United States).

4.2.6 JC-1 mitochondrial health assay

JC-1 assay was conducted on treated cells as mentioned above. Cells were incubated for 20 minutes protected from light and then washed once with saline (PBS, 0.154 M NaCl, 0.001 M KH2PO4, 0.003 M Na2HPO4; pH 7.4) and fluorescence was measured at 495/530nm for green light and 530/580nm for red light with the Victor Nivo Multimode Plate Reader (PerkinElmer, Waltham, Massachusetts, United States). Ratio of red light to green light was determined for each well.

4.2.7 Annexin V/PI flow cytometry assay

UM cells were treated with UC2288 (5μM in 0.1% DMSO) in their respective medium containing 1% (v/v) FBS with 0.1% DMSO as control. Cells were collected at 48 hours and washed twice with PBS and stained with annexin V-FITC and Propidium iodine for 15 minutes according to manufacturer's protocol. Samples were analysed for mode of cell death using a Guava easy®cyte flow cytometer (Merck Millipore, Bayswater, VIC, Australia).

4.2.8 Cell cycle assay

Cells were seeded and treated as mentioned in flow cytometry assay and as described in previous paper (314). Cells were harvested and washed twice in PBS before fixed in ice cold ethanol (70%vlv) and stored in -20°C overnight. Ethanol was removed and cells were washed with PBS prior to analysis and stained with propidium iodide for 15 to 30 minutes protected from light. Analysis was conducted using Guava easy®cyte flow cytometer (Merck Millipore, Bayswater, VIC, Australia).

4.2.9 Transwell cell migration assay

Cells were seeded onto the inner chamber of a 24 well transwell plate with 8µM pore size (Corning, New York, United States). Cells were incubated in 10% medium overnight to ensure attachment. A concentration gradient was formed using 1% FBS medium in the inner chamber and 3% FBS medium in the outer chamber, then cells were treated with UC2288 (3µM) and further incubated at 37°C to allow for migration. All the inner chambers were cleansed with PBS and cotton swab and then incubated in 100% methanol for 30 minutes to fixate the cells. Fixed cells were then dyed using crystal violet. The number of cells per well is determined by taking the average of the number of cells within photos of the 4 sides and a photo in the middle. The migration rate was mathematically calculated as below.

$$Migration\ rate\ (\%) = \frac{\frac{average\ cell\ number}{Area(viewing\ field)}\ x\ Area(transwell\ insert)}{number\ of\ cells\ seeded}\ x\ 100$$

- Area (viewing field) = area of the microscope viewing field at the magnification used to take photos
- Area (transwell insert) = area of the member in the inner chamber of the transwell

4.2.10 Transwell cell invasion assay

Cells were seeded in the same manner as cell migration assay. Matrigel layer (Corning, New York, United States) was added prior to addition of cells mimic the extra cellular matrix of organs. Cells were treated and incubated at 37°C alike to cell migration assay. Average number

of cells per well were identified as described above and invasion rate was calculated with the same equation described in the migration assay.

4.2.11 Colony formation assay

Colony formation assay was conducted as previously described (84). Cells were plated onto 12 well plates and treated with UC2288 (3μM) for 24 hours. Cells were then harvested and reseeded onto 24 well plates (100 cell/well) and incubated for 6-8 days (37°C, 5%CO_2). On the day of analysis, cells were fixed with 100% methanol then stained with 0.01% crystal violet (w/v). A colony was defined microscopically as a cluster of a minimum 50 cells. Wells were scanned using the Essen IncuCyte S3^R, (Sartorius, Dandenong South, VIC, Australia) at 4x objective using the whole well scan mode and Image J was used to estimate the amount of cell colony formation.

4.1.12 Western blotting

Cells were plated into 6 well plates and treated with UC2288 (3μM) for 48 hours. Cells were harvested and lysed with NP-40(1% IGEPAL, 150 mM NaCl and 50 mM Tris, pH 7.8 with 1% protease inhibitors). the lysate was then centrifuged at 15,000 rpm (5 min, 4 °C) to separate supernatant containing protein samples from the cell debris. Lamini buffer was added, and samples were denatured at 50°C for 30 minutes on a heat block. Samples were stored in -20°C.

Electrophoresis was conducted to separate the protein sample, and proteins were transferred onto a PVDF membrane before blocking with 5% non-fat milk in PBST for 1 hour. The blots were incubated with their respective primary antibody and placed on an orbital shaker at 4 °C overnight. Membrane was washed with PBST 3 times before second antibody was added and incubated at room temperature for 1 hour. Protein signal was detected using Immobilon Western Chemiluminescent HRP Substrate (Merck Millipore, Macquarie Park, NSW, Australia) and visualized with ImageQuant LAS500 (GE health care, Silverwater, NSW, Australia).

4.2.13 Primary UM tumour derived cell lines

Human UM tumour samples were obtained with approval from St. Vincent's Hospital Sydney Human Ethics Committee (HREC/17/SVH/346) and experiments were conducted as per the

major guidelines and regulations. Tumours was surgically removed and washed in PBS (pH7.4) for three times. Tumours were processed to separate into individual cells and cultured at 37°C with 5% CO_2 in RPMI-1640 medium containing 20% FBS (v/v), 1% L-glutamine, 1% P/S, 1% ITS and 2% GCT. All experiments were conducted with the passage numbers between 2 to 5.

4.2.14 3D bio printed UM cell models

Rastrum 3D bioprinter (Inventia Life Science, Alexandria, New South Wales) was utilised to generate 3D spheroids on PEG-based hydrogel at Px01.71, ~0.7 kPa, containing RGD (fibronectin), DYIGSR (Collagen I), CNYYSNS (collagen IV) forming a complex matrix mimicking the tumour environment. The 3D Large Plug Model was chosen; the printing protocol was created using the Rastrum Cloud (Inventia Life Science). All bio printed cultures was conducted on 96 well flat bottom plates according to manufacturer's protocol. Priming and printing of the base inert layer was first conducted to better facilitate matrix adhesion. Cells were suspended at a concentration of $5x10^6$/mL within the activator, then printing was conducted by alternating bioink and cell containing activator to form a covalent interaction suspending the cells within the matrix. 150µL of RPMI-1640 medium supplemented with 10% (v/v) FBS, 1% P/S and 1% L-Glutamine was added to each well and cells were incubated at 37°C for 5 days prior to the subsequent analysis.

4.2.15 Xenograft mouse model and in vivo imaging

Animal ethics approval was obtained from the Laboratory Animal Ethics Committee of Jiangsu Institute of Nuclear Medicine (Wuxi, China) and animal experiments were performed in strict accordance with the relevant guidelines and regulations. BALB/c nude mice (5 weeks old; male; Chang Zhou Cavens Laboratory Animal Co., Ltd, Changzhou, China) were intravitreally injected with 92.1-Luc cells overexpressing luciferase (5×10^6) dissolved in saline and then mixed with Matrigel at a 2:1 ratio (315, 316). After 7 days, mice were intraperitoneally injected with D-luciferin (15 mg/mL) and imaged using the Xenogen Living Image system (Alameda, CA, USA) (315, 316). Upon confirmed the formation of tumours in the eyes, mice were randomly assigned to the control (n=6) or UC2288 treatment (n=7) group. Treatment group was orally administered with UC2288 (15 mg/kg) or vehicle every day for two weeks. At the end of treatment duration, the mice were injected with D-luciferin again and imaged using the Xenogen Living Image

system. Then the mice were anesthetised and euthanized. The tumours and some other key tissues (i.e., the heart, liver, spleen, lung and kidney) were removed, fixed with formalin, embedded in paraffin, and sectioned for subsequent analysis.

4.2.16 Histology and immunohistochemical analysis

The tissue sections were processed for Hematoxylin & Eosin, Ki67, and ATF4 staining. Tumour sections were incubated with Hematoxylin and eosin, anti-Ki67 or anti-ATF4 antibody overnight at 4 ℃. The immunohistochemically stained sections were incubated with HRP-conjugated secondary antibody for 2 h at room temperature and visualised using the DAB kit (Beyotime, Nantong, China). Images were captured with the Olympus light microscope (Olympus IX53, Tokyo, Japan).

4.2.17 Statistic

Data is shown as the mean ± standard deviation (SD) with significance defined as $p < 0.05$. A cell culture studies were done in triplets with 3 repeats at separate times. Statistical analysis was conducted using one-way ANOVA then Dunnett's post-hoc test when comparing multiple independent groups in GraphPad Prism 7.0.

4.3 Results

4.3.1 UC2288 has a potent anti-cancer effect in UM

In our preliminary testing of several sorafenib analogues (commercially available or in-house customised) (Suppl. Fig. 4), UC2288 demonstrated a relatively most potent effect in decreasing cell viability across all the tested UM cell lines. Thus, UC2288 was chosen as our candidate compound to be further studied.

92.1 is a classic primary tumour derived UM cell lines, whereas OMM2.5 is derived from liver metastatic lesion of UM (317-319). Thus, these two cell lines were adopted as the *in vitro* UM models in the current study. First, we investigated the anti-cancer potency of UC2288 in these UM cell lines. As shown in Fig. 11A, the IC_{50} values of UC2288 are 2.7 μM and 1.9 μM,

respectively. In accordance with this, 3uM was chosen as the optimal concentration of UC2288 treatment for further testing.

To evaluate the tumour selectivity of UC2288, the treatment was conducted on UM cell lines as well as the typical non-tumour ocular cell lines (i.e., MIO-M1 and ARPE-19 cells) as well as primary culture of human melanocytes. Here, MIO-M1 is the commonly used human Müller cell line while ARPE-19 is the classic human retinal pigmented epithelial cell line. UC2288 displayed optimal tumour selectivity with no cytotoxicity on ARPE-19 and MIO-M1 (Fig. 11B) as well as a mild cytotoxicity on primary melanocytes.

It is well known that the classic two-dimensional (2D) culture (cell monolayers) cannot demonstrate the complex characteristics of solid tumours. In contrast, three0-dimentional (3D) cultures are emerging to better mimic tumour physiological in the recent decades. The previous studies showed that UM cell lines had different responses to drug treatment when cultured in monolayer or in 3D structure (320). Till now, the 3D culture models of UM cell lines were mainly generated by force floating or Matrigel-embedded method (320). In the current study, we are the first to establish the UM 3D culture model using bioprinting technology, in which tumour cell growth was better supported by biomimicking extracellular matrix (ECM). The 3D bio printed UM cells were treated with UC2288 for extended duration considering the existence of ECM may hinder drug penetration. Consistently, UC2288 significantly decreased cell viability in both UM cell lines (0.14 folds of cell viability in 92.1 and 0.44 folds in OMM2.5 cells when compared to the control) (Fig. 11C), which suggested that this candidate drug is capable of penetrating solid tumours and inducing tumour cell death.

It is a general concern that immortalised tumour cell lines cannot well represent heterogenous tumour characteristics in drug testing. To validate our finding, our study has also adopted three UM primary cell lines derived from three independent UM patients. Our data showed that UC2288 consistently demonstrated a significant effect in decreasing cell viability in the *ex vivo* models (Fig. 11D).

Overall, UC2288 has shown to be a potent and promising candidate drug against UM with a potent anti-cancer effect not only in 2D but also in 3D cultured UM tumour cells as well as in patient tumour-derived UM primary cultures.

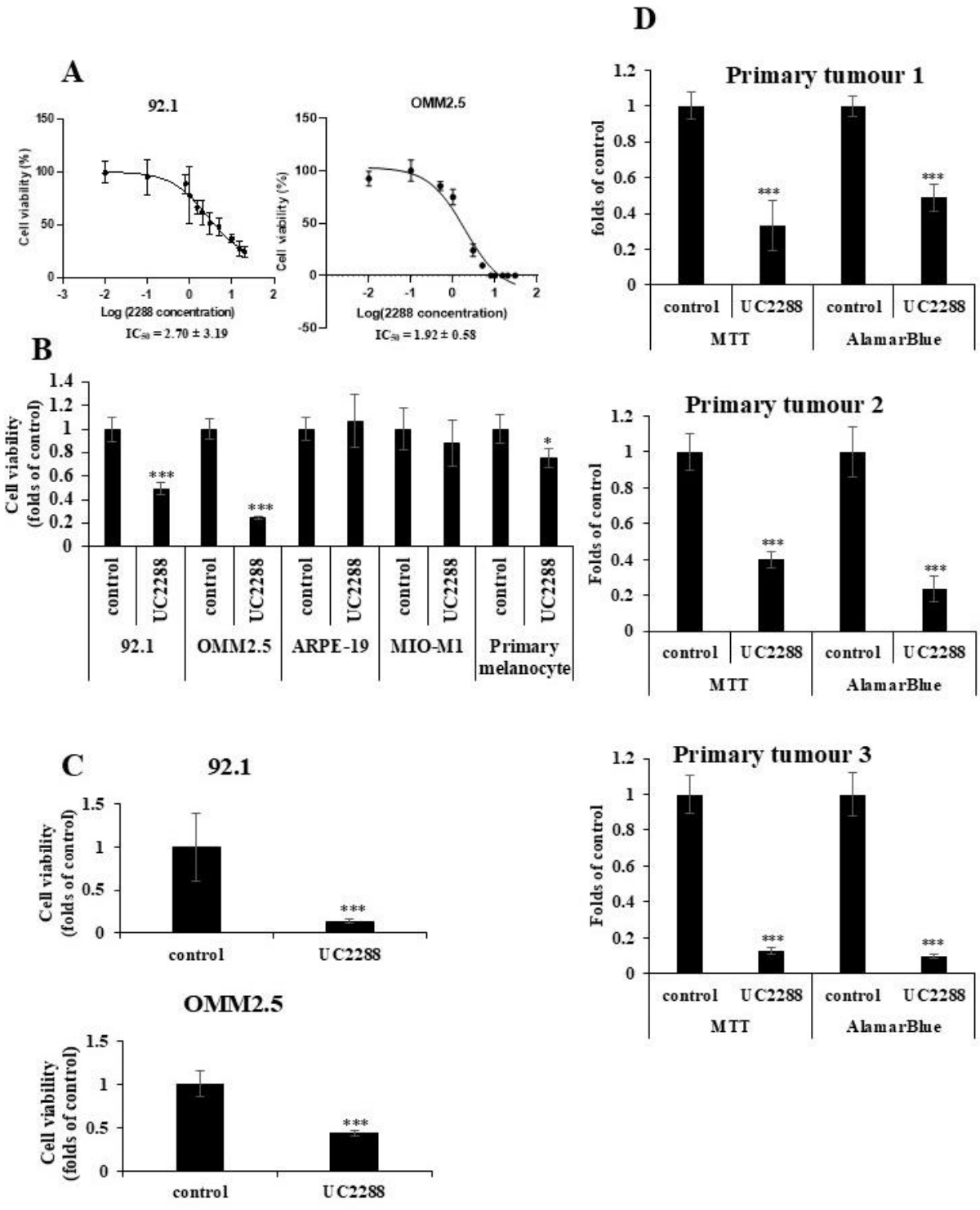

Figure 11. Molecular characterisation of the anti-cancer effect of UC2288 in UM cell lines. UC2288 demonstrates tumour selective reduction in cell viability in UM cell lines. UM cells were treated with or without UC2288 in medium supplemented with 1% FBS. (A) IC_{50} of

*UC2288 in UM cell lines. UM cells were treated with UC2288 at a concentration from 0.01μM to 20μM. Cell viability was evaluated using MTT cytotoxicity assays. The experiments were conducted in triplicate, with three independent replicates performed for each experiment (n = 3). The results are expressed as a percentage of the control, presented as mean ± standard deviation (SD). IC_{50} values were determined using GraphPad Prism 9.0. (B) cell viability study with tumour and non-tumour cell lines. Cells were treated with UC2288 (3μM). Cell viability was determined using MTT cytotoxicity assay. (C) 3D Rastrum Bio-printed cell model. Cells were embedded with PEG-hydrogel and incubated for 5 days to allow 3D structure formation. Cells were treated for 96hrs with UC2288 (3μM), and cell viability assay was conducted using AlamarBlue assay. (D) patient primary tumour derived cell cultures. 3 different Patient tumour was utilised and cells were extracted and cultured. Cells were treated with UC2288, and viability was determined with both MTT and AlamarBlue assay. The experiments were conducted in triplicate, with three independent replicates performed for each experiment (n = 3). *p < 0.05; **p < 0.01; ***p < 0.001 vs. control by unpaired Student's t test.*

4.3.2 UC2288 induces cytotoxicity and promotes autophagy-related necrosis through disrupting mitochondrial function and health

The reduced cell viability upon UC2288 treatment may be resulted from an induced cell death and/or suppressed cell proliferation. Subsequently, we performed LDH assay cytotoxicity to further characterise the anti-cancer effect of UC2288. Our data showed that UC2288 has a potent cytotoxic effect on both UM cell lines (2.62 folds of cytotoxicity in 92.1 and 2.71 folds in OMM2.5 cells when compared to the control) (Fig. 12A).

As both MTT and AlamarBlue cell viability assays are based on mitochondrial function, we hypothesise that the potent anti-cancer effect of UC2288 is also in part due to its impact on cell mitochondria. We then employed further analysis to assess mitochondria function and health. ROS assay utilises the non-specific indicator CM-H2DCFDA to assess the ROS level in cells. Our data demonstrated that there was an increase of 3.98 folds of ROS accumulation in 92.1 and 2.04 folds in OMM2.5, respectively (Fig. 12B). This finding indicates that UC2288 treatment results in a significant ROS accumulation in UM cells.

JC-1 assay was employed to explore mitochondria health through measuring the mitochondria membrane potential. Our data revealed that mitochondria membrane potential was significantly disrupted in both cell lines after the treatment of UC2288 (Fig. 12C). This suggests that UC2288 exerts its effect by disrupting mitochondrial health and function. In addition, the cytotoxicity of UC2288 was further evaluated by Annexin V/PI staining flow cytometry cell death assay. Necrosis was observed as the main form of cell death upon UC2288 treatment in 92.1 and OMM2.5 cells (Fig. 12D).

It is known that autophagy can trigger necrosis (321). And the previous studies showed that agents modulate autophagy may induce UM cell death (322). Thus, we assessed the autophagic protein makers to see whether such mechanism is involved in the anti-UM effect of UC2288. As shown in Fig. 12E and 12F, there is a significant decrease of P62 protein expression and a cleavage of LC3-I into the activated LC3-II isoform in UM cells treated with UC2288 when compared to the control. The UC2288-induced P62 protein change has a delayed effect in OMM2.5 compared to that of 92.1 cells. P62 activation occurs during the initial autophagy response in attempts to retain homeostasis through digestion of stress causing organelles. OMM2.5 is a metastatic cell line shown to have more aggressive phenotype and different reaction to drug treatment when compared to 92.1. Furthermore, such difference in cell phenotype may contribute towards changes in autophagic response when treated with UC2288 as seen in Figure 12E, 12F. Overall, UC2288 has a potent cytotoxicity and can induce autophagy-related cell death via impacting on mitochondrial function and health.

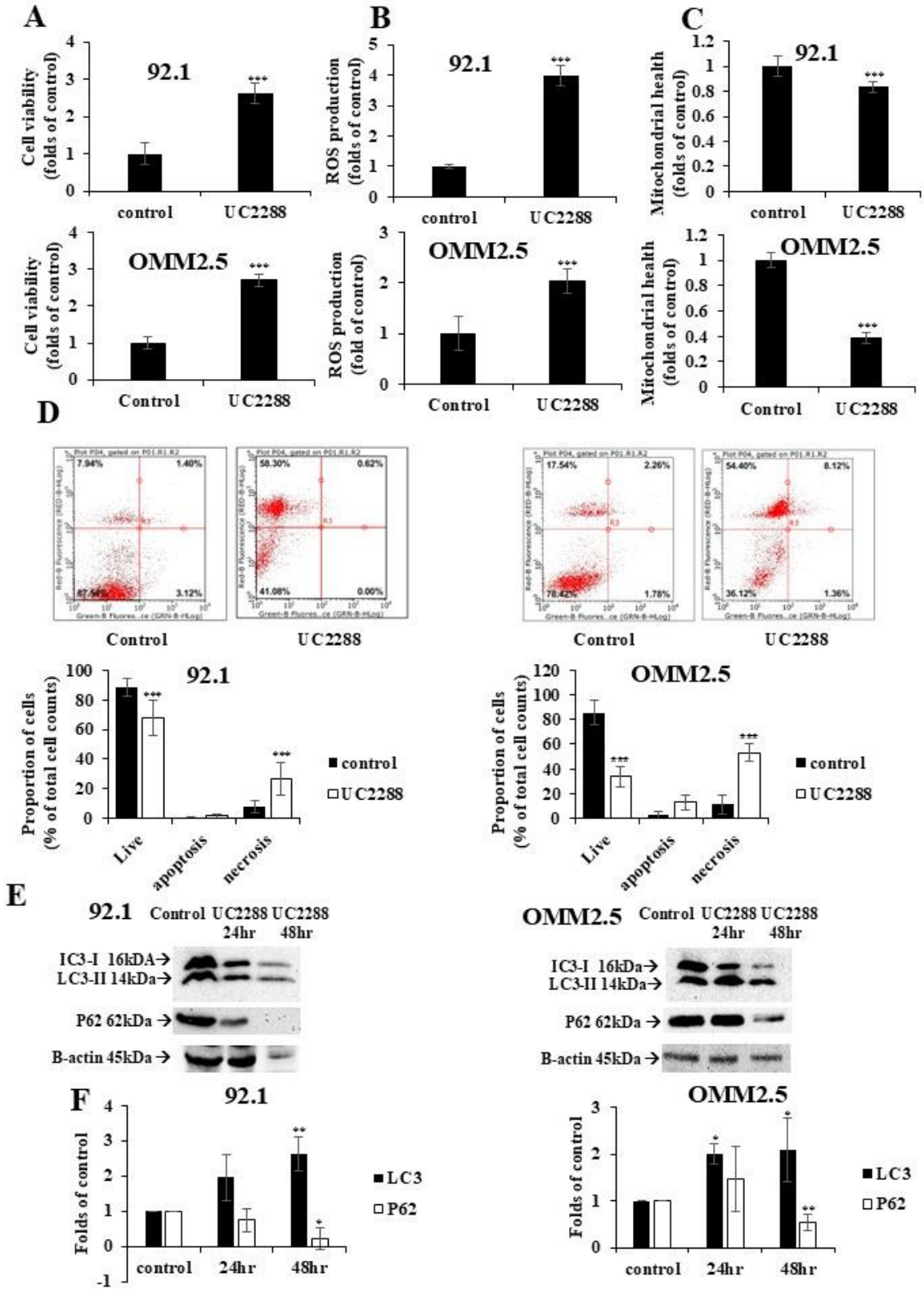
A
92.1
Cell viability (folds of control)
control
UC2288
OMM2.5
Control
UC2288
B
92.1
ROS production (folds of control)
OMM2.5
ROS production (fold of control)
C
92.1
Mitochondrial health (folds of control)
OMM2.5
D
Control
UC2288
92.1
Proportion of cells (% of total cell counts)
Live
apoptosis
necrosis
control
UC2288
OMM2.5
E
92.1 Control UC2288 UC2288
24hr 48hr
IC3-I 16kDA→
LC3-II 14kDa→
P62 62kDa →
B-actin 45kDa →
OMM2.5 Control UC2288 UC2288
24hr 48hr
F
92.1
Folds of control
control
24hr
48hr
LC3
P62
OMM2.5

*Figure 12. The effect of UC2288 on UM cell death. Further studies have been implemented to better evaluate the effect of UC2288 on UM cell lines. Cells were treated with 3μM of 2288 before assays were conducted. (A) The LDH assay utilises the supernatant of UM cells only. Equal parts of supernatant and LDH assay was combined and incubated for 30 minutes before absorbance was measured. (B) CM-H2DCF-DA. was diluted with PBS according to manufacturer's instructions before incubating it with cells for up to 1.5 hours (37°C). (C) JC-1 assay was prepared according to manufacturer's instructions and incubated with cells for 20 minutes (37°C) before measured twice at differing wavelength. All data is presented as folds of activity compared to control (mean ± SD) and statistical analysis done by unpaired Student's t test. Cell death profile in response to UC2288 treatment is depicted with annexin V/PI staining flow cytometry. Cells were separated into viable, necrotic, or apoptotic. Representative image as well as graphical presentation as percentage compared to control (mean ± SD) are presented (D) and statistical assessment was done using Two-way ANOVA with Šídák post hoc test. Specific cell death markers for autophagy were assessed using western blot. Cells were treated with differing length to assess overall changes in time. Representative images of each marker are shown in (E), and densitometry assessment was conducted (F) where data are presented as fold of control (mean ± SD) and statistical analysis was done with unpaired Student's t test. All experiments were done in triplicate with n=3 in each repeat. *p < 0.05; **p < 0.01; ***p < 0.001 vs. control.*

4.3.3 UC2288 potently suppresses cell cycle progress in UM cell lines

PI staining flow cytometry assay was used to determine the effect of UC2288 on cell cycle. Our findings revealed a significant increase in the proportion of cells arrested in the S phase in both UM cell lines, 92.1 displayed moderate elevation in the G2/M phase whilst OMM2.5 showed a decrease in G2/M phase. The G0/G1 phase showed a marked decrease in both UC2288-treated UM cell lines. (Fig. 13A). We also assessed the expression of two cell cycle protein markers (i.e. Cyclin E1 and Cyclin A2) to validate our findings. Our data showed an increase in cyclin E1 expression but a decrease in cyclin A2 level upon the treatment of UC2288 (Fig. 13B and 13C). In detail, Cyclin E1 was increased to 2.40 folds of control in 92.1 and 2.10 folds in OMM2.5;

while that of Cyclin A2 was decreased to 0.35 folds of control in 92.1 and 0.58 folds in OMM2.5. This finding is aligned with the S phase halt.

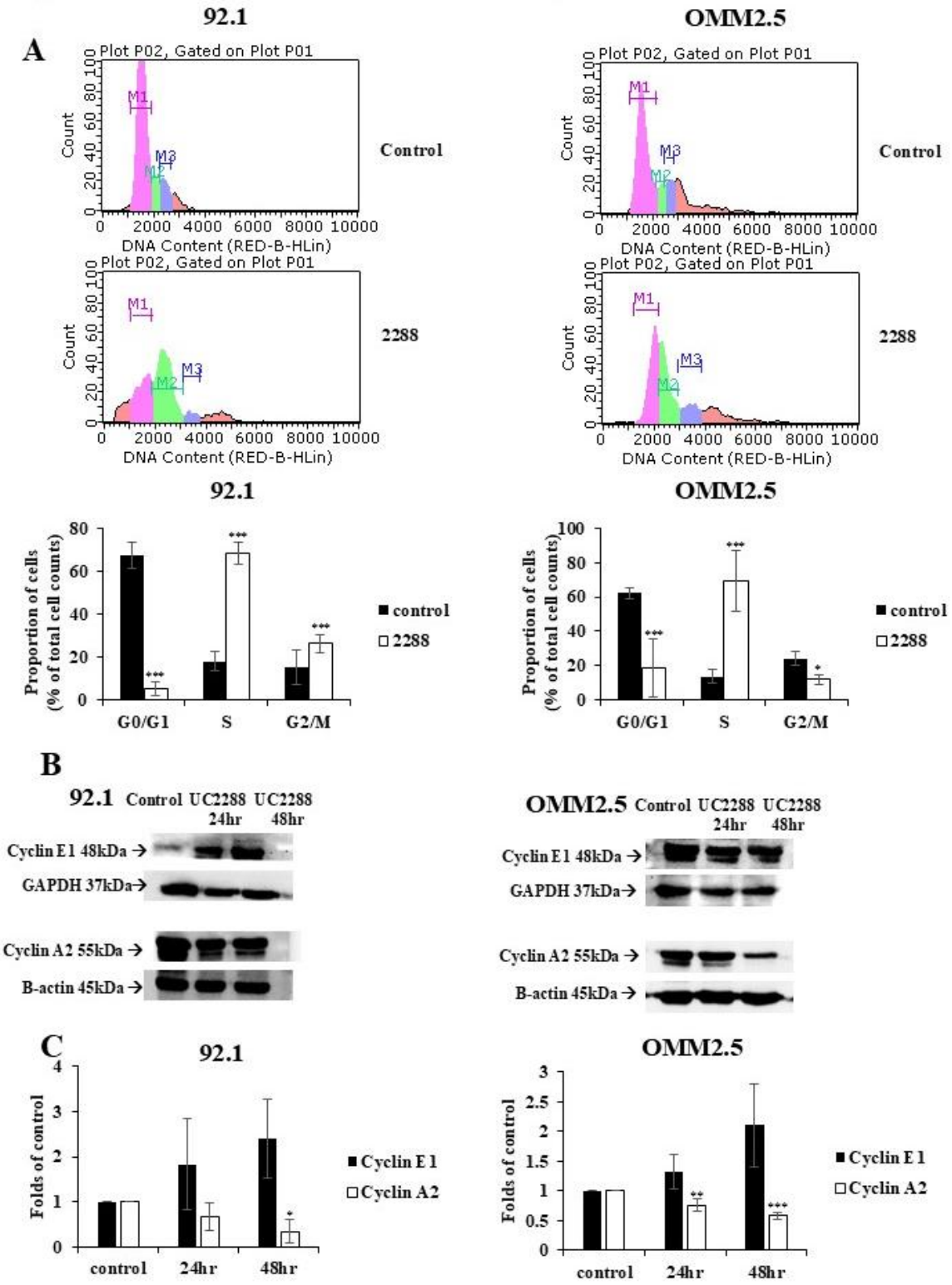

*Figure 13. The effect of UC2288 on UM cell cycle. The influence of UC2288 on cell cycle was assessed in both cell lines. Cells were treated with 3μM UC2288 and fixed with 70% ethanol. Fixed cells are resuspended in PBS with RNAse A and stained with propidium iodide for flow cytometry analysis to determine cell cycle profiles. Cell cycle distribution in G0/G1, S or G2/M phases are presented as percentages of total cells (mean ± SD) (A) and statistical assessment was done using Two-way ANOVA with Šídák post hoc test. Key cell cycle stage markers cyclin E1 and cyclin A2 were assessed using western blot analysis. Cells were treated with 3μM UC2288 at varying times to observe the changes. Representative images are shown in (B). Densitometry assessment was conducted (C) where data are presented as fold of control (mean ± SD) and statistical analysis was done with unpaired Student's t test. All experiments were done in triplicate with n=3 in each repeat. *p < 0.05; **p < 0.01; ***p < 0.001 vs. control.*

4.3.4 UC2288 also exerts its anti-UM effect via inducing endoplasmic reticulum stress

To further evaluate the cell death mechanism of UM cells exposed to UC2288, we selected the specific inhibitors of necroptosis, ferroptosis or endoplasmic reticulum **(**ER) stress to be co-treated with UC2288 (Fig. 14A). Our data showed that ER stress inhibitors Salubrinal and integrated stress response inhibitor (ISRIB) can effectively relieve the effect of UC2288 in reducing UM cell viability. Salubrinal is a direct inhibitor of eukaryotic initiation factor 2 alpha (eIF2α) signalling through inhibition its dephosphorylation. Whereas ISRIB functions allosterically by binding to eukaryotic initiation factor 2B (eIF2B), it activates eIF2B which mitigates the impact of eIF2α phosphorylation, leading to the resumption of protein synthesis during cellular stress (323). Our results indicates that UM cell death is reversed by Salubrinal in 92.1 cell line whereas reserved in OMM2.5 cell line (Fig. 14A).

ER is well known to be involved in cancer development and progression (324). ER stress is prone to induce cell death in many cancer cells. To further explore the role of ER stress in UC2288-induced UM cell death, we assessed the protein expression of several ER stress protein markers. Our data showed the eIF2α/ATF4 pathway was activated upon UC2288 treatment in 92.1 cell line (Fig. 14B). The expression of the direct ER stress sensor protein BIP has been shown to be increased in UM cells exposed to UC2288. It is known that BIP chaperone protein

dissociates from the transducer proteins to activate the UPR pathway (325). Thus, we further explore its downstream signalling's. We found that the eIF2α protein is highly activated as well as its downstream effector proteins including ATF4 and caspase 9 (Fig. 14C). In OMM2.5, BIP and eIF2α did not show increase in activation but end-point cell death effects were still observed through ATF4 and Caspase 9 activation (Fig. 14B, 14C). This corresponds to the effect of ISRIB as it does not only inhibit eIF2α dephosphorylation but also mitigate its downstream effect by preventing the reduction of protein synthesis (323) This suggests that UC2288 exerts its anti-UM effect through inducing ER stress via the activation of eIF2α/ATF4 pathway in primary UM tumour cells but plays a different role in metastatic cells.

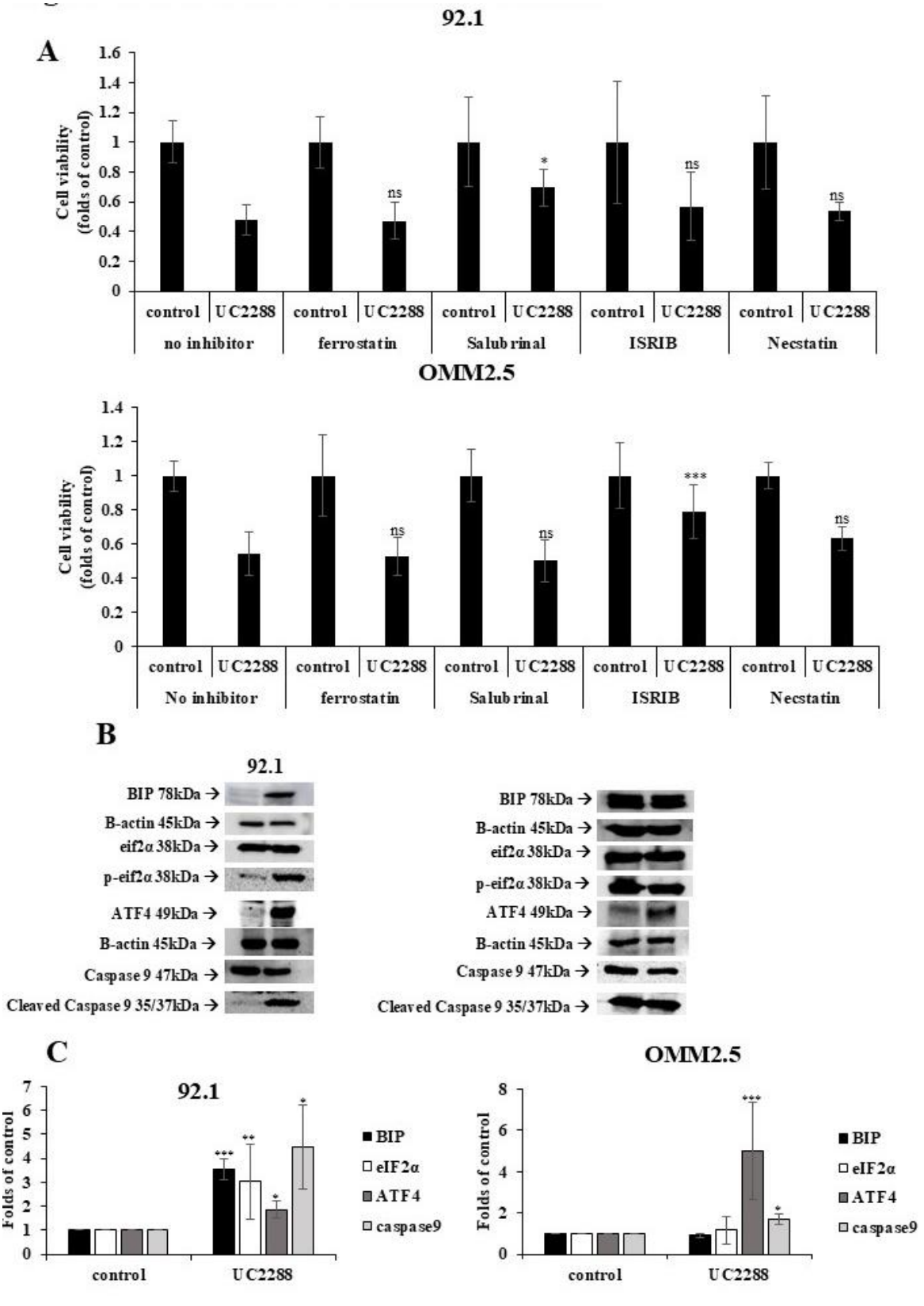
92.1
A
Cell viability (folds of control)
control
UC2288
no inhibitor
ferrostatin
Salubrinal
ISRIB
Necstatin
OMM2.5
No inhibitor
B
92.1
BIP 78kDa
B-actin 45kDa
eif2α 38kDa
p-eif2α 38kDa
ATF4 49kDa
Caspase 9 47kDa
Cleaved Caspase 9 35/37kDa
C
92.1
OMM2.5
Folds of control
BIP
eIF2α
ATF4
caspase9

*Figure 14. UC2288 induced ER stress in UM cells UC2288 treatment induces ER stress in UM cell lines. Specific cell death inhibitors were chosen as co-treatment with UC2288 on UM cell lines. cells were co-treated with UC2288 and cell death inhibitors before cell viability was assessed with MTT assay. Cell death inhibitor alone was used as control for each treatment pair and the differences in cell viability was evaluated using Two Way ANOVA with Dunnett post hoc test comparing the folds of reduction in cell viability between control group and cell death inhibitor groups. Eif2α associated ER stress signalling pathway was chosen to be evaluated based on the results of cell death inhibitors. BIP, eif2α, ATF4 and caspase 9 were chosen as key signalling markers for the pathway. Representative images are shown in (B). Densitometry assessment was conducted (C) where data are presented as fold of control (mean ± SD) and statistical analysis was done with unpaired Student's t test. All experiments were done in triplicate with n=3 in each repeat. *p < 0.05; **p < 0.01; ***p < 0.001 vs. control.*

4.3.5 UC2288 inhibits cell migration, invasion, and reproductive cell growth in UM cell lines

As mentioned above, metastasis is the leading cause of death in UM patients. Thus, it is critical to evaluate the anti-metastatic potential of UC2288. We conducted cell migration, invasion, and colony formation assays accordingly. The ability of UM cells to migrate with or without Matrigel was assessed to determine local and inter-organ movement, respectively. In the presence of Matrigel, UM cells need to break through the extracellular matrix invading into other organs (326)

UC2288 treatment exhibited a reduced migration rate compared to that of the control (0.47 fold of the control in 92.1 cells and 0.38 folds of the control in OMM2.5 cells) (Fig. 15A and 15B). Furthermore, the invasion rate of UM cells was also significantly decreased upon the treatment of UC2288 (0.35 in 92.1 cells and 0.27 in OMM2.5 cells) (Fig. 15C). The ability to reproduce post treatment is also a critical hallmark of tumour metastasis. As the micro-metastasis to other organs is often under detection in UM, it is a highly desired feature of candidate drugs in treating this cancer. Thus, the influence of UC2288 on cell reproductive growth was evaluated with colony formation assay (Fig. 15D). UC2288 was shown to significantly inhibit the reproductive cell growth of UM cells (0.51 folds of the control in 92.1 cells and 0.28 folds of the control in

OMM2.5 cells). Overall, it is evident that UC2288 is potent in inhibiting cell migration and invasion as well promoting reproductive cell death in UM cells.

The inhibitory effect of UC2288 on tumour metastasis was further explored through the expression of key epithelial-mesenchymal transition (EMT) marker proteins (i.e., Matrix Metalloproteinase-2 (MMP2) and β-catenin) (Fig. 15E). Our results suggest EMT was disrupted by UC2288 treatment with a decreased expression of MMP2 (0.53 folds of the control in 92.1 and to 0.64 folds of the control in OMM2.5) as well as β-catenin (0.78 folds of the control in 92.1 and to 0.64 folds of the control in OMM2.5). Consistently, UC2288 is shown to prohibit the metastasis of UM cells to neighbouring and distant organs suggesting a reduced metastatic potential.

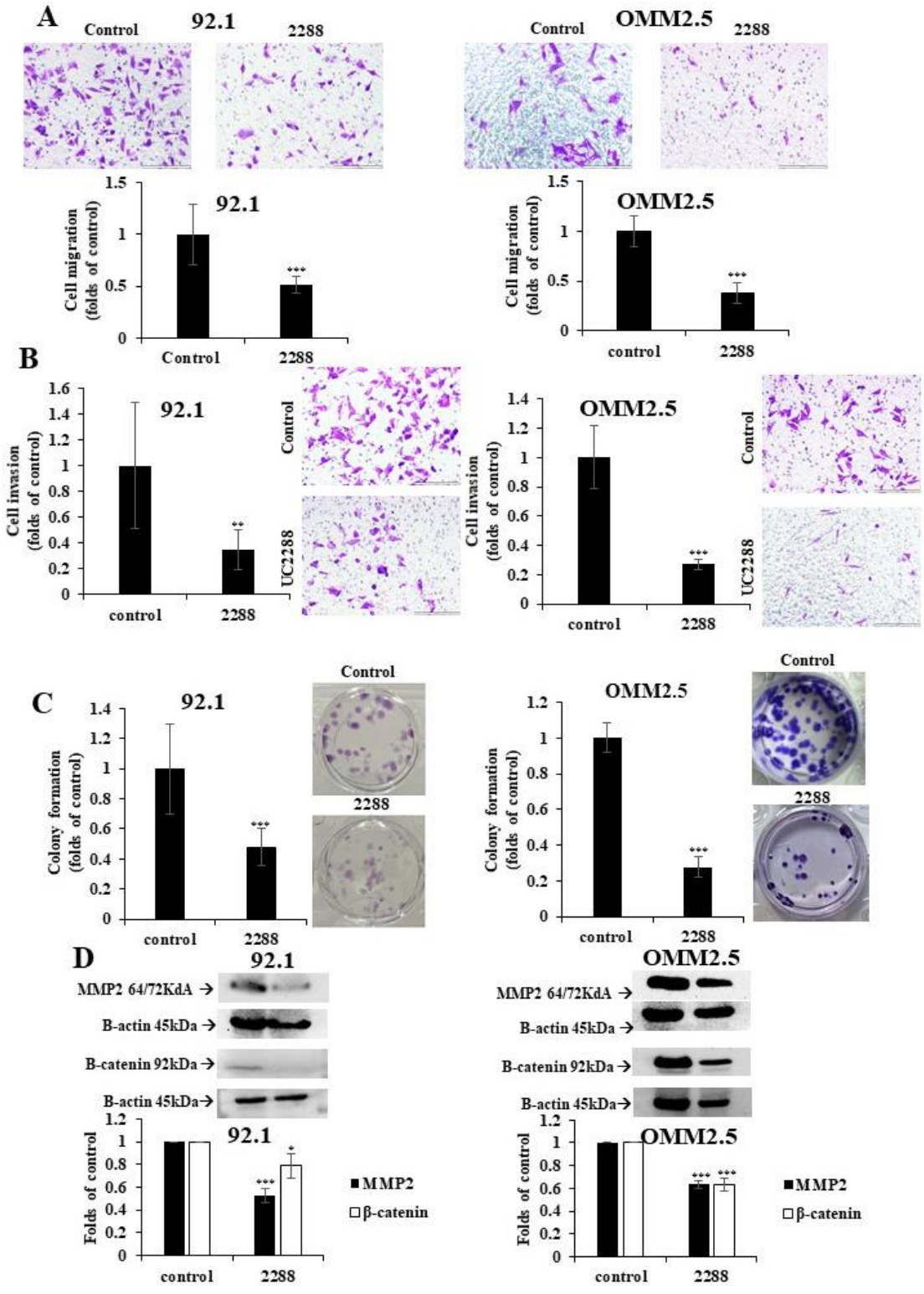

Figure 15. UC2288 impacts on the metastatic potential of UM. UC2288 can prevent cell migration and invasion as well as inhibit reproductive cell death in UM cell lines. Transwell assay was adapted with or without Matrigel (200μg/ml) to assess the influence on cell migration

*(A) and cell invasion (B). Cells were only seeded onto the inner chamber while UC2288 (3μM) was added to both inner and outer chamber. Cells were stained with crystal violet and the number of cells migrated was compared to the initial seeding number. Both the representative image and the quantitative graphic analysis is shown. Inhibition of colony formation was determined through pre-treating cells with UC2288 (3μM) or control (1% FBS supplemented medium) and re-seeded at 200 cells per well and incubated (37°C). The number of colonies formed are shown as folds against control (C). Key protein markers for EMT formation in cells have been assessed with western blot. The relative activity of MMP2 and β-catenin was compared to β-actin which was used as the loading control. (D) show the representative images as well as the densitometry study. All experiments were done in triplicate with n=3 in each repeat. *p < 0.05; **p < 0.01; ***p < 0.001 vs. control.*

4.3.6 The anti-cancer effect of UC2288 in the UM xenograft mouse model

It is important to evaluate the anti-UM effect of UC2288 in *in vivo* models. We have successfully established a primary xenograft mouse model via intravitreally injected the 92.1-LUC cells (316). Mice was orally administered with UC2288 (15mg/kg every day) for two weeks and the in vivo imaging system (IVIS) was adopted to analyse the tumours. VIS images indicated that UC2288 significantly suppressed the tumour progression in the xenograft mice (Fig. 16A).

Our also performed histological and immunohistochemical staining on the tumour tissues (Fig. 16B). Our data demonstrated a significantly disrupted tissue structure and a markedly decreased Ki67 staining post treatment, which confirmed the cytotoxicity of UC2288. In addition, we observed an elevated ATF4 staining in the tumour tissues of UC2288 group, which is consistent with the molecular finding above that UC2288 induces ER stress to exert its anti-UM effect (Fig. 14). Meanwhile, UC2288 treatment did not induce significant tissue damages in other key organs, suggesting its favourable tumour selectivity (Fig. 16C). Overall, our data proved that UC2288 has a potent anti-UM effect in the *in vivo* UM model.

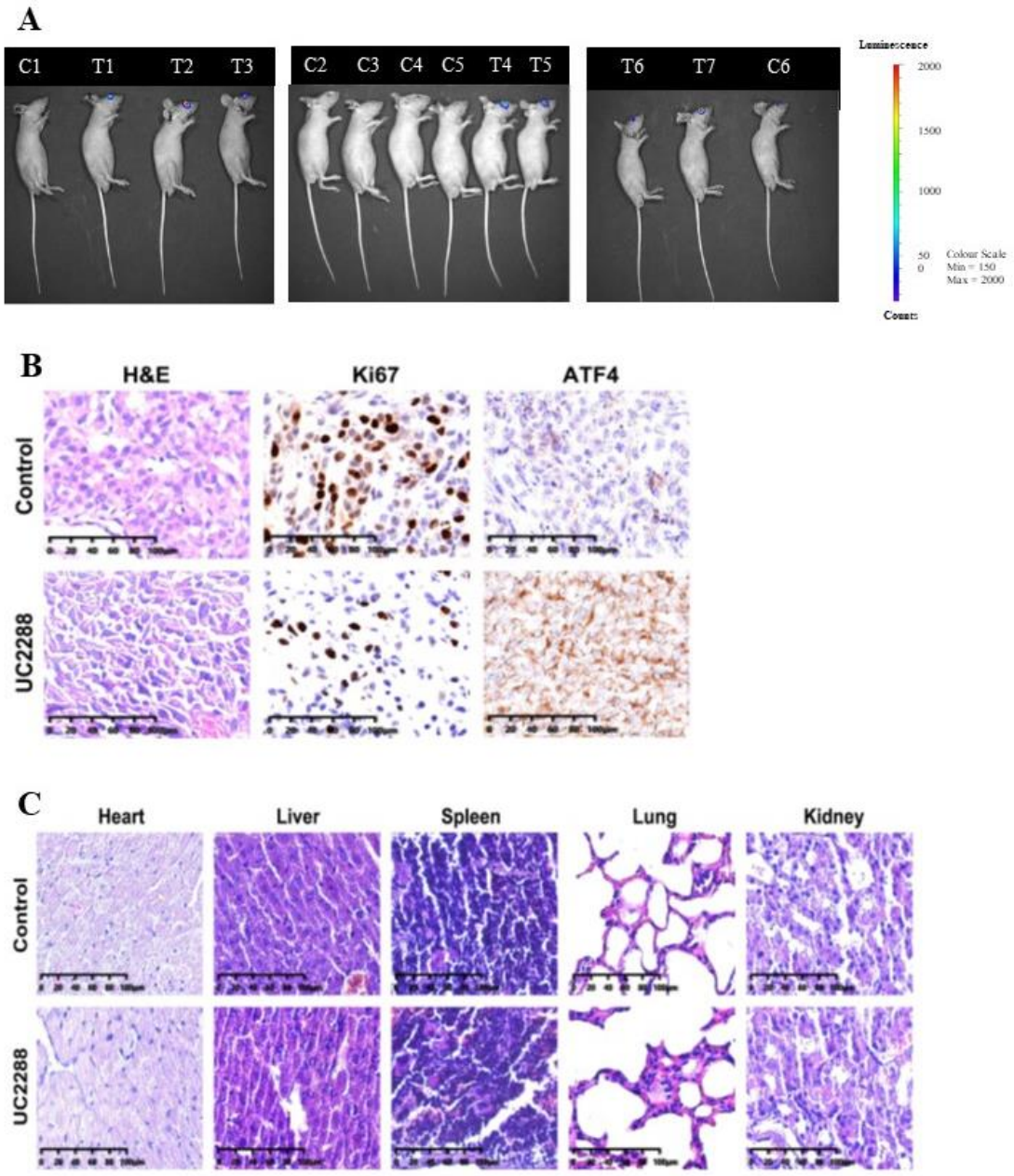

Figure 16. In vivo evaluation of the anti-cancer effect of UC2288.

UC2288 inhibits tumour growth in UM cell xenograft models. BALB/c nude mice were inoculated with 92.1 intravitreally. After tumour formation is confirmed, mice were randomly assigned to oral UC2288 (15 mg/kg) (n=7) or vehicle (n=6) every day for two weeks. (A) shows representative images from vivo imaging system depicting UM xenograft within the eye after UC2288 treatment. Paraffin embedded tissue cryostats from treatment and control were both

taken and stained with hematoxylin and eosin, Ki67 and ATF4 staining (B). Tumour selectivity was confirmed in vivo through staining or other key organs in mice after UC2288 treatment (C).

4.4 Discussion

UM is a rare but deadly cancer. Its drug development pipeline has been greatly hindered by its distinct tumour biology, resistance to conventional therapies, and limited response to immune checkpoint inhibitors (327). Within the current clinical setting, it is well known that metastasis is the most concerning outcome for UM patients as it drastically decreases their overall survival and leads to a rapid decay in health and even death soon after diagnosis (4, 307). It is worse the common therapies for UM are non-pharmacological and only effective for small size of primary tumours with an early detection (21, 35). Although the newly approved Tebentafusp has been approved for unresectable metastatic UM in a sub-group of patients with a distinct genotype, there is only a mild increase in OS and PFS. Thus there is an urgent need for novel, effective and generalised therapeutics to better treat the primary and metastatic UM (46). In the current study, we identified UC2288 as a potent candidate drug with a favourable anti-cancer and anti-metastatic effect.

UC2288 demonstrated potent cytotoxicity in both primary and metastatic UM cell lines with the IC_{50} values superior to many other drugs reported before (Fig. 10A) (48, 84). More importantly, UC2288 has also showed a favourable tumour selectivity against non-tumour eye cells and healthy melanocytes (Fig. 10B), which is a preferred feature of drug therapies in preserving normal eye functions.

The major hurdle of anti-cancer drug development is a lack of physiologically relevant models for pre-clinical drug research. It is highly recognised that the traditional 2D cell monolayers cannot represent the ECM and interactions between tumour and adjacent cells that forms the tumour microenvironment (TME) (328). ECM remodelling along with changes in secretory factors are closely linked to tumour progression, metastasis and immune evasion (329). The ECM has also been identified to contribute to chemotherapy resistance and impact on the efficacy of non-pharmacological treatments (330). Thus, we developed the novel 3D UM culture

models utilising the advanced bioprinting technology for the first time, to better characterise our candidate drug. This model is superior to the traditional 3D culture models, as it has a better control of culture conditions and a long-term supply of oxygen and nutrients (331). UC2288 showed a good penetrability and a consistent anti-cancer effect in the 3D culture models with UM spheroids formed on the optimised hydrogel matrix (Fig. 10C).

It has been noticed that many candidate drugs with superior efficacy in treating cancer cells in *in vitro* models, fail to display the consistent effect in *in vivo* settings. This largely attributes to that in vivo culture models cannot mimic the heterogeneity of tumours (332, 333). Accordingly, we have employed the primary cultures derived from three independent UM patient tumours to validate our findings regarding UC2288. It demonstrated a consistent effect on all the primary cultures indicating the versatile effect of UC2288 in treating UM.

Our further molecular characterisation of UC2288's anti-UM effect showed that it exerts its effect via inducing cytotoxicity and effecting on mitochondria (Fig. 12A-C). Particularly, it is potent in disrupting mitochondrial membrane potential and triggering ROS accumulation, which in turn, impacts on mitochondrial health and function. Mitochondria is considered the "powerhouse" of cells, which controls the survival, proliferation, and metabolism of tumour cells (334). One of the major functions of mitochondria is to produce ROS, which can promote genetic mutations, activate oncogenic signalling pathways, and increase tumour progression. It is also well known that an excessive accumulation of ROS can induce cell death. Thus, agents disrupt mitochondria and/or acting on it to elevate the ROS level, has been considered as a viable strategy in treating cancers.

In addition, our cell death analysis explored the mechanism of cell death associated with UC2288 treatment. Necrosis is shown to be the primary form of cell death (Fig. 12D). And the analysis on the expression of LC3 and P62 suggested that autophagy is likely involved in UC2288-induced necrosis. Autophagy is a regulated cellular process to maintain cell homeostasis via recycling damaged organelles, misfolded proteins and cell debris, which can either protect cells or induce cell death depending on the actual autophagic process (335, 336). In contrast, necrosis is a non-programmed, uncontrolled and inflammatory type of cell death in response to stresses (337). Although autophagy and necrosis are two different cellular processes, they have a complex crosstalk under specific cellular environment, stress conditions and disease states (337).

In the case of overactivated autophagy, it can result in an excessive “self-digestion” of cellular organelles, proteins and cell debris and an induction of ROS production, leading to necrosis (338). The autophagy-related proteins may also interact with necrotic pathways to promote such cell death (339). Thus, our findings suggested that UC2288 is capable of advancing autophagic process leading to necrotic cell death.

To further investigate the UC2288-induced cell death in UM cells, we included the co-treatment of several cell death inhibitors. Our data showed that two chemical inhibitors can potently relieve the effect of UC2288 in reducing UM cell viability (Fig. 14A). Salubrinal and ISRIB are known to inhibit ER stress via inhibiting eIF2α phosphatase enzymes and mitigating the effect of eIF2α phosphorylation through stabilising eIF2B, respectively. The discrepancy of findings from both UM cell lines is likely due to the differences in tumour origins. 92.1 is a primary UM tumour whereas OMM2.5 is derived from a liver metastasis. Metastatic cells are often more aggressive and resistant to treatment harbouring difference epigenetic mutations resulting in the differences in protein signalling (340). In the case of 92.1 and OMM2.5, studies have shown that OMM2.5 indeed display qualities such as increased migration and proliferative properties in xenograft zebrafish models (341). Likewise, OMM2.5 displayed variability in treatment efficacy when compared to primary UM cell lines like 92.1 (317). This results further solidifies the current findings with ER stress variability between the two UM cell lines. UC2288 may also have multitude actions in the ER stress spectrum resulting in the divergence effect upstream that converge into an endpoint of ER stress related cell death.

The ER has a well-documented role in cancer development and progression (324). It is the organelle responsible for the bioprocess of proteins including protein synthesis, folding and maturation. Despite of a rigorous quality control system, up to 30% of all proteins translocated into the ER are folded defectively (342, 343). Thus, a build-up of mis-folded and unfolded proteins triggers ER stress that initiates the unfolded protein response (UPR) - a cascade of protein response to remedy and mitigate stress factors (100) External factors such as hypoxia, nutrients, ROS accumulation and pH change contribute to ER stress. The protein kinase RNA-like ER kinase (PERK)-eIF2α is one of the key sensors to activate UPR (Fig. 17). PERK phosphorylates eIF2α to induce a global reduction of protein synthesis and an activation of ATF4 that modulates genes involved in, redox homeostasis, stress adaptation and cell death.

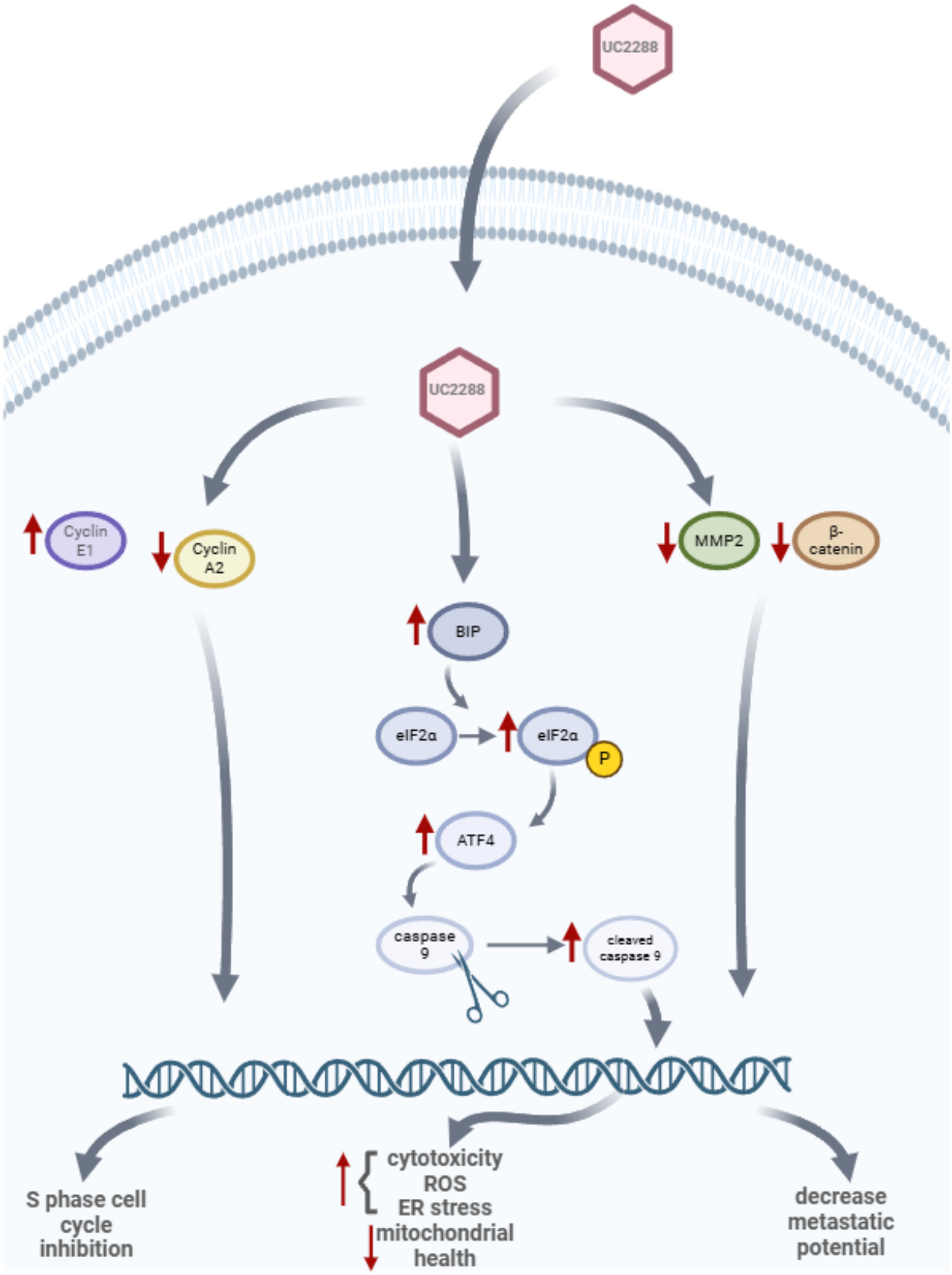
UC2288
UC2288
Cyclin E1
Cyclin A2
MMP2
β-catenin
BIP
eIF2α
eIF2α
P
ATF4
caspase 9
cleaved caspase 9
S phase cell cycle inhibition
cytotoxicity
ROS
ER stress
mitochondrial health
decrease metastatic potential

Figure 17. The proposed molecular mechanism for UC2288. UC2288 simultaneously acts on multiple cellular signalling pathways to induce overall anti-cancer effects in UM cell lines. UC2288 causes S phase cell cycle arrest through modulating cyclin proteins, prevent metastasis through decreasing EMT proteins (e.g. MMP2 and β-catenin) and induces increased ROS production, ER stress and ultimately autophagic cell death through the eIF2α-related UPR cascade.

The ER interacts with the mitochondria to regulate cell homeostasis and proliferation through the Mitochondria-associated membranes (MAMs) (91). The MAMs function as couriers to relocate the ROS produced in the mitochondria into the ROS processing organelle the ER. Likewise, the UPR proteins also act as MAMs and ER stress regulates MAM components. ER stress potentiates autophagy in attempts to restore homeostasis (342, 344-346). In the case of prolonged ER stress, ATF4 remained activated to induce ROS accumulation and mitochondrial dysfunction, trigger autophagy progressing to an advanced stage, eventually leading to cell death (347, 348).

It is worth to mention that the TME often prompts ER stress acting as a double-sided blade for cancer progression. An adaptive ER stress promotes nutrient recycling to prioritise nutrient supply towards the rapidly proliferating tumour cells, facilitates angiogenesis through the activation of downstream UPR pathways and accelerates the epithelial–mesenchymal transition causing an increase of metastatic risk (89). Under prolonged ER stress, the balance of ER stress and cell survival is no longer maintained, thus cell death occurs (89).

Studies have widely explored the crosstalk of ER stress and autophagy in cancer treatment, but little has been known in UM (269, 349-351). In the current study, our findings indicated that the anti-cancer effect of UC2288 is likely mediated through a crosstalk of ER stress, autophagy, and necrotic cell death pathways. It is plausible that UC2288 treatment prompts the autophagic progress to an advanced level in UM cells, which results in a sustained activation of eIF2α-mediated ER stress signalling and a constant mitochondrial dysregulation, disrupting cellular homeostasis and leading to cell death.

It has been noticed that a reduced cell viability can be a result of inducing cell death and/or inhibiting cell proliferation. Thus, we also assessed the influence of UC2288 on UM cell

proliferation. Our data indicated that it could induce S phase cell cycle halt in UM cells (Fig. 13A). Cyclin proteins are the pinnacle marker protein of cell cycle transgression in cancer cells. The cyclin super family is activated by one or more for cells to progress through the different stages of cell cycle (352). In particular, Cyclin E1 activation along with an induction of downstream signalling pathways occurs to allow for cell progress from the preparation G1 phase into the active cell cycle S phase. And Cyclin A2 is required for cells to progress further into S and G2 phase, where DNA is synthesised with quality control prior to mitosis (352, 353). In the current study, the expression of cyclin E1 was increased, whereas that of cyclin A2 was decreased upon the treatment of UC2288 treatment (Fig. 13B). This is consistent with the observed S phase arrest. Abnormalities within the cell cycle are often documented in cancer cells as unrestricted cell cycle progression facilitates tumour growth and metastasis. To this end, cell cycle inhibitors have been explored as potential anti-cancer therapies when administered individually or in combination with other agents. Mills *et al.* assessed the therapeutic effect of a range of cell cycle modulators in combination with conventional chemotherapies in both adult and paediatric cancers. They found a promising result of improved patient outcomes (354). As to the findings of the current study, UC2288 may also serve as a potential adjuvant therapy to improve patient outcomes in UM.

As mentioned above, metastasis is the primary cause of death in UM. Thus, it is important for us to explore the anti-metastatic effect of UC2288. Tumour migration and invasion were assessed using transwell migration and invasion assays in the presence or absence of Matrigel (a pseudo-ECM widely adopted in cancer research) as well as colony formation assay. UC2288 can potently reduce tumour migration and invasion; and also promotes a reproductive cell death (Fig. 15A-D). This is further validated with the expression of EMT markers. MMP2 is an endopeptidase involved in ECM degradation (355). It plays a key role in tumour metastasis and EMT by breaking down ECM components. β-catenin is a key factor involved in Wnt signalling pathway contributing to cell adhesion and transcriptional regulation (356). It is also known that in EMT, β-catenin accumulates in the cytoplasm and translocate to the nucleus to activate EMT transcription factors and enhance mesenchymal markers favouring tumour cell migration and invasion. Our findings indicated that the expression of both MMP2 and β-catenin are decreased drastically after UC2288 treatment (Fig. 15E). Noteworthy, the previous study showed that

autophagy activation downregulates EMT (357), which is aligned with our observation that UC2288-induced autophagy is accompanied with a decreased expression of EMT markers.

UC2288 was previously reported as a p21 inhibitor (358). It is known that p21 is an oncogenic protein and a downstream target of p53. It acts as a cell cycle regulator and its activation can potentiate cancer cell death. In our study, UC2288 shows a potent tumour suppressive effect, which is contradicted to its role of a p21 inhibitor. Indeed, we observed a moderate increase of cell viability in UM cells upon p21 siRNA silencing (Suppl. Fig. 5). Thus, we consider p21 is not likely involved in the anti-UM effect of UC2288.

More importantly, our *in vivo* testing showed that UC2288 has exhibited superior effect in tumour suppression in a UM xenograft model (Fig. 16A). Tumour tissues were significantly disrupted upon its treatment (Fig. 16B), but it has minimal impact on the key non-tumour tissues (Fig. 16C). This suggests that UC22888 has a favourable tumour selectivity in *in vivo* setting, complimentary to our *in vitro* observation (Fig. 10B). It has induced a significant cell death in the tumour tissues, which is accompanied with an elevated level of ATF4 (Fig. 14B), which findings is also consistent with our *in vitro* observation that it can induce ER stress and cell death (Fig.12 and 14).

4.5 Conclusion

In this study, we have identified UC2288 as a novel and effective agent in treating UM. It has displayed a consistent cytotoxicity in in vitro, ex vivo and in vivo UM models with a favourable tumour selectivity and tissue penetration. Its effect is mediated through an induction of ROS accumulation, mitochondrial disruption, eIF2α-involved ER stress and autophagy-involved cell death. It also shows superior anti-metastatic effect in UM cells. Our *in vivo* testing yielded a consistent result for its anti-UM role. Overall, our findings shed a new insight on introducing UC2288 as a potent candidate drug to be further evaluated in clinical setting for its role in the treatment of primary and metastatic UM, which application may also be an adjuvant therapy to existing regimens.

Chapter 5: UC2288 increases in efficacy when treated in glucose depletion culture medium in uveal melanoma cell lines

Abstract

Purpose

Uveal melanoma (UM) is the primary intraocular malignancy in adults. It is associated with a poor prognosis, as metastasis occurs in over 50% of cases. Metabolic reprogramming is a well-known hallmark of cancers and changes in nutrient uptake can affect tumour cell survival. This study provides an insight on the glucose-dependent metabolism in UM cell lines. The previous chapter has indicated UC2288 as a potent anti-UM candidate drug. In this study, we further explored the synergistic effect of glucose deprivation in UC2288 treatment against UM

Methods

UM cell lines were treated with various nutrient deficient medium to ascertain macronutrient deficiency. This effect was validated with the treatment of metabolic inhibitors. The effect of glucose deprivation on UC2288 treatment was analysed using cell viability, reactive oxygen species, lactate dehydrogenase and glycolytic rate assays. The synergistic effect of glucose depletion and UC2288 was also verified in patient tumour-derived primary cultures.

Results

Glucose deficiency was shown to have the greatest impact on UM cell survival. Glucose depletion further increased UC2288-induced cell death, ROS production and cytotoxicity in UM cell lines. Such effect was also observed in UM spheroids generated through 3D bio-printing. Furthermore, consistent findings were obtained in patient tumour-derived primary cultures. Surprising results was shown with IC_{50} where it remained similar in both glucose depleted and glucose sufficient medium. However, Emax was obtained at a lower dose in glucose depleted

medium suggesting synergism occurs when cells are co-treated making UC2288 more efficacious.

Conclusion

Glucose deprivation and UC2288 co-treatment showed a synergistic effect in inducing cell death in UM models. Molecular characterisation indicated that glucose depletion may not enhance the potency of UC2288 but confer metabolic disturbance through additive effects. UC2288 in glucose restricted condition may promise for an improved treatment effect in UM patients.

5.1 Introduction

In cells, metabolism generates energy to support cellular functions. Nutrients for energy production and biosynthesis are obtained from external resources and bio transformed by cellular enzymes to meet the needs of cell growth, development and reproduction (359). Cells rely on the tricarboxylic acid (TCA) cycle to produce energy, which process mainly involves the metabolism of glucose, amino acid, and fatty acids.

In healthy cells, dietary carbohydrates are broken down into individual hexoses and further utilised either anaerobically through oxidation to pyruvate and then into lactate, or aerobically with pyruvate transported into the mitochondria as a part of the TCA cycle and Oxidative Phosphorylation (OXPHOS) reactions (360). Amino acids are key building blocks for a range of cellular events including energy production and anabolic growth. They can generally be classified into 2 groups: the essential amino acids that can only be obtained through dietary intake and the non-essential amino acids that can be synthesised in cells. Both types of amino acids are utilised in the proteolytic pathway to generate energy for cellular functions (359, 361). Lipids like triglycerides, cholesterol, and fatty acids (FAs), play a range of roles in cells. Dietary lipids are absorbed through the intestinal wall, resynthesised and packaged in the enterocytes to be redistributed throughout the body. The packaged lipoproteins are important for energy storage as well as the formation of cell membrane and signalling molecules (362).

Unlike healthy cells whereby energy production and metabolism are highly regulated, tumour cells are well known to carry mutations in genes involved in multiple signalling pathways resulting in distinct characteristics such as extensive cell replication, evasion of cell death and

enhanced invasiveness and metastasis (363, 364). To maintain a high proliferative profile, tumour cells attain metabolic changes to adapt to environmental limitations such as a limited resource of nutrients and lack of oxygen. With the flexibility in metabolic pathways, tumour cells can maintain a rapid ATP production to sustain energy needs, an enhanced macromolecule biosynthesis, and a strict regulation of cellular redox balance (365).

The Warberg effect is one of the hallmarks of tumour cells. Stepping away from the mitochondrial OXPHOS, they heavily rely on aerobic glycolysis for ATP production. In addition, there is also an increased level of metabolic intermediates that are precursors for biosynthesis of macromolecules (366). In mitochondrial OXPHOS, 36 moles of ATP can be produced with every mole of glucose compared; while in glycolysis, only 2 moles of ATP can be obtained with every mole of glucose. However, glycolysis occurs at a much faster rate than OXPHOS in tumour cells, allowing for rapid attainment of energy that is needed for cell proliferation (367). Moreover, glucose transformed into lactate in tumour cells, in favour of speeding up the ATP production as well as energy production in a low oxygen environment (368).

Amino acid metabolism is also greatly impacted in tumour cells. Glutamine is the most abundant amino acid in the body; protein synthesis is yet to meet the largely enhanced need for glutamine in tumour cells (369). In addition to meet the nitrogen supply, tumour cells also partially oxidise glutamine to be fed into the TCA cycle to generate ATP and NADPH (370). Glutamine usage for energy production and reactive oxygen species (ROS) neutralisation is recognised as a hallmark of oncogenesis, termed as glutaminolysis (370). Apart from altered glutamine metabolic profile, tumour cells also display enhanced arginine and tryptophan catabolism for cellular growth and proliferation (371). L-arginine is a critical nutrient for T-cell activation and formation of memory T-cells. Likewise, tryptophan is also widely involved in immune activation and regulation. In tumour cells, enzymes are upregulated to increase the catabolic rates of these two amino acids as required by tumour microenvironment (TME). This effectively reduces the amount of immune cells in the surrounding areas leading to immune evasion (371).

Lipid metabolism is also dramatically altered in tumour cells. Lipids such as FAs, cholesterol and triglycerides are essential building blocks for cell membranes, signalling factors and energy storage (372). A shift towards *de novo* synthesis as the traditional dietary uptake of FAs is often deemed too slow for the rapidly proliferating tumour cells (373). *De novo* synthesis allows for

versatility in usage such as lipid modification for inter- and intra-cellular membranes, protein acylation and lipid mediator formation (373). Excess FAs are converted into triglycerides and cholesterol esters to be stored in droplet forms in tumour cells. The abundance of lipid drops is another hallmark of tumour formation (374).

Uveal melanoma (UM) is a rare yet deadly malignancy that arises from the melanocytes within the uveal track of the eye. Up to 90% of cases arise from the choroid, but some can also occur from the iris (3% - 5%) and the ciliary body (5% - 8%) (375). The median age of UM patients is around 62 years old, and the risk of UM increases with age. UM occurrence is evenly distributed between male and female, however, incidence of UM is significantly higher in Caucasians compared to other ethnic groups (376). Extensive research has identified several genetic mutations associated with UM, notably in the GNAQ, GNA11, BAP1, EIF1AX, and SF3B1 genes. These mutations significantly influence tumour behaviour and patient prognosis. For instance, mutations in GNAQ and GNA11 are present in approximately 90% of UM cases, may indicate early oncogenic events. Loss-of-function mutations in BAP1 are strongly linked to metastatic progression, whereas mutations in SF3B1 and EIF1AX are generally associated with a more favourable prognosis (377). In addition to these genetic mutations, chromosomal abnormalities such as monosomy 3, loss of chromosome 8p, and gain of chromosome 8q are prevalent in UM with an association with an increased metastatic risk and poor patient outcomes (378). Despite advancement in understanding the genetic and chromosomal profiles of UM, these insights have yet to be translated into therapeutic treatments (379).

Despite the extensively studied metabolic alterations in many types of cancers, metabolic information in rare cancers like UM remains little. The development of targeted drug therapies for UM has encountered significant challenges, necessitating the exploration of innovative treatment strategies. In the current study, we investigated the glucose metabolic profile in UM. More importantly, we evaluated the anti-cancer effect of a previously identified potent drug candidate UC2288 in UM cells with or without glucose depletion.

5.2 Material and methods

5.2.1 Reagents

2',7'-dichlorodihydrofluorescein diacetate (CM-H2DCFDA), AlamarBlue Cell Viability Reagent, CyQUANT LDH Cytotoxicity Assay, dimethyl sulfoxide (DMSO), eBioscience Annexin V-FITC Apoptosis Detection Kit, L-glutamine, Penicillin-Streptomycin (P/S), and Roswell Park Memorial Institute Medium (RPMI-1640) with and without glucose were obtained from Thermo Scientific (Lidcombe, NSW, Australia). Foetal bovine serum was supplied by CellSera (Rutherford, NSW, Australia), while thiazolyl blue tetrazolium bromide (MTT) was acquired from Chem-Supply (Gillman, SA, Australia). PVDF membranes were procured from Merck Millipore (Bayswater, VIC, Australia), and JC-1 dye was sourced from Sapphire Bioscience (Redfern, NSW, Australia).

5.2.2 Cell lines

Human 92.1 cell line was gifted by Prof. M.J. Jager (Leiden University Medical Centre, Leiden, Netherlands). OMM2.5 cell line was a kind gift from Dr. S Manisha (University of Melbourne, Melbourne, Australia). All cell lines were authenticated by commercial suppliers through DNA sequencing and comparison. To maintain mycoplasma-free cultures, cells were periodically tested for mycoplasma contamination every four months using the MycoAlert Mycoplasma Detection Kit (Lonza, Mount Waverley, VIC, Australia). 92.1 and OMM2.5 cells were maintained in RPMI medium supplemented with 10% heat-inactivated foetal bovine serum (FBS) (v/v), 1% Penicillin-Streptomycin (P/S), and 1% L-Glutamine. Cultures were incubated at 37°C in a humidified atmosphere with 5% CO_2. To preserve genetic integrity, all cells were used within 30 passages

5.2.3 Cell viability assay

Cells were plated in a 96-well plate at 90% confluency and allowed to adhere overnight. Following incubation, cells were treated with 2288, which was dissolved in DMSO and diluted in the appropriate culture medium supplemented with 1% FBS. After 24 hours of treatment, MTT (0.5 mg/mL) was added, and the cells were incubated for up to 4 hours until purple crystals

were visible under the microscope. The resulting purple formazan crystals were dissolved in DMSO, and the plate was shaken for 5 minutes at room temperature to ensure complete solubilization. Absorbance was recorded at 550 nm using the Multiskan SkyHigh Microplate Spectrophotometer (Thermo Fisher, Lidcombe, NSW, Australia). The IC50 value was determined using the MTT assay and analysed through non-linear regression of cell viability versus drug concentration in GraphPad Prism 7.0 (San Diego, CA, USA).

5.2.4 AlamarBlue assay

The AlamarBlue assay was performed to confirm the results of MTT assay. Cells were seeded and treated following the same conditions as described above. AlamarBlue was diluted (1:9) in FBS-free medium and added to the treated cells. After an incubation period starting with 30 minutes until colour change from blue towards pink is visible, absorbance was measured at 550/590 nm using the Victor X Multilabel Plate Reader (PerkinElmer, Waltham, MA, USA).

5.2.5 Lactate dehydrogenase (LDH) cytotoxicity assay

The LDH assay was carried out alongside the MTT assay by using the supernatant from the treated cells. The supernatant was collected and transferred from the treatment plate, followed by the addition of the LDH assay reagent. The mixture was incubated at room temperature for 30 minutes with shaking on a plate shaker while being protected from light. A stop solution was then added, and absorbance was recorded at 490/655 nm using a microplate reader (Model 680, Bio-Rad, Gladesville, NSW, Australia).

5.2.6 Reactive oxygen species (ROS) assay

Reactive oxygen species (ROS) levels were assessed using the CM-H2DCFDA probe, a general ROS indicator. The reagent was prepared following the manufacturer’s instructions, and cells were incubated in the dark for at least 1 hour and a maximum of 1.5 hour. Fluorescence intensity was then recorded at 450/500 nm using the Victor X Multilabel Plate Reader (PerkinElmer, Waltham, MA, USA)

5.2.7 3D bio-printed cell culture

The Rastrum 3D bioprinter (Inventia Life Science, Alexandria, NSW) was used to create tumour cells encapsulated in a PEG-based hydrogel, forming a complex matrix that simulates the tumour microenvironment. The 3D Large Plug Model was selected, and the structure along with the printing protocol was designed using the Rastrum Cloud platform (Inventia Life Science). Printing was performed in a 96-well flat-bottom plate (Corning) following the manufacturer's instructions. To enhance matrix adhesion, a base inert layer was primed and printed first. Cells were suspended at a concentration of 5×10^6/mL in an activator solution obtained from Inventia Life Science. Printing was then carried out by alternating layers of bioink and cell-containing activator, enabling covalent interactions that embed the cells within the matrix. This alternating droplet technique ensured uniform gelation and an even distribution of cells. Following the printing process, 150 µL of medium supplemented with 10% (v/v) FBS was added, and the cells were incubated at 37°C for five days before drug treatment.

5.2.8 Primary UM tumour derived cell lines and melanocyte primary cultures

Human uveal melanoma (UM) tumour samples were collected with approval from the St. Vincent's Hospital Sydney Human Ethics Committee (HREC/17/SVH/346), and all experiments were performed in accordance with established ethical guidelines and regulations. Following surgical excision, tumours were transported to the laboratory, washed three times in PBS (pH 7.4), and treated with Trypsin-EDTA to dissociate individual cells. The isolated cells were then cultured, ensuring all processing was completed within 24 hours of tumour removal. Isolated cells were then cultured at 37°C in a humidified incubator with 5% CO_2 using RPMI-1640 medium supplemented with 20% FBS (v/v), 1% L-glutamine, 1% penicillin-streptomycin (P/S), 1% ITS, and 2% GCT.

Human primary melanocytes were isolated from healthy donor eyes with the approval from the University of Sydney and the South-East Illawarra Area Human Research Ethics Committees. Primary melanocytes were isolated as previously described (380) and maintained in Ham's F12 supplemented with 10% FBS (v/v), 1% L-glutamine, 10 ng/ml cholera toxin, 100 nM PMA (phorbol 12-myristate 13-acetate) and 0.1 mM isobutylmethylxanthine (IBMX) at 37 °C and 5% CO_2. All experiments were carried out using cells at passages 2 to 5.

5.2.9 Agilent Seahorse Real time analysis

Cells were seeded according to the manufacturer's instructions and incubated over night to allow cells to settle. Analyser cartridge is hydrated on cell seeding day with manufacturer's pH buffer. Cells were treated for either 24 hours as extended treatment time or 4 hours for short treatment time. Rot/AA and 2-DG was diluted and added into the analyser injection wells according to manufacturer's instructions. Statistical tests were conducted within the analyser using the glycolytic rate assay template.

5.2.10 Statistical analysis

All data are presented as mean ± standard deviation (SD), with statistical significance set at $p < 0.05$. Cell culture experiments were performed in triplicates, with three independent repetitions conducted at different time points. Statistical analyses were carried out using one-way ANOVA, followed by Dunnett's post-hoc test for comparisons between multiple independent groups, utilizing GraphPad Prism 7.0.

5.3 Results

5.3.1 UM cells rely on glucose metabolism for cell survival and proliferation

We selected the primary tumour-derived 92.1 and metastatic tumour-derived OMM2.5 cell lines in the current study, which cell lines have been adopted in the study shown in Chapter 4 and in many other studies (317-319). These UM cell lines were incubated in the glucose- or glutamine-free medium for 24 hours. As shown in Fig. 18A, 92.1 and OMM2.5 cell lines both exhibited a decreased cell viability (0.17 folds of the control for 92.1; 0.30 folds of the control for OMM2.5) in glucose-free medium, while that was only mildly reduced in glutamine-free medium (0.75 folds of the control for 92.1; 0.80 folds of the control for OMM2.5). Noteworthy, the treatment was performed in the medium supplied with a reduced percentile of FBS (1% for treatment vs. 10% for culture maintenance). This aims to minimize the influence from other nutrients, hormones and lipids. And subsequent experiments using 2-deoxyl glucose (2DG) for glucose metabolism inhibition, benzylserine for glutamine metabolism inhibition and etomoxir for fatty acid oxidation inhibition were performed to further confirm such findings (Fig. 18B).

Consistently, cell viability of 92.1 was reduced to 0.01 folds of the control upon the treatment of 2DG ($p<0.001$); however, that of benzylserine and etomoxir treatment did not change. In the case of OMM2.5 cells, the viability was also significantly decreased to 0.70 folds of the control in 2DG treatment group ($p<0.01$); while that of benzylserine and etomoxir were only slightly decreased (0.89 and 0.83 folds of the control, respectively). Through targeted nutrient deprivation and metabolic inhibition experiments, we explored the roles of the three main energy recourses in UM cells.

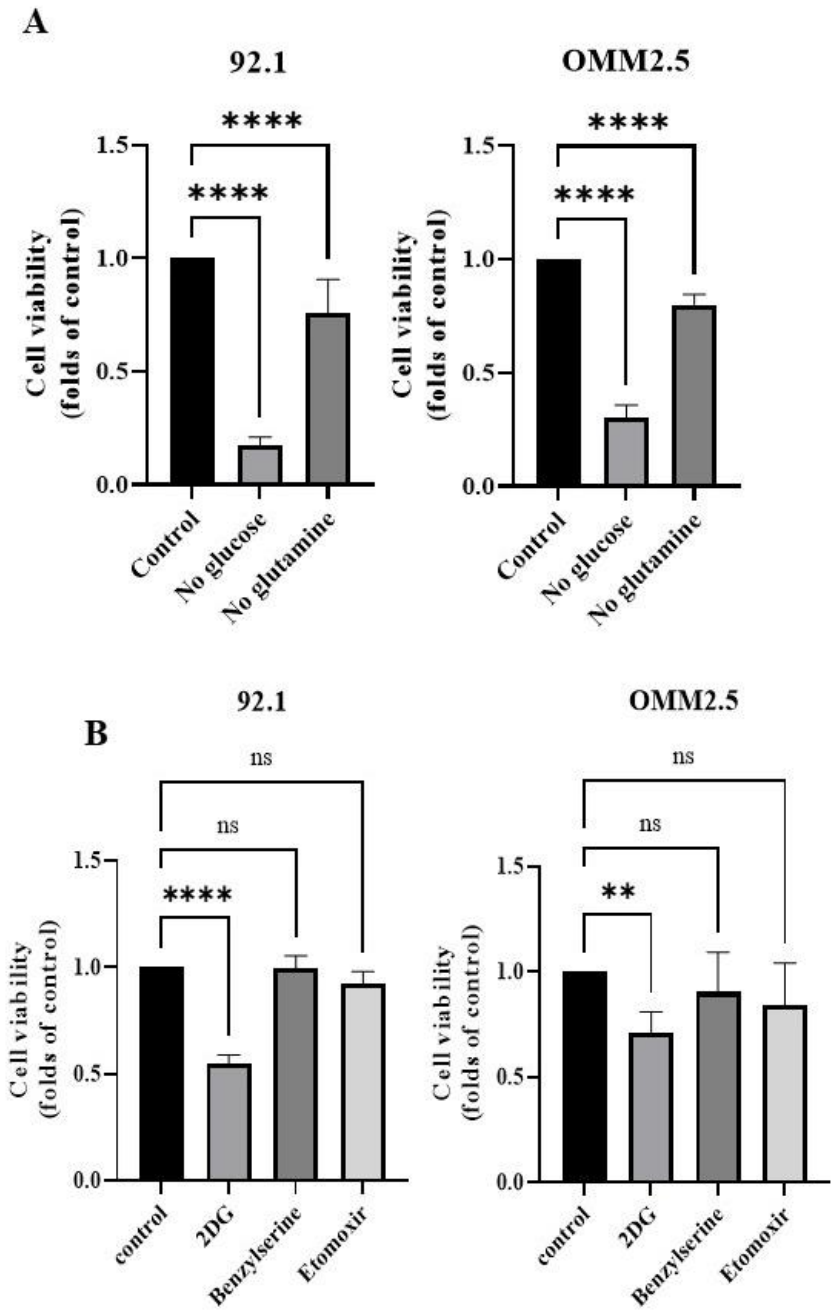

Figure 18. Molecular characterisation of metabolic effect in UM cell lines. Um cell lines demonstrate glucose dependence when treated in nutrient depleted medium. Nutrient depleted medium was brought to exclude either glucose or glutamine, all medium was supplemented with 1% FBS and cells were treated for 24 hours, and MTT cell viability assay was conducted as end point assay to determine cell viability (A). Metabolic activity was further validated using metabolic inhibitors. 2 deoxyl-glucose (2DG) (2mM) was used for glucose metabolism,

*benzylserine (1mM) was used for glutamine metabolism and etomoxir (40µM) was used for fatty acid oxidation. All cells were treated for 24 hours then MTT assay was conducted as end point assay to determine cell viability. The experiments were conducted in triplicate, with three independent replicates performed for each experiment (n = 3). *p < 0.05; **p < 0.01; ***p < 0.001 vs. control by unpaired Student's t test using GraphPad Prism 9.0.*

5.3.2 Glucose depletion promotes the anti-cancer effect of UC2288 in UM cell lines

Considering glucose deprivation significantly reduced cell viability, it is important to know whether there are any clinical applications in the treatment of UM, especially when combined with other pharmacological treatments. To this end, we treated UM cell lines with the candidate compounds identified in our laboratory that have potent anti-cancer effect with or without glucose deprivation. Interestingly, we found that glucose depletion has a pronounced synergistic effect on UC2288, but no other drugs tested (Fig 19A). 92.1 cell line displayed a further 0.37-fold reduction in glucose free medium ($p<0.001$) and OMM2.5 showed a further 0.62-fold decrease in cell viability ($p<0.001$). Such effect was not observed in other drugs tested especially afatinib (84), suggesting a specific influence on UC2288 activity.

Confirmatory analysis was conducted using AlamarBlue cell viability assay. 92.1 showed a further reduction of 0.37 folds and OMM2.5 showed a further reduction of 0.54 folds ($p<0.001$) (Fig. 19B). Furthermore, the anti-cancer potential of UC2288 was estimated as to its IC50 values in both cell lines. Our result showed that the IC50 values did not differ with or without glucose deprivation (IC50 of 2.70 ± 3.19 with glucose and 3.57 ± 1.35 without glucose in 9.21; IC50 of 1.92 ± 0.58 with glucose and 1.92 ± 1.33 without glucose in OMM2.5) (Fig. 19C). However, it is observed that the maximal effect of UC2288 in the absence of glucose was greatly improved achieving a complete cell killing at a significantly lower concentration (3µM) compared to treatment with glucose (8µM). This indicated that the synergistic effect of glucose deprivation does not influence the potency of UC2288 but largely promote its maximal effect in UM cell lines.

As indicated in Chapter 4, UC2288 demonstrated a favourable selectivity to UM tumour cells. Accordingly, further analysis was conducted on human non-tumour eye cell lines as well as three

independent melanocyte primary cultures. The Müller glial cell MIO-M1 and retinal pigment epithelium cell ARPE were selected as to be aligned with our previous study. In addition, we also included three healthy melanocyte primary cultures obtained from three independent healthy donors. As shown in Fig. 19D, glucose deprivation did not change the cellular effect of UC2288 in non-tumour cells; thus, its synergistic effect is specific to UM tumour cells.

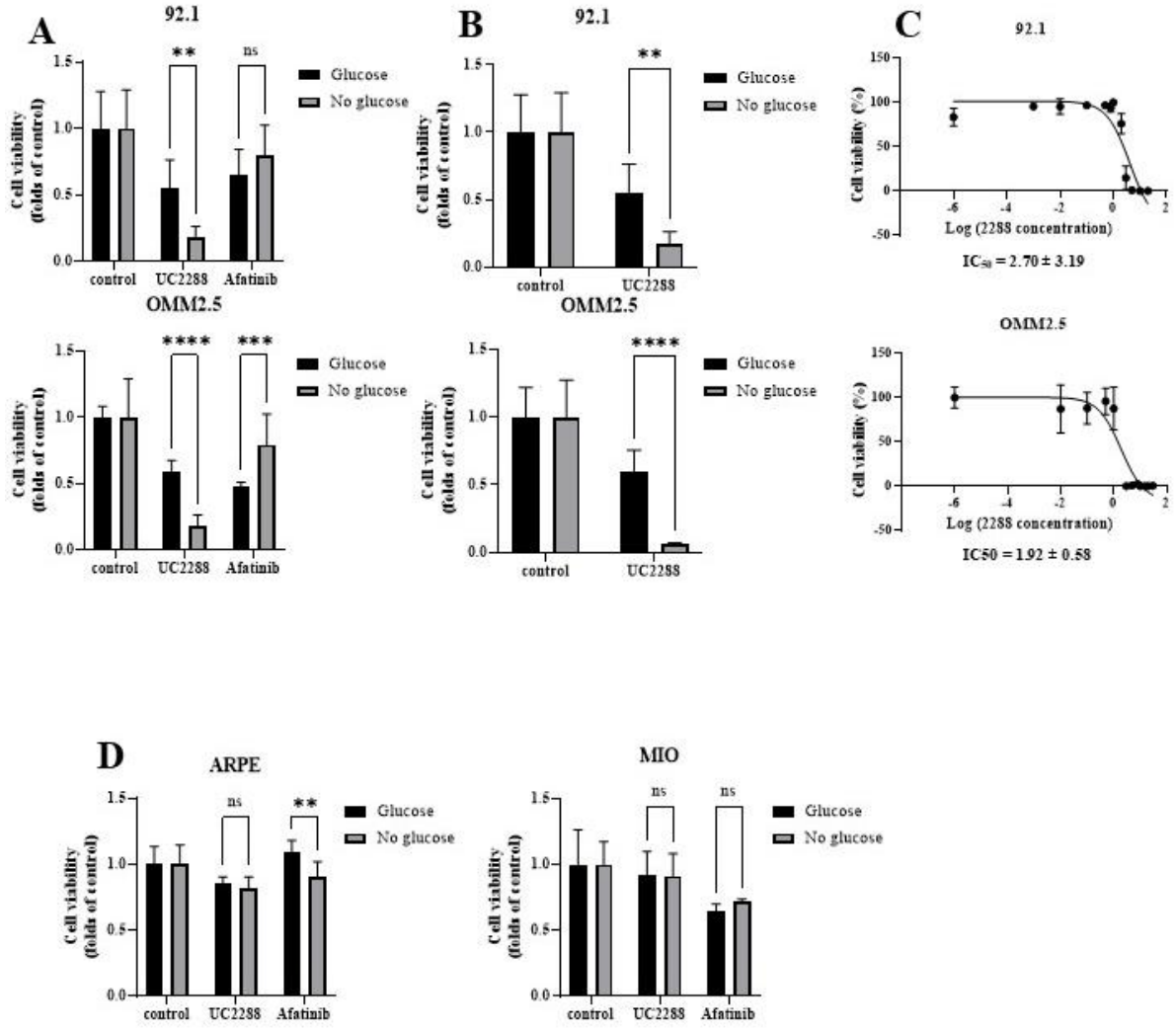

Figure 19. Molecular characterisation of UC2288 effect in UM cell lines when treated with glucose depleted medium. The effects of UC2288 co-treatment with glucose depleted medium is tested on UM cells for potential additive effects. Cell viability study was conducted with cells seeded and treated with UC2288 (3μM) and afatinib (5μM) in glucose depleted medium for 24

*hours. Cell viability was determined using MTT cytotoxicity assay (A). Confirmatory study was conducted under similar condition with AlamarBlue assay (B). IC_{50} of UC228 in UM cell lines was estimated using Graphpad Prism as described in the previous chapter. Non-tumour cell lines ARPE and MIO-M1 were also tested with UC2288 (3μM) in glucose depleted medium. Cell viability was tested with MTT assay (D). The experiments were conducted in triplicate, with three independent replicates performed for each experiment (n = 3). *p < 0.05; **p < 0.01; ***p < 0.001 vs. control by unpaired Student's t test using GraphPad Prism 9.0.*

5.3.3 Glucose deprivation enhanced the molecular effect of UC2288 on UM cell lines

As shown in Chapter 4, UC2288 exhibited a significant cytotoxicity in UM cells, accompanied with an elevated ROS level and impaired mitochondrial health. Thus, the molecular effect of UC2288 was further investigated in glucose-containing and glucose-free media accordingly. 92.1 displayed an increased cytotoxicity from 1.35 folds to 2.09 folds upon the treatment of UC2288 in the presence and absence of glucose, respectively (Fig. 20A). A similar result was also observed in the case of OMM2.5 cells (UC2288 cytotoxicity increased from 1.50 folds to 3.63 folds in the presence and absence of glucose). ROS level often reflects oxidative damage and cytotoxic effects of drug treatment. 92.1 exhibited an increase in ROS production from 1.95 folds to 5.57 folds in the presence and absence of glucose, respectively (Fig. 20B), while a consistent result was yield in OMM2.5 cells (an increase of ROS level from 2.00 folds to 18.17 folds in the presence and absence of glucose). These findings collectively indicated that glucose-free medium significantly promoted cytotoxicity and ROS production upon UC2288 treatment in UM cells, suggesting a critical role of metabolic stress in amplifying oxidative damage of UC2288 in conjunction with glucose deprivation.

Mitochondrial health is also a key indicator of cell survival. JC-1 assay was adopted to assess mitochondrial membrane potential, enabling a more thorough evaluation of cellular health and metabolic function following UC2288 exposure. Surprisingly, although UC2288-induced mitochondria health damage was more dramatic in the absence of glucose in both cell lines (Fig. 20C), such effect was to a much less extent compared to that observed in ROS production and cytotoxicity (a further 0.17 fold decrease in 92.1 and 0.16 fold decrease in OMM2.5). This

suggested that the synergistic effect of glucose deprivation may primarily impact on mitochondrial function rather than influence its health.

As indicated in Chapter 4, the traditional 2D monolayer cannot represent the complex tumour physiology. It is highly desired that 3D culture models can be used in cancer drug development. Accordingly, the current study evaluated the anti-cancer effect of UC2288 under glucose-deprived condition in the 3D bio-printed UM cell cultures. In such an advanced model, UM cells were encapsulated in hydrogel matrix to mimic the tumour microenvironment and better assess drug distribution and efficacy. UC2288 was able to achieve greater cell death in glucose free medium at a lower dose in 3D bio-printed UM cultures (Fig. 20D). Cell viability decreased to 0.29 folds in glucose free medium compared to 0.54 folds with glucose in 92.1 cells ($p<0.05$). These findings suggest that glucose-free medium enhances the drug's effectiveness, allowing for a greater therapeutic impact at a lower dose.

Given that tumour heterogeneity has consistently presented a significant challenge to achieving effective tumour suppression, it remains a critical factor in the development of targeted therapeutic strategies. To better validate UCC2288, three patient-derived tumour primary cultures were utilized to assess the effectiveness of UC2288 in the presence or absence of glucose. Such a clinically relevant *ex vivo* model is desired to evaluate the therapeutic potential of UC2288 in a physiologically representative environment. As shown in Fig. 20E, treatment in glucose free medium has further promoted the efficacy of UC2288 in reducing UM cell viability. UM primary cultures displayed a further decrease in cell viability, a further increase in ROS accumulation across all primary cultures. The primary culture 3 showed no significance in the effect of UC2288 with or without glucose as both conditions achieved close to complete killing. This may be due to the heterogenous nature of UM tumours with diverse sensitivity to drugs. Thus, UC2288 was effective to induce a significant anti-UM effect in an heterogenous tumour environment and its effect was greatly amplified by glucose deprivation.

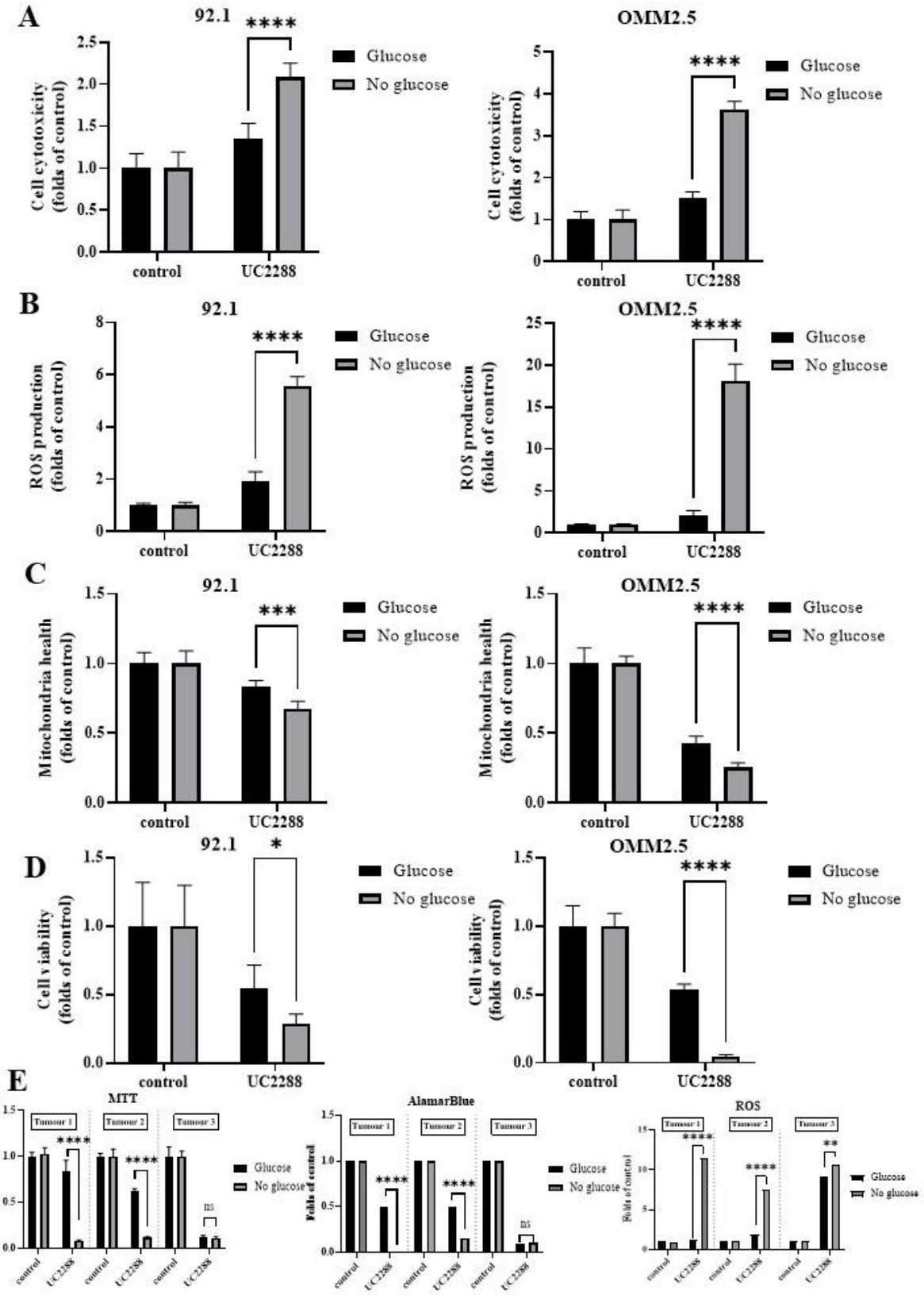
A
92.1
OMM2.5
Cell cytotoxicity (folds of control)
Glucose
No glucose
control
UC2288
****
B
ROS production (folds of control)
C
Mitochondria health (folds of control)
***
D
Cell viability (folds of control)
*
E
MTT
AlamarBlue
ROS
Folds of control
Tumour 1
Tumour 2
Tumour 3
ns
**

*Figure 20. The cell death profile of UC2288 and glucose depletion on UM cell death. Further studies have been implemented to better evaluate the effect of UC2288 and glucose depletion on UM cell lines. The LDH assay (A) is superimposed on the MTT assay as it only requires the supernatant of the treated cells. equal amounts of LDH assay are added to extracted medium and incubated before absorbance is read. ROS assay utilises the chemical CM-H2DCF-DA which was diluted PBS according to manufacturer's instructions before incubating it with cells for up to 1.5 hours (37°C) (B). JC-1 assay was diluted and according to the manufacturer's instructions and incubated with cells for 20 minutes (37°C) before measured twice at differing wavelength as written in the protocol (C). (D) Cells were printed with PEG-hydrogel and incubated to allow 3D structure formation for 5 days, then cells were treated with UC2288 with and without glucose for further 4 days before tested with AlamarBlue assay. (E) UC2288 and glucose depletion was tested on patient tumour derived primary cell lines. Cells were treated as described in the previous assays and MTT, AlamarBlue and ROS assay was performed in the same way as described as before. Data are presented as fold of control (mean ± SD) and statistical analysis was done with unpaired Student's t test. All experiments were done in triplicate with n=3 in each repeat. *p < 0.05; **p < 0.01; ***p < 0.001 vs. control using GraphPad Prism 9.0.*

5.3.4 The impact of UC2288 on glucose metabolism in UM cells

As shown in Chapter 4, UC2288 can impact on mitochondrial health and lead to ROS accumulation in UM cells. In the current study, glucose depletion exhibited a synergistic effect in further enhancing its effect. Thus, it is possible that the pharmacological effect of UC2288 may partially be attributed to disturbing glucose metabolism and TCA cycle in UM cells, in line with the observation that glucose deprivation more impacts on UC2288-induced mitochondrial dysfunction rather than impairing its health (Fig. 20B and C).

UC2288 boosts the effects of glucose omission. Through the Agilent Seahorse Glycolytic Rate Assay, real-time extracellular acidification was evaluated, providing critical insights into the dynamic changes of glycolytic activity and metabolic adaptations of the UM cells in response to UC2288 treatment. UM cells were treated for 4 and 24 hours to assess their glycolytic rates in a short or long duration. The basal glycolic rate was changed over time in both cells. The

glycolytic rate was elevated for the short treatment duration (92.1 depicted an increase of 152.82 glycoPER and OMM2.5 showed an increase of 76.4 glycoPER (pmol/min/Cells)) but returned to normal level in the long run (Fig. 21A). Compensatory glycolytic rates remained steady with an acute treatment of UC2288 but decreased with a prolonged duration (92.1 showed a decrease of 308.77 glycoPER and OMM2.5 showed a decrease of 45.8 glycoPER (pmol/min/Cells)) (Fig. 21B). The difference in the degree of change between the 2 samples may be due to the difference in cell line origin. Metastatic UM cells has been discussed in the previous chapters and is known to possess mutations that increase aggressive and proliferation. With an increase in drug treatment resistance. It is understandable the changes in OMM2.5 is not as high when compared to 92.1. UC2288 likely increases basal glycolysis in UM cells to engage in compensatory glycolysis, ultimately leading to metabolic stress and decreased cell viability. And glucose

deprivation aggravates such effect to promote its impact on cellular metabolism.

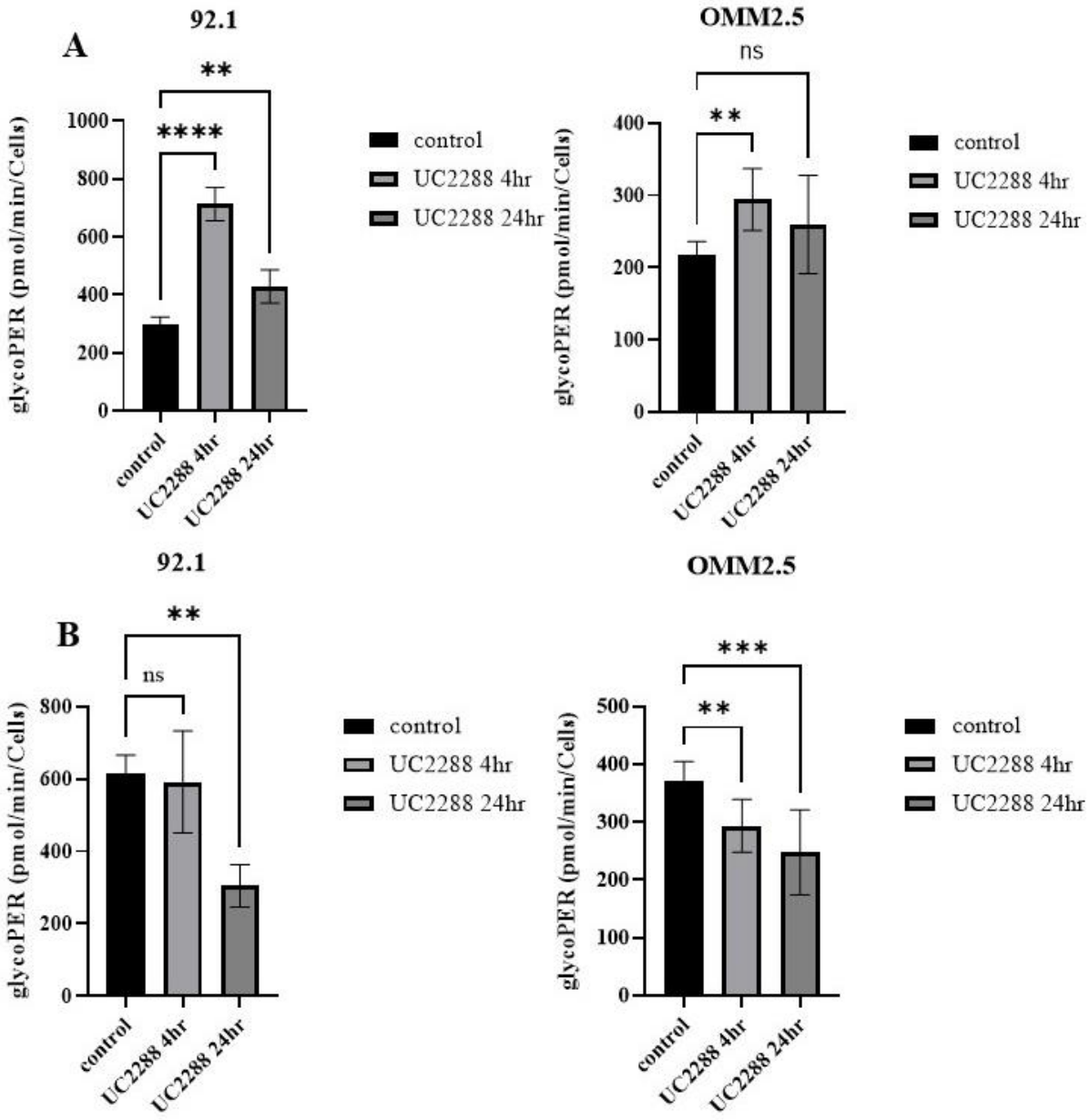

Figure 21. Glycolysis changes over time when UM cells are treated with UC2288. UM cells undergo specialised analysis utilising the real-time metabolic change analyser Agilent Seahorse. Cells were seeded according to manufacturer's instructions and analysing cartridge was hydrolysed a day prior as advised. UC2288 (3µM) was treated at 2 time points with 24 hours as extended treatment and 4 hours and immediate treatment. Rot/AA and 2DG was injected into assay wells as pre-determined by the manufacturer's assay settings and resulting analysis was

*calculated by the analyser using raw values. (A) shows the basal glycolysis of UM cells prior to metabolism inhibition induced by the analyser. (B) shows the compensatory increase in glycolysis due to mitochondria oxidation inhibition by Rot/AA. where data are presented as glycoPER (mean ± SD), and statistical analysis was done with one way ANOVA. All experiments quadruplet with n=1 in each repeat. *p < 0.05; **p < 0.01; ***p < 0.001 vs. control using GraphPad Prism 9.0*

5.4 Discussion

UM is the most common intraocular malignancy in adults and its treatment options remain limited, particularly for metastatic diseases (379). Despite advancements in cancer drug development, effective systemic therapies for UM are not proved (308, 311). UM is associated with a high mortality rate (up to 52% within 35 years), with approximately 80% of UM-related deaths occurring within the first 10 years of diagnosis (4). Its poor prognosis is significantly exacerbated by metastasis, as up to 50% of patients have developed metastatic diseases resulting in rapid decay of health and quality of life. This emphasises the urgent need for novel and effective drug therapies in the treatment UM and its metastatic diseases. Novel strategies such as exploiting metabolic dependencies and signalling pathways, may improve patient outcomes and address the challenges associated with such tumour progression and metastasis.

Among the three main mechanisms involved in the TCA cycle, tumour cells incline to heavily rely on aerobic glycolysis for ATP production. This study first investigated the role of glucose, fatty acid and glutamine metabolism played in sustain UM cell survival with the approaches of nutrient exclusion or metabolic inhibitor treatment. As shown in Fig. 18, UM cells significantly dependent on glycolysis for cell growth compared to other macronutrients. This suggested the clinical applications of glucose deprivation as a combination therapy to drug treatment.

As shown in Chapter 4, UC2288 has been shown to have a potent anti-cancer effect in UM cells. The current study obtained evidence to demonstrate that glucose deprivation can specifically amplify the anti-UM effect of UC2288 (Fig. 19A and B). Noteworthy, such synergistic effect of glucose deprivation to UC2288 is also tumour selective (Fig. 19D).

A decreased cell viability may be a result of increased cytotoxicity and/or reduced cell proliferation. Further molecular analysis showed that glucose depletion largely aggravates the cytotoxicity of UC2288 and its impact on mitochondrial function and mildly promoted its influence on mitochondrial health (Fig. 20).

Interestingly, glucose deprivation did not change the potency of UC2288 (IC_{50} values) in reducing cell viability but greatly enhanced its maximum efficacy (Fig. 19C). This finding suggests that glucose is extensively involved in the mode of action of UC2288, possibly inducing metabolic stress or modulating cellular signalling pathways. As the mitochondria generally provides energy and biomaterials for all cellular functions, this suggests a potential divergence in the underlying mechanisms.

Given that mitochondrial dysfunction and ER stress are the primary outcomes of UC2288 treatment in UM cells, it is worth to further investigate the underlying mechanisms of UC2288-induced anti-cancer effect in relation to glucose metabolism. The well-established Agilent Seahorse XF analysis measures extracellular acidification rate (ECAR) and oxygen consumption rate (OCR) to calculate cellular glycolysis over time. ECAR determines the conversion of pyruvate to lactate, including basal OXPHOS levels; while OCR isolates and subtracts OXPHOS to derive basal glycolysis (glycolysis at rest). Mitochondrial function is inhibited by Rotenone and Antimycin A (Rot/AA), suppressing OXPHOS and increasing glycolysis to sustain cellular function, termed as compensatory glycolysis (381).

The outcome of the assay generally indicates the glycolytic rate of UM cells. In the current experimental setting, UM cell lines were treated with UC2288 for a short and long period. The acute treatment of UC2288 induced an initial spike in basal glycolysis, which gradually returned to baseline level with a prolonged treatment duration (Fig. 21A). Notably, no compensatory glycolysis was observed immediately following UC2288 administration, but the capacity for compensatory glycolysis was further declined over time (Fig. 21B). These findings suggest that UC2288 may induce a metabolic reprogramming with an accelerated glycolysis to meet the needs for cell survival initially. However, as to a prolonged treatment, the mitochondria is overloaded with accumulated stress, ultimately leading to cell death. Thus, glucose deprivation likely disrupts the initial metabolic reprogramming and in turn, promoted the maximal efficacy of UC2288.

Metabolic reprograming is a definitive feature of tumours and plays a pivotal role in tumour progression and survival. Tumour cells shift metabolic processes to meet the need for their rapid growth and survival in a highly dynamic and unforgiving manner (382). Cell metabolism in tumours is highly influenced by external stresses such as blood perfusion, nutrient uptake and waste secretion (383). Blood perfusion is imbalanced within solid tumours as aberrant formation of vascular network resulting in fluctuations in blood flow and oxygen delivery (383). Hypoxia in tumours encourage the production and secretion of Hypoxia-inducible factor 1-alpha (HIF-1α), which in turn, alters metabolic profile to favour glycolysis through increasing glucose transporter expression (384). Paradoxically, irregular vasculature limits nutrient supply leading to a change in nutrient gradients in tumours (385). It has been noticed that lower glucose levels were widely found in tumour tissues and surrounding extracellular fluids. Conversely, glucose metabolism is often accelerated in tumours (385, 386). To accommodate the discrepancies in nutrients and oxygen levels, tumour cells exhibit remarkable flexibility and plasticity in metabolism to sustain their growth. Namely, utilising amino acid such as glutamine, lipids like fatty acids and glucose metabolites such as lactate to fuel the TCA cycle in energy production and anabolism (387).

Through the dedicated works of Otto Warburg, glucose metabolic reprogramming is one of the most well-known hallmarks of cancer progression (388). Normal cells in nonmonic condition can generate up to 36 mol of ATP through 1 mol of glucose via OXPHOS. In contrast, cancer cells preferentially convert pyruvate to lactate via glycolysis instead of channelling pyruvate into the TCA cycle, even though the net yield of ATP is drastically smaller than that of OXPHOS (389). To meet their increased glucose demands, cancer cells enhance glucose uptake by upregulating glucose transporters such as GLUT1. This upregulation facilitates greater glucose influx, supporting accelerated glycolysis (390). This preference is due to the upregulation of LDH, which regenerates NAD^+ from NADH, sustaining high glycolytic rates. The lactate produced is then exported into the TME, aiding nutrient distribution to tumour cells (389). Such symbiosis between lactate production and consumption in tumour cells effectively mitigate issues such as hypoxia and nutrient deficiency within the tumour mass (391). Moreover, lactate production from pyruvate also generates NADPH, a ROS scavenger, thereby reducing oxidative stress in cancer cells (392). Additionally, lactate within the TME promotes metalloprotease activity, facilitating extracellular matrix degradation and enhancing cancer metastasis and invasion (393).

Apart from being a major source of energy production for cancer cells, metabolite intermediates from the glycolytic pathways are also utilised in multiple anabolic processes including nucleic acid, protein and lipid biosynthesis (394). This metabolic reprogramming supports the rapid proliferation of cancer cells.

Given the multitude of glycolysis has on tumour growth, invasion as well as management of nearby non-cancer cells, it is second nature to attempt to target glycolysis through inhibiting glucose transporters, key enzymes involved in the glycolytic pathways such as hexokinase and phosphofructokinase, as well as glucose transformation enzymes like pyruvate dehydrogenase kinase and lactate dehydrogenase (395). Indeed, glucose metabolism has been correlated with metastatic UM. Metastatic lesion with higher glucose uptake levels were associated with up to a 4-fold reduction in overall survival (396). In monosomy 3 UM samples, a compensatory increase in GLUT1 transporters was observed, likely due to the decreased expression of GLUT2, located on chromosome 3q26.2 (397). Evidently, quercetin was found to impair UM proliferation through interfering glucose uptake and metabolism (398). Although advancements have been made to identify the relationship between glucose metabolism inhibition and anti-tumour effect in UM cells, limited research has been conducted with glucose inhibition as an additive effect to enhance UM treatment. Here we propose glucose inhibition not as a form of treatment but as an effective addition to enhance drug treatment outcomes in UM.

The findings of this study indicated a predominant reliance on glucose metabolism in UM cells in comparison to glutamine or fatty acid metabolism. Glucose consumption was further enhanced upon the treatment of UC2288. Thus, a disruption of glucose supply synergistically aggravates the effect of UC2288. Consistently, we observed that UC2288 impedes on UM metabolic activity, in particular glucose consumption.

As glutamine consumption and fatty acid oxidation inhibition showed minimal impact on UM cell viability (Fig. 18B), it is plausible that UC2288 may specifically influence glucose metabolism and/or fatty acid synthesis. Accordingly, future investigation will be required to elucidate the detailed mode of action of UC2288 in relationship to these specific metabolic pathways. As glycolysis is increased to produce lactate, it may bypass the mitochondria electron transport chain and TCA cycle to produce energy. Identifying glycolysis metabolite intermediates may examine the influence of UC2288 in glucose metabolism.

In the realm of macronutrient metabolism, lipid metabolism reprograming has been newly identified as a hallmark of cancer malignancy (399). Lipids are widely used by tumour cells to create basic cellular structures for growth. Owing to this, tumour cells often have an increased lipid uptake, storage and lipogenesis to meet their growing needs for rapid proliferation (400). It is well known that fatty acid metabolism remodelling, especially *de novo* fatty acid synthesis is greatly increased in tumour cells when compared to normal counterparts due to their increased metabolic demands and a reduction in serum lipid availability (399, 401). On the other hand, glucose and glutamine are used as substrates in the TCA cycle to produce acetyl-CoA for fatty acid synthesis under nonmonic conditions. Due to hypoxia, nutrient imbalance is often encountered in tumour masses requiring an alternative source of fatty acids. In hypoxic cells, *de novo* fatty acid synthesis is bypassed through scavenging serum fatty acid and those in the TME (402). As a matter of fact, the cell killing effect of FA synthesis was reversed with the addition of the FA palmitate (403). The significance of fatty acid synthesis and lipid metabolism in cancer lies in their essential roles in supporting tumour growth, survival, and therapy resistance, making them promising targets for novel therapeutic strategies.

Lipid metabolism plays a critical role in the progression of UM, driving tumour growth, survival, and metastasis through the reprogramming of fatty acid synthesis and lipid utilization pathways. In particular, recent findings indicate acetyl-CoA carboxylase (ACC) was shown to be elevated in UM increasing FA synthesis (404). ACC is the rate limiting enzyme found in the ER that is responsible for the initiation of long chain FA synthesis. This enzyme irreversibly acetyl CoA to malonyl CoA to be used for both energy and FA synthesis (401). Additionally, UM cell cytoplasm is found to contain high levels of lipid droplets as well as the production structural protein adipophilin. Under hypoxic or high energy dependence conditions, decreased levels of adipophilin emphasised the increase in lipid usage and were associated with an increased metastatic risk and more aggressive phenotypes (405, 406). Indeed, studies have found co-treatment targeting metabolic pathways such as fatty acid synthase (FASN) and mTOR was successful in inhibiting UM growth (407).

Likewise, metabolite composition may also be explored to elucidate lipid metabolism with or without UC2288 treatment in UM cells. And the expression of protein markers such as ACC, FASN and SREBP1 that are key regulatory proteins in fatty acid synthesis may be assessed to

indicate the likely signalling pathways involved. And *in vivo* validation of the current findings is highly desired in UM xenograft mouse models to consolidate the clinical application of current findings.

Overall, this study demonstrated that UM cells are primarily dependent on glucose rather than glutamine or fatty acid oxidation for its metabolism. Glucose deprivation has shown a synergistic effect in promoting the anti-cancer effect of UC2288 in UM cells, which is mainly mediated through further increasing ROS production and its cytotoxicity. There is an increase in glucose consumption in UM cells when treated with UC2288, which may provide molecular mechanism to support the synergistic effect of glucose deprivation in UC2288 treatment in UM. Although the results are yet to be solidified, glucose deprivation may serve as an effective combined therapy to boost the anti-cancer effect of UC2288 in the treatment of UM.

Chapter 6: conclusion and future directions

6.1 conclusion

UM is one of the most common eye cancers in adults with a ~50% metastasis rate. There is a diminishing survival rate of UM, once metastasis is confirmed (4). Though genotypical risks factors such as mutations within GNAQ/11, BAP1 and monosomy 3 and phenotypical risks such as Caucasian decent, fair skin and iris colour and increasing in residential latitude, have been identified for UM. This information has yet to be translated therapeutically. In fact, common therapeutic options for UM patients remain non-pharmacologically with a potential irreversible impact on vision (19). Advancement in non-pharmacological therapeutical development is now effective in treating primary UM, however micro-metastasis has often formed prior to the initial diagnosis (310). Currently, there is only one drug approved for the treatment of unresectable metastatic UM. Nonetheless, due to genetic limitations, only a portion of patients may benefit from tebentafusp for a mild increase of survival (46). As previously discussed, numerous clinical trials investigating pharmacological interventions in UM have yielded disappointing outcomes. Consequently, mortality rates associated with this deadly cancer remain high, underscoring the critical need for effective therapeutic drugs to improve patient outcomes.

It is imperative that novel therapeutic targets are highly desired in UM. Here we recontextualize an established receptor - epidermal growth factor receptors (EGFR) for the treatment of UM. EGFR is a family of transmembrane proteins with four subfamilies of receptor tyrosine kinases: EGFR (HER1), HER2, HER3 and HER4 (125). Although EGFR (HER1) has limited effects in UM (84), the other receptors have yet to be explored. Here using afatinib (84) and lapatinib (Chapter 2) as representative drugs, we showed that HER2 is a targetable receptor in the treatment of UM. Targeting HER2 receptors in UM was able to greatly reduce cell viability, prevent metastasis and reproductive cell growth. The effect of HER2 inhibition was tested in *in vitro*, *ex vivo* and *in vivo* models to ensure wholistic effect. HER2 inhibition-induced anti-UM effect was shown to be tumour selective with minimal disturbance in healthy eye cell lines and no apparent side effects in xenograft mouse models. Thus, HER2 has been proven to be a viable therapeutic target in treating UM.

Building upon the concept of reimagining classical paradigms, we have undertaken an in-depth exploration of cell death signalling pathways to identify novel therapeutic approaches derived from traditional ideas. This endeavour involves examining established mechanisms such as apoptosis, necrosis and the unconventional cell death method – autophagy. Autophagy holds both tumorigenic and tumour suppressive effect. It was initiated thought to maintain homeostasis and sustain cell survival in stressful environments (20). A prolonged progress of autophagy often results in an overload leading to cell death. In Chapter 3 and 4, we uncover that autophagy may be closely linked to ER stress and ROS production in UM. UC2288 is a novel small molecule compound with potent anti-UM effect in *in vitro*, *in vivo* and *ex vivo* models. As UC2288 is a soluble epoxide hydrolase (sEH) and p21 inhibitor, it was thought to exert its anti-cancer effect through regulating epoxy fatty acid metabolism or disrupting p21 signalling. Surprisingly, we showed that either mechanism is related to its anti-UM effect.

More excitingly, our study shown in Chapter 5 indicated that UM cells primarily depend on glucose metabolism for survival and proliferation. And glucose depletion has a selective synergistic effect to UC2288 in inducing cell death and ROS accumulation. Further studies showed that glucose depletion does not directly impact on the potency of UC2288 but exerts an additive effect to its anti-UM effect. It is hypothesised that UC2288 may induce a metabolic reprograming involving glycolysis and/or fatty acid synthesis. Future studies with pathway identification and metabolite intermediate determination are expected to better understand such synergistic effect of glucose deprivation.

6.2 Future directions

Although progress has been made for receptor and novel compound identification, detailed studies in regard to mechanism of action through signalling pathways and adjustment of novel molecule chemistry to better target UM is greatly desired. Future research in this direction may include:

1. Our study has demonstrated that HER2 receptors are expressed in both UM cell lines and patient tumour samples, with further validation through TCGA database analysis. Emerging evidence suggests that HER2 expression may play a role in tumour progression,

survival signalling, and therapeutic resistance, highlighting its potential as a therapeutic target in UM. This finding also raises the possibility that other receptor subfamilies, previously overlooked, may have therapeutic relevance in UM. Therefore, we advocate for a re-evaluation of common oncogenic factors, including hypoxia-inducible factors, tumour necrosis factors, and vascular endothelial growth factors, along with their respective receptors. A deeper investigation into these pathways may reveal novel, previously unrecognized therapeutic targets for UM.

2. UC2288 has demonstrated potent anti-UM effects both *in vitro* and *in vivo*, inducing cell death and inhibiting metastasis. However, its primary effector receptor remains unidentified. Detailed proteomic and pathway analyses could provide a breakthrough in uncovering key protein changes, leading to the identification of upstream signalling pathways and the drug's target protein responsible for initiating the cell death cascade. Identifying these targets could enhance UC2288's selectivity and specificity, improving its potency while minimizing adverse effects.
3. The combination of glucose inhibition and UC2288 resulted in a significantly greater increase in cell death compared to other anti-cancer drugs. However, the full extent of its additive effect remains unclear, limiting its clinical application. Further studies, such as proteomic analysis to assess changes in key protein expression, could provide deeper insights into this synergy. A better understanding of this interaction may facilitate optimized clinical trial designs, enabling improved glucose depletion strategies through combination dosing or dietary modifications to enhance its feasibility in clinical settings.
4. Similarly, metabolite composition analysis should be conducted to obverse the difference in metabolite concentration in UC2288 treatment with and without glucose to identify the potential inhibition caused by UC2288. This can identify key proteins that is responsible for UC2288's enhanced effect. This is proposed to be down through HPLC analysis of protein lysates to identify increases or decreases in glucose and lipid metabolites.
5. Due to the eye's secluded nature and restricted systemic accessibility, effective drug delivery into the aqueous humour remains a major challenge in ocular treatment. While UC2288's high potency makes it a viable candidate for intraocular micro-injection, less invasive approaches, such as nanoparticles and extracellular vehicles (EVs), represent the forefront of drug delivery innovations. Conjugating UC2288 with nanoparticles or EVs

could enhance its ocular delivery, improving therapeutic efficacy while minimizing invasiveness.

6. Given the heterogeneity of UM tumours, the wide range of cellular mutations in patient tumours remains a significant barrier to achieving effective *in vivo* responses in clinical trials. Many drugs that initially showed promise *in vitro* have demonstrated lacklustre effect in Phase II and III trials, leading to disappointing outcomes. To address this issue, we utilized primary patient-derived ex vivo models to better mimic tumour heterogeneity. However, UC2288 was tested on only one primary and one metastatic cell line. Considering the vast number of UM cell lines, it is essential for future studies to incorporate a broader panel of cell lines representing common mutations, such as GNAQ/11 and BAP1, to ensure a more comprehensive evaluation of UC2288's therapeutic potential in UM.

By integrating classical and emerging paradigms, my PhD project identifies innovative therapeutic strategies for UM. Through re-evaluating established receptors and cell death mechanisms, we have discovered novel therapeutic target, a lead compound as well as potential combined therapies that are effective in treating UM. These innovative discoveries serve as critical steppingstones toward improving UM patient outcomes and paving the way for more effective treatments in the future.

Acknowledgments

This research reported in this thesis was supported by the award of a Research Training Program scholarship to the PhD Candidate.

Reference

1. Damato EM, Damato BE. Detection and Time to Treatment of Uveal Melanoma in the United Kingdom: An Evaluation of 2384 Patients. Ophthalmology. 2012;119(8):1582-9.
2. Singh AD, Topham A. Incidence of uveal melanoma in the United States: 1973–1997. Ophthalmology. 2003;110(5):956-61.
3. Yonekawa YMD, Kim IKMD. Epidemiology and Management of Uveal Melanoma. Hematology/oncology clinics of North America. 2012;26(6):1169-84.
4. Kujala E, Mäkitie T, Kivelä T. Very Long-Term Prognosis of Patients with Malignant Uveal Melanoma. Investigative Ophthalmology & Visual Science. 2003;44(11):4651-9.
5. Stålhammar G. Delays between Uveal Melanoma Diagnosis and Treatment Increase the Risk of Metastatic Death. Ophthalmology. 2024;131(9):1094-104.
6. Gragoudas ES, Egan KM, Seddon JM, Glynn RJ, Walsh SM, Finn SM, et al. Survival of patients with metastases from uveal melanoma. Ophthalmology. 1991;98(3):383-9; discussion 90.
7. Diener-West M, Hawkins BS, Markowitz JA, Schachat AP. A Review of Mortality From Choroidal Melanoma: II. A Meta-Analysis of 5-Year Mortality Rates Following Enucleation, 1966 Through 1988. Archives of Ophthalmology. 1992;110(2):245-50.
8. Shields CL, Furuta M, Thangappan A, Nagori S, Mashayekhi A, Lally DR, et al. Metastasis of Uveal Melanoma Millimeter-by-Millimeter in 8033 Consecutive Eyes. Archives of Ophthalmology. 2009;127(8):989-98.
9. Kiuru M, Busam KJ. The NF1 gene in tumor syndromes and melanoma. Laboratory investigation; a journal of technical methods and pathology. 2017;97(2):146-57.
10. Mandalà M, Merelli B, Massi D. Nras in melanoma: targeting the undruggable target. Critical reviews in oncology/hematology. 2014;92(2):107-22.
11. Van Raamsdonk CD, Bezrookove V, Green G, Bauer J, Gaugler L, O'Brien JM, et al. Frequent somatic mutations of GNAQ in uveal melanoma and blue naevi. Nature. 2009;457(7229):599-602.
12. Raamsdonk CDV, Griewank KG, Crosby MB, Garrido MC, Vemula S, Wiesner T, et al. Mutations in GNA11 in Uveal Melanoma. New England Journal of Medicine. 2010;363(23):2191-9.
13. Harbour JW, Onken MD, Roberson EDO, Duan S, Cao L, Worley LA, et al. Frequent Mutation of BAP1 in Metastasizing Uveal Melanomas. Science. 2010;330(6009):1410-3.
14. Harbour JW, Roberson EDO, Anbunathan H, Onken MD, Worley LA, Bowcock AM. Recurrent mutations at codon 625 of the splicing factor SF3B1 in uveal melanoma. Nature Genetics. 2013;45(2):133-5.
15. Martin M, Maßhöfer L, Temming P, Rahmann S, Metz C, Bornfeld N, et al. Exome sequencing identifies recurrent somatic mutations in EIF1AX and SF3B1 in uveal melanoma with disomy 3. Nat Genet. 2013;45(8):933-6.
16. Yavuzyigitoglu S, Koopmans AE, Verdijk RM, Vaarwater J, Eussen B, van Bodegom A, et al. Uveal Melanomas with SF3B1 Mutations: A Distinct Subclass Associated with Late-Onset Metastases. Ophthalmology. 2016;123(5):1118-28.
17. White VA, Chambers JD, Courtright PD, Chang WY, Horsman DE. Correlation of cytogenetic abnormalities with the outcome of patients with uveal melanoma. Cancer. 1998;83(2):354-9.
18. Onken MD, Worley LA, Ehlers JP, Harbour JW. Gene Expression Profiling in Uveal Melanoma Reveals Two Molecular Classes and Predicts Metastatic Death. Cancer Research. 2004;64(20):7205-9.

19. Branisteanu DC, Bogdanici CM, Branisteanu DE, Maranduca MA, Zemba M, Balta F, et al. Uveal melanoma diagnosis and current treatment options (Review). Exp Ther Med. 2021;22(6):1428.
20. Bhutia SK, Mukhopadhyay S, Sinha N, Das DN, Panda PK, Patra SK, et al. Autophagy: cancer's friend or foe? Advances in cancer research. 2013;118:61-95.
21. Group TCOMS. The COMS Randomized Trial of Iodine 125 Brachytherapy for Choroidal Melanoma, III: Initial Mortality Findings: COMS Report No. 18. Archives of Ophthalmology. 2001;119(7):969-82.
22. Shields CL, Shah SU, Bianciotto CG, Emrich J, Komarnicky L, Shields JA. Iris Melanoma Management with Iodine-125 Plaque Radiotherapy in 144 Patients: Impact of Melanoma-Related Glaucoma on Outcomes. Ophthalmology. 2013;120(1):55-61.
23. Gragoudas ES, Lane AM, Munzenrider J, Egan KM, Li W. Long-term risk of local failure after proton therapy for choroidal/ciliary body melanoma. Transactions of the American Ophthalmological Society. 2002;100:43-8; discussion 8-9.
24. Horgan N, Shields CL, Mashayekhi A, Salazar PF, Materin MA, O'Regan M, Shields JA. Periocular Triamcinolone for Prevention of Macular Edema after Plaque Radiotherapy of Uveal Melanoma: A Randomized Controlled Trial. Ophthalmology. 2009;116(7):1383-90.
25. Gragoudas E, Li W, Goitein M, Lane AM, Munzenrider JE, Egan KM. Evidence-Based Estimates of Outcome in Patients Irradiated for Intraocular Melanoma. Archives of Ophthalmology. 2002;120(12):1665-71.
26. Egger E, Zografos L, Schalenbourg A, Beati D, Bhringer T, Chamot L, Goitein G. Eye retention after proton beam radiotherapy for uveal melanoma. International Journal of Radiation Oncology, Biology, Physics. 2003;55(4):867-80.
27. Gragoudas ES, Goitein M, Verhey L, Munzenreider J, Suit HD, Koehler A. Proton Beam Irradiation: An Alternative to Enucleation for Intraocular Melanomas. Ophthalmology. 1980;87(6):571-81.
28. Akbaba S, Foerster R, Nicolay NH, Arians N, Bostel T, Debus J, Hauswald H. Linear accelerator-based stereotactic fractionated photon radiotherapy as an eye-conserving treatment for uveal melanoma. Radiation Oncology. 2018;13(1):140.
29. Zehetmayer M, Kitz K, Menapace R, Ertl A, Heinzl H, Ruhswurm I, et al. Local tumor control and morbidity after one to three fractions of stereotactic external beam irradiation for uveal melanoma. Radiotherapy and Oncology. 2000;55(2):135-44.
30. Oosterhuis JA, Journée-de Korver HG, Keunen JEE. Transpupillary Thermotherapy: Results in 50 Patients With Choroidal Melanoma. Archives of Ophthalmology. 1998;116(2):157-62.
31. Shields CL, Shields JA, Perez N, Singh AD, Cater J. Primary transpupillary thermotherapy for small choroidal melanoma in 256 consecutive cases: outcomes and limitations1 1The authors have no proprietary interests in any of the devices mentioned in this article. Ophthalmology. 2002;109(2):225-34.
32. Marinkovic M, Horeweg N, Fiocco M, Peters FP, Sommers LW, Laman MS, et al. Ruthenium-106 brachytherapy for choroidal melanoma without transpupillary thermotherapy: Similar efficacy with improved visual outcome. European Journal of Cancer. 2016;68:106-13.
33. Blasi MA, Laguardia M, Tagliaferri L, Scupola A, Villano A, Caputo CG, Pagliara MM. BRACHYTHERAPY ALONE OR WITH NEOADJUVANT PHOTODYNAMIC THERAPY FOR AMELANOTIC CHOROIDAL MELANOMA: Functional Outcomes and Local Tumor Control. Retina. 2016;36(11):2205-12.
34. Turkoglu EB, Pointdujour-Lim R, Mashayekhi A, Shields CL. PHOTODYNAMIC THERAPY AS PRIMARY TREATMENT FOR SMALL CHOROIDAL MELANOMA. RETINA. 2019;39(7).
35. Rundle P. Treatment of posterior uveal melanoma with multi-dose photodynamic therapy. British Journal of Ophthalmology. 2014;98(4):494.

36. Damato B, Groenewald C, McGalliard J, Wong D. Endoresection of choroidal melanoma. British Journal of Ophthalmology. 1998;82(3):213.
37. Konstantinidis L, Groenewald C, Coupland SE, Damato B. Long-term outcome of primary endoresection of choroidal melanoma. British Journal of Ophthalmology. 2014;98(1):82.
38. Karkhaneh R, Chams H, Amoli FA, Riazi-Esfahani M, Ahmadabadi MN, Mansouri MR, et al. LONG-TERM SURGICAL OUTCOME OF POSTERIOR CHOROIDAL MELANOMA TREATED BY ENDORESECTION. RETINA. 2007;27(7).
39. Gündüz K, Bechrakis NE. Exoresection and endoresection for uveal melanoma. Middle East African journal of ophthalmology. 2010;17(3):210-6.
40. Damato BE. Local resection of uveal melanoma. Bulletin de la Societe belge d'ophtalmologie. 1993;248:11-7.
41. Shields JA, Shields CL. Management of Posterior Uveal Melanoma: Past, Present, and Future: The 2014 Charles L. Schepens Lecture. Ophthalmology. 2015;122(2):414-28.
42. Zimmerman LE, McLean IW, Foster WD. Statistical Analysis of Follow-up Data Concerning Uveal Melanomas, and the Influence of Enucleation. Ophthalmology. 1980;87(6):557-64.
43. Damato B, Lecuona K. Conservation of eyes with choroidal melanoma by a multimodality approach to treatment: An audit of 1632 patients. Ophthalmology. 2004;111(5):977-83.
44. Kersten RC, Tse DT, Anderson RL, Blodi FC. The Role of Orbital Exenteration in Choroidal Melanoma with Extrascleral Extension. Ophthalmology. 1985;92(3):436-43.
45. Baum SH, Westekemper H, Bechrakis NE, Mohr C. Conjunctival and uveal melanoma: Survival and risk factors following orbital exenteration. Eur J Ophthalmol. 2022;32(1):612-9.
46. Hassel JC, Piperno-Neumann S, Rutkowski P, Baurain J-F, Schlaak M, Butler MO, et al. Three-Year Overall Survival with Tebentafusp in Metastatic Uveal Melanoma. New England Journal of Medicine. 2023;389(24):2256-66.
47. de Melo AC, Lucena E, de Oliveira DCM, Viola JPB. Frequency of HLA-A*02:01 in the Brazilian population and its impact on uveal melanoma systemic treatment. The Oncologist. 2024;29(8):e1098-e9.
48. Wang JZ, Lin V, Toumi E, Wang K, Zhu H, Conway RM, et al. Development of new therapeutic options for the treatment of uveal melanoma. The FEBS Journal. 2021;288(21):6226-49.
49. Shoushtari AN, Carvajal RD. Treatment of Uveal Melanoma. In: Kaufman HL, Mehnert JM, editors. Melanoma. Cham: Springer International Publishing; 2016. p. 281-93.
50. Shoushtari AN, Carvajal RD. GNAQ and GNA11 mutations in uveal melanoma. Melanoma research. 2014;24(6).
51. Carvajal RD, Sosman JA, Quevedo JF, Milhem MM, Joshua AM, Kudchadkar RR, et al. Effect of selumetinib vs chemotherapy on progression-free survival in uveal melanoma: a randomized clinical trial. Jama. 2014;311(23):2397-405.
52. Carvajal RD, Piperno-Neumann S, Kapiteijn E, Chapman PB, Frank S, Joshua AM, et al. Selumetinib in Combination With Dacarbazine in Patients With Metastatic Uveal Melanoma: A Phase III, Multicenter, Randomized Trial (SUMIT). Journal of clinical oncology : official journal of the American Society of Clinical Oncology. 2018;36(12):1232-9.
53. Falchook GS, Lewis KD, Infante JR, Gordon MS, Vogelzang NJ, DeMarini DJ, et al. Activity of the oral MEK inhibitor trametinib in patients with advanced melanoma: a phase 1 dose-escalation trial. The Lancet Oncology. 2012;13(8):782-9.
54. Shoushtari AN, Ong LT, Schoder H, Singh-Kandah S, Abbate KT, Postow MA, et al. A phase 2 trial of everolimus and pasireotide long-acting release in patients with metastatic uveal melanoma. Melanoma research. 2016;26(3):272-7.

55. Ambrosini G, Musi E, Ho AL, de Stanchina E, Schwartz GK. Inhibition of Mutant GNAQ Signaling in Uveal Melanoma Induces AMPK-Dependent Autophagic Cell Death. Molecular Cancer Therapeutics. 2013;12(5):768-76.
56. Babchia N, Calipel A, Mouriaux F, Faussat A-M, Mascarelli F. The PI3K/Akt and mTOR/P70S6K Signaling Pathways in Human Uveal Melanoma Cells: Interaction with B-Raf/ERK. Investigative Ophthalmology & Visual Science. 2010;51(1):421-9.
57. Jirousek MR, Goekjian PG. Protein kinase C inhibitors as novel anticancer drugs. Expert Opinion on Investigational Drugs. 2001;10(12):2117-40.
58. Wu X, Zhu M, Fletcher JA, Giobbie-Hurder A, Hodi FS. The Protein Kinase C Inhibitor Enzastaurin Exhibits Antitumor Activity against Uveal Melanoma. PLOS ONE. 2012;7(1):e29622.
59. Chen X, Wu Q, Tan L, Porter D, Jager MJ, Emery C, Bastian BC. Combined PKC and MEK inhibition in uveal melanoma with GNAQ and GNA11 mutations. Oncogene. 2014;33(39):4724-34.
60. Wu X, Li J, Zhu M, Fletcher JA, Hodi FS. Protein kinase C inhibitor AEB071 targets ocular melanoma harboring GNAQ mutations via effects on the PKC/Erk1/2 and PKC/NF-κB pathways. Mol Cancer Ther. 2012;11(9):1905-14.
61. Mendelsohn J. The epidermal growth factor receptor as a target for cancer therapy. Endocrine-related cancer. 2001;8(1):3-9.
62. Amaro A, Mirisola V, Angelini G, Musso A, Tosetti F, Esposito AI, et al. Evidence of epidermal growth factor receptor expression in uveal melanoma: Inhibition of epidermal growth factor-mediated signalling by Gefitinib and Cetuximab triggered antibody-dependent cellular cytotoxicity. European Journal of Cancer. 2013;49(15):3353-65.
63. Patel SP, Kim KB, Papadopoulos NE, Hwu WJ, Hwu P, Prieto VG, et al. A phase II study of gefitinib in patients with metastatic melanoma. Melanoma research. 2011;21(4):357-63.
64. All-Ericsson C, Girnita L, Seregard S, Bartolazzi A, Jager MJ, Larsson O. Insulin-like Growth Factor-1 Receptor in Uveal Melanoma: A Predictor for Metastatic Disease and a Potential Therapeutic Target. Investigative Ophthalmology & Visual Science. 2002;43(1):1-8.
65. Yan F, Liao R, Farhan M, Wang T, Chen J, Wang Z, et al. Elucidating the role of the FoxO3a transcription factor in the IGF-1-induced migration and invasion of uveal melanoma cancer cells. Biomedicine & Pharmacotherapy. 2016;84:1538-50.
66. Macaulay VM, Middleton MR, Protheroe AS, Tolcher A, Dieras V, Sessa C, et al. Phase I study of humanized monoclonal antibody AVE1642 directed against the type 1 insulin-like growth factor receptor (IGF-1R), administered in combination with anticancer therapies to patients with advanced solid tumors. Annals of oncology : official journal of the European Society for Medical Oncology. 2013;24(3):784-91.
67. Koch S, Claesson-Welsh L. Signal transduction by vascular endothelial growth factor receptors. Cold Spring Harbor perspectives in medicine. 2012;2(7):a006502.
68. el Filali M, Ly LV, Luyten GP, Versluis M, Grossniklaus HE, van der Velden PA, Jager MJ. Bevacizumab and intraocular tumors: an intriguing paradox. Molecular vision. 2012;18:2454-67.
69. Moser JC, Pulido JS, Dronca RS, McWilliams RR, Markovic SN, Mansfield AS. The Mayo Clinic experience with the use of kinase inhibitors, ipilimumab, bevacizumab, and local therapies in the treatment of metastatic uveal melanoma. Melanoma research. 2015;25(1):59-63.
70. Niederkorn JY. Ocular immune privilege and ocular melanoma: parallel universes or immunological plagiarism? Frontiers in immunology. 2012;3:148.
71. Alexander M, Mellor JD, McArthur G, Kee D. Ipilimumab in pretreated patients with unresectable or metastatic cutaneous, uveal and mucosal melanoma. Medical Journal of Australia. 2014;201(1):49-53.

72. Zimmer L, Vaubel J, Mohr P, Hauschild A, Utikal J, Simon J, et al. Phase II DeCOG-study of ipilimumab in pretreated and treatment-naïve patients with metastatic uveal melanoma. PLoS One. 2015;10(3):e0118564.
73. Namikawa K, Takahashi A, Mori T, Tsutsumida A, Suzuki S, Motoi N, et al. Nivolumab for patients with metastatic uveal melanoma previously untreated with ipilimumab: a single-institution retrospective study. Melanoma research. 2020;30(1):76-84.
74. Kottschade LA, McWilliams RR, Markovic SN, Block MS, Villasboas Bisneto J, Pham AQ, et al. The use of pembrolizumab for the treatment of metastatic uveal melanoma. Melanoma research. 2016;26(3):300-3.
75. Royer-Bertrand B, Torsello M, Rimoldi D, El Zaoui I, Cisarova K, Pescini-Gobert R, et al. Comprehensive Genetic Landscape of Uveal Melanoma by Whole-Genome Sequencing. American journal of human genetics. 2016;99(5):1190-8.
76. Nell RJ, Versluis M, Cats D, Mei H, Verdijk RM, Kroes WGM, et al. Identification of diagnostic and prognostic genetic alterations in uveal melanoma using RNA sequencing. Scientific reports. 2025;15(1):8167.
77. Cao X, Zhang Y, Ding Y, Wan Y. Identification of RNA structures and their roles in RNA functions. Nature Reviews Molecular Cell Biology. 2024;25(10):784-801.
78. Chen B, Dragomir MP, Yang C, Li Q, Horst D, Calin GA. Targeting non-coding RNAs to overcome cancer therapy resistance. Signal Transduction and Targeted Therapy. 2022;7(1):121.
79. Uppaluri KR, Challa HJ, Gaur A, Jain R, Krishna Vardhani K, Geddam A, et al. Unlocking the potential of non-coding RNAs in cancer research and therapy. Translational oncology. 2023;35:101730.
80. Barbagallo C, Stella M, Broggi G, Russo A, Caltabiano R, Ragusa M. Genetics and RNA Regulation of Uveal Melanoma. Cancers. 2023;15(3):775.
81. Dewaele S, Delhaye L, De Paepe B, de Bony EJ, De Wilde J, Vanderheyden K, et al. The long non-coding RNA SAMMSON is essential for uveal melanoma cell survival. Oncogene. 2022;41(1):15-25.
82. Milán-Rois P, Quan A, Slack FJ, Somoza Á. The Role of LncRNAs in Uveal Melanoma. Cancers (Basel). 2021;13(16).
83. Sergina NV, Moasser MM. The HER family and cancer: emerging molecular mechanisms and therapeutic targets. Trends Mol Med. 2007;13(12):527-34.
84. Shu W, Zhu X, Wang K, Cherepanoff S, Conway RM, Madigan MC, et al. The multi-kinase inhibitor afatinib serves as a novel candidate for the treatment of human uveal melanoma. Cellular oncology (Dordrecht, Netherlands). 2022;45(4):601-19.
85. Booth L, Roberts JL, Spasojevic I, Baker KC, Poklepovic A, West C, et al. GZ17-6.02 kills PDX isolates of uveal melanoma. Oncotarget. 2024;15(1).
86. Forsberg EMV, Lindberg MF, Jespersen H, Alsén S, Bagge RO, Donia M, et al. HER2 CAR-T Cells Eradicate Uveal Melanoma and T-cell Therapy–Resistant Human Melanoma in IL2 Transgenic NOD/SCID IL2 Receptor Knockout Mice. Cancer Research. 2019;79(5):899-904.
87. Trocmé E, Mougiakakos D, Johansson CC, All-Eriksson C, Economou MA, Larsson O, et al. Nuclear HER3 is associated with favorable overall survival in uveal melanoma. International Journal of Cancer. 2012;130(5):1120-7.
88. O'Malley J, Kumar R, Inigo J, Yadava N, Chandra D. Mitochondrial Stress Response and Cancer. Trends in cancer. 2020;6(8):688-701.
89. Zhang W, Shi Y, Oyang L, Cui S, Li S, Li J, et al. Endoplasmic reticulum stress—a key guardian in cancer. Cell Death Discovery. 2024;10(1):343.

90. Yang X, Zhuang J, Song W, Shen W, Wu W, Shen H, Han S. Mitochondria-associated endoplasmic reticulum membrane: Overview and inextricable link with cancer. Journal of Cellular and Molecular Medicine. 2023;27(7):906-19.
91. An G, Park J, Song J, Hong T, Song G, Lim W. Relevance of the endoplasmic reticulum-mitochondria axis in cancer diagnosis and therapy. Experimental & Molecular Medicine. 2024;56(1):40-50.
92. Yu H, Sun C, Gong Q, Feng D. Mitochondria-Associated Endoplasmic Reticulum Membranes in Breast Cancer. Frontiers in Cell and Developmental Biology. 2021;9.
93. Bononi A, Giorgi C, Patergnani S, Larson D, Verbruggen K, Tanji M, et al. BAP1 regulates IP3R3-mediated Ca(2+) flux to mitochondria suppressing cell transformation. Nature. 2017;546(7659):549-53.
94. Xie J, Wu H, Dai C, Pan Q, Ding Z, Hu D, et al. Beyond Warburg effect--dual metabolic nature of cancer cells. Scientific reports. 2014;4:4927.
95. Fu Y, Zou T, Shen X, Nelson PJ, Li J, Wu C, et al. Lipid metabolism in cancer progression and therapeutic strategies. MedComm. 2021;2(1):27-59.
96. Liu J, Wu Y, Meng S, Xu P, Li S, Li Y, et al. Selective autophagy in cancer: mechanisms, therapeutic implications, and future perspectives. Molecular Cancer. 2024;23(1):22.
97. Zhu X, Zou W, Meng X, Ji J, Wang X, Shu H, et al. Elaiophylin Inhibits Tumorigenesis of Human Uveal Melanoma by Suppressing Mitophagy and Inducing Oxidative Stress via Modulating SIRT1/FoxO3a Signaling. Front Oncol. 2022;12:788496.
98. Senft D, Ronai ZA. UPR, autophagy, and mitochondria crosstalk underlies the ER stress response. Trends in biochemical sciences. 2015;40(3):141-8.
99. Bellini L, Strub T, Habel N, Pandiani C, Marchetti S, Martel A, et al. Endoplasmic reticulum stress mediates resistance to BCL-2 inhibitor in uveal melanoma cells. Cell Death Discovery. 2020;6(1):22.
100. Zhang S, Wang K, Zhu X, Cherepanoff S, Conway RM, Madigan MC, et al. The unfolded protein response and the biology of uveal melanoma. Biochimie. 2022;197:9-18.
101. Rodrigues M, de Koning L, Coupland SE, Jochemsen AG, Marais R, Stern M-H, et al. So Close, yet so Far: Discrepancies between Uveal and Other Melanomas. A Position Paper from UM Cure 2020. Cancers. 2019;11(7):1032.
102. Chang AE, Karnell LH, Menck HR. The National Cancer Data Base report on cutaneous and noncutaneous melanoma. Cancer. 1998;83(8):1664-78.
103. McLaughlin CC, Wu X-C, Jemal A, Martin HJ, Roche LM, Chen VW. Incidence of noncutaneous melanomas in the U.S. Cancer. 2005;103(5):1000-7.
104. Singh AD, Turell ME, Topham AK. Uveal Melanoma: Trends in Incidence, Treatment, and Survival. Ophthalmology. 2011;118(9):1881-5.
105. Ah-Fat FG, Damato BE. Delays in the diagnosis of uveal melanoma and effect on treatment. Eye. 1998;12(5):781-2.
106. Damato BE, Heimann H, Kalirai H, Coupland SE. Age, Survival Predictors, and Metastatic Death in Patients With Choroidal Melanoma: Tentative Evidence of a Therapeutic Effect on Survival. JAMA Ophthalmology. 2014;132(5):605-13.
107. Gamel JW, McLean IW, McCurdy JB. Biologic distinctions between cure and time to death in 2892 patients with intraocular melanoma. Cancer. 1993;71(7):2299-305.
108. Damato B. Current management of uveal melanoma. European Journal of Cancer Supplements. 2005;3(3):433-5.
109. Freton A, Chin KJ, Raut R, Tena LB, Kivelä T, Finger PT. Initial PET/CT Staging for Choroidal Melanoma: AJCC Correlation and Second Nonocular Primaries in 333 Patients. European Journal of Ophthalmology. 2012;22(2):236-43.

110. Gupta S, Bedikian AY, Ahrar J, Ensor J, Ahrar K, Madoff DC, et al. Hepatic artery chemoembolization in patients with ocular melanoma metastatic to the liver: response, survival, and prognostic factors. American journal of clinical oncology. 2010;33(5):474-80.
111. Nathan P, Cohen V, Coupland S, Curtis K, Damato B, Evans J, et al. Uveal Melanoma UK National Guidelines. European Journal of Cancer. 2015;51(16):2404-12.
112. Gomez D, Wetherill C, Cheong J, Jones L, Marshall E, Damato B, et al. The Liverpool uveal melanoma liver metastases pathway: Outcome following liver resection. Journal of Surgical Oncology. 2014;109(6):542-7.
113. Mariani P, Piperno-Neumann S, Servois V, Berry MG, Dorval T, Plancher C, et al. Surgical management of liver metastases from uveal melanoma: 16 years' experience at the Institut Curie. European Journal of Surgical Oncology (EJSO). 2009;35(11):1192-7.
114. Johansson PA, Brooks K, Newell F, Palmer JM, Wilmott JS, Pritchard AL, et al. Whole genome landscapes of uveal melanoma show an ultraviolet radiation signature in iris tumours. Nature Communications. 2020;11(1):2408.
115. Dousset L, Poizeau F, Robert C, Mansard S, Mortier L, Caumont C, et al. Positive Association Between Location of Melanoma, Ultraviolet Signature, Tumor Mutational Burden, and Response to Anti–PD-1 Therapy. JCO Precision Oncology. 2021(5):1821-9.
116. Liau S, Wang JZ, Zagarella E, Paulus P, Dang N, Rawling T, et al. An update on inflammation in uveal melanoma. Biochimie. 2023;212:114-22.
117. Singh N, Singh R, Bowen RC, Abdel-Rahman MH, Singh AD. Uveal Melanoma in BAP1 Tumor Predisposition Syndrome: Estimation of Risk. American journal of ophthalmology. 2021;224:172-7.
118. Akin-Bali DF. Bioinformatics analysis of GNAQ, GNA11, BAP1, SF3B1,SRSF2, EIF1AX, PLCB4, and CYSLTR2 genes and their role in the pathogenesis of Uveal Melanoma. Ophthalmic Genetics. 2021;42(6):732-43.
119. Sisley K, Rennie IG, Cottam DW, Potter AM, Potter CW, Rees RC. Cytogenetic findings in six posterior uveal melanomas: Involvement of chromosomes 3, 6, and 8. Genes, Chromosomes and Cancer. 1990;2(3):205-9.
120. Spagnolo F, Caltabiano G, Queirolo P. Uveal melanoma. Cancer Treatment Reviews. 2012;38(5):549-53.
121. Amaro A, Gangemi R, Piaggio F, Angelini G, Barisione G, Ferrini S, Pfeffer U. The biology of uveal melanoma. Cancer Metastasis Rev. 2017;36(1):109-40.
122. Croce M, Ferrini S, Pfeffer U, Gangemi R. Targeted Therapy of Uveal Melanoma: Recent Failures and New Perspectives. Cancers. 2019;11(6):846.
123. Goh AY, Layton CJ. Evolving systemic targeted therapy strategies in uveal melanoma and implications for ophthalmic management: a review. Clinical & Experimental Ophthalmology. 2016;44(6):509-19.
124. Niu Y, Wang K, Zhu X, Zhang S, Cherepanoff S, Conway RM, et al. The application of natural compounds in uveal melanoma drug discovery. J Pharm Pharmacol. 2022;74(5):660-80.
125. Hsu JL, Hung MC. The role of HER2, EGFR, and other receptor tyrosine kinases in breast cancer. Cancer Metastasis Rev. 2016;35(4):575-88.
126. Yarden Y, Sliwkowski MX. Untangling the ErbB signalling network. Nature reviews Molecular cell biology. 2001;2(2):127-37.
127. Sharma B, Singh VJ, Chawla PA. Epidermal growth factor receptor inhibitors as potential anticancer agents: An update of recent progress. Bioorganic Chemistry. 2021;116:105393.
128. Oh D-Y, Bang Y-J. HER2-targeted therapies — a role beyond breast cancer. Nature Reviews Clinical Oncology. 2020;17(1):33-48.

129. Topcu-Yilmaz P, Kiratli H, Saglam A, Söylemezoglu F, Hascelik G. Correlation of clinicopathological parameters with HGF, c-Met, EGFR, and IGF-1R expression in uveal melanoma. Melanoma research. 2010;20(2):126-32.
130. Hurks HMH, Metzelaar-Blok JAW, Barthen ER, Zwinderman AH, De Wolff-Rouendaal D, Keunen JEE, Jager MJ. Expression of Epidermal Growth Factor Receptor: Risk Factor in Uveal Melanoma. Investigative Ophthalmology & Visual Science. 2000;41(8):2023-7.
131. Ma D, Niederkorn JY. Role of epidermal growth factor receptor in the metastasis of intraocular melanomas. Investigative Ophthalmology & Visual Science. 1998;39(7):1067-75.
132. Knight LA, Di Nicolantonio F, Whitehouse P, Mercer S, Sharma S, Glaysher S, et al. The in vitroeffect of gefitinib ('Iressa') alone and in combination with cytotoxic chemotherapy on human solid tumours. BMC Cancer. 2004;4(1):83.
133. Mallikarjuna K, Pushparaj V, Biswas J, Krishnakumar S. Expression of Epidermal Growth Factor Receptor, Ezrin, Hepatocyte Growth Factor, and c-Met in Uveal Melanoma: An Immunohistochemical Study. Current Eye Research. 2007;32(3):281-90.
134. Amaro A, Mirisola V, Angelini G, Musso A, Tosetti F, Esposito AI, et al. Evidence of epidermal growth factor receptor expression in uveal melanoma: inhibition of epidermal growth factor-mediated signalling by Gefitinib and Cetuximab triggered antibody-dependent cellular cytotoxicity. Eur J Cancer. 2013;49(15):3353-65.
135. Nahta R, Yuan LX, Du Y, Esteva FJ. Lapatinib induces apoptosis in trastuzumab-resistant breast cancer cells: effects on insulin-like growth factor I signaling. Mol Cancer Ther. 2007;6(2):667-74.
136. Daniels KJ, Boldt HC, Martin JA, Gardner LM, Meyer M, Folberg R. Expression of type VI collagen in uveal melanoma: its role in pattern formation and tumor progression. Laboratory investigation; a journal of technical methods and pathology. 1996;75(1):55-66.
137. Yu X, Ambrosini G, Roszik J, Eterovic AK, Stempke-Hale K, Seftor EA, et al. Genetic analysis of the 'uveal melanoma' C918 cell line reveals atypical BRAF and common KRAS mutations and single tandem repeat profile identical to the cutaneous melanoma C8161 cell line. Pigment Cell Melanoma Res. 2015;28(3):357-9.
138. Welch DR, Bisi JE, Miller BE, Conaway D, Seftor EA, Yohem KH, et al. Characterization of a highly invasive and spontaneously metastatic human malignant melanoma cell line. Int J Cancer. 1991;47(2):227-37.
139. Iwamoto S, Burrows RC, Kalina RE, George D, Boehm M, Bothwell MA, Schmidt R. Immunophenotypic differences between uveal and cutaneous melanomas. Arch Ophthalmol. 2002;120(4):466-70.
140. Leviskas B, Valyi-Nagy T, Munirathinam G, Bork M, Valyi-Nagy K, Skwor T. Metalloporphyrin Pd(T4) Exhibits Oncolytic Activity and Cumulative Effects with 5-ALA Photodynamic Treatment against C918 Cells. Int J Mol Sci. 2020;21(2).
141. Jiu X, Liu Y, Wen J. Artesunate combined with verteporfin inhibits uveal melanoma by regulation of the MALAT1/yes-associated protein signaling pathway. Oncol Lett. 2021;22(2):597.
142. Hua X, Wu P, Gao GS, Ye XL. Combination of oridonin and TRAIL induces apoptosis in uveal melanoma cells by upregulating DR5. Int J Ophthalmol. 2021;14(12):1834-42.
143. Percie du Sert N, Hurst V, Ahluwalia A, Alam S, Avey MT, Baker M, et al. The ARRIVE guidelines 2.0: updated guidelines for reporting animal research. BMJ Open Sci. 2020;4(1):e100115.
144. Levy DE, Darnell JE. STATs: transcriptional control and biological impact. Nature Reviews Molecular Cell Biology. 2002;3(9):651-62.
145. Bromberg JF. Activation of STAT proteins and growth control. BioEssays. 2001;23(2):161-9.

146. Konecny GE, Venkatesan N, Yang G, Dering J, Ginther C, Finn R, et al. Activity of lapatinib a novel HER2 and EGFR dual kinase inhibitor in human endometrial cancer cells. British journal of cancer. 2008;98(6):1076-84.
147. Scaltriti M, Verma C, Guzman M, Jimenez J, Parra JL, Pedersen K, et al. Lapatinib, a HER2 tyrosine kinase inhibitor, induces stabilization and accumulation of HER2 and potentiates trastuzumab-dependent cell cytotoxicity. Oncogene. 2009;28(6):803-14.
148. Taskar KS, Rudraraju V, Mittapalli RK, Samala R, Thorsheim HR, Lockman J, et al. Lapatinib Distribution in HER2 Overexpressing Experimental Brain Metastases of Breast Cancer. Pharmaceutical Research. 2012;29(3):770-81.
149. Forsberg EMV, Lindberg MF, Jespersen H, Alsen S, Bagge RO, Donia M, et al. HER2 CAR-T Cells Eradicate Uveal Melanoma and T-cell Therapy-Resistant Human Melanoma in IL2 Transgenic NOD/SCID IL2 Receptor Knockout Mice. Cancer Res. 2019;79(5):899-904.
150. Ma J, Han H, Liu D, Li W, Feng H, Xue X, et al. HER2 as a promising target for cytotoxicity T cells in human melanoma therapy. PLoS One. 2013;8(8):e73261.
151. Cohen P. Protein kinases — the major drug targets of the twenty-first century? Nature Reviews Drug Discovery. 2002;1(4):309-15.
152. Zhang J, Yang PL, Gray NS. Targeting cancer with small molecule kinase inhibitors. Nature Reviews Cancer. 2009;9(1):28-39.
153. Hynes NE, MacDonald G. ErbB receptors and signaling pathways in cancer. Current Opinion in Cell Biology. 2009;21(2):177-84.
154. Gross S, Rahal R, Stransky N, Lengauer C, Hoeflich KP. Targeting cancer with kinase inhibitors. The Journal of Clinical Investigation. 2015;125(5):1780-9.
155. Yang J, Manson DK, Marr BP, Carvajal RD. Treatment of uveal melanoma: where are we now? Therapeutic Advances in Medical Oncology. 2018;10:1758834018757175.
156. Scholes AG, Hagan S, Hiscott P, Damato BE, Grierson I. Overexpression of epidermal growth factor receptor restricted to macrophages in uveal melanoma. Arch Ophthalmol. 2001;119(3):373-7.
157. Vertuani S, Dubrovska E, Levitsky V, Jager MJ, Kiessling R, Levitskaya J. Retinoic acid elicits cytostatic, cytotoxic and immunomodulatory effects on uveal melanoma cells. Cancer Immunol Immunother. 2007;56(2):193-204.
158. Medina PJ, Goodin S. Lapatinib: A dual inhibitor of human epidermal growth factor receptor tyrosine kinases. Clinical Therapeutics. 2008;30(8):1426-47.
159. Higa GM, Abraham J. Lapatinib in the treatment of breast cancer. Expert Review of Anticancer Therapy. 2007;7:1183+.
160. eviQ. Breast metastatic capecitabine and laPAtinib Alexandria NSW 1435: Cancer Insititute NSW; 2020 [updated 12 October 2020.
161. Geyer CE, Forster J, Lindquist D, Chan S, Romieu CG, Pienkowski T, et al. Lapatinib plus Capecitabine for HER2-Positive Advanced Breast Cancer. New England Journal of Medicine. 2006;355(26):2733-43.
162. Li D, Ambrogio L, Shimamura T, Kubo S, Takahashi M, Chirieac LR, et al. BIBW2992, an irreversible EGFR/HER2 inhibitor highly effective in preclinical lung cancer models. Oncogene. 2008;27(34):4702-11.
163. Dratkiewicz E, Pietraszek-Gremplewicz K, Simiczyjew A, Mazur AJ, Nowak D. Gefitinib or lapatinib with foretinib synergistically induce a cytotoxic effect in melanoma cell lines. Oncotarget. 2018;9(26):18254-68.
164. Thakur V, Lu J, Roscilli G, Aurisicchio L, Cappelletti M, Pavoni E, et al. The natural compound fucoidan from New Zealand Undaria pinnatifida synergizes with the ERBB inhibitor lapatinib enhancing melanoma growth inhibition. Oncotarget. 2017;8(11):17887-96.

165. Nakata S, Fujita M, Nakanishi H. Efficacy of Afatinib and Lapatinib Against HER2 Gene-amplified Trastuzumab-sensitive and -resistant Human Gastric Cancer Cells. Anticancer Res. 2019;39(11):5927-32.
166. Garrett TP, McKern NM, Lou M, Elleman TC, Adams TE, Lovrecz GO, et al. The crystal structure of a truncated ErbB2 ectodomain reveals an active conformation, poised to interact with other ErbB receptors. Mol Cell. 2003;11(2):495-505.
167. Stark A, Hulka BS, Joens S, Novotny D, Thor AD, Wold LE, et al. HER-2/neu Amplification in Benign Breast Disease and the Risk of Subsequent Breast Cancer. Journal of Clinical Oncology. 2000;18(2):267-.
168. Slamon DJ, Godolphin W, Jones LA, Holt JA, Wong SG, Keith DE, et al. Studies of the HER-2-neu proto-oncogene in human breast and ovarian cancer. Science. 1989;244:707+.
169. Hudis CAMD. Trastuzumab -- Mechanism of Action and Use in Clinical PracticeDrug Therapy. The New England Journal of Medicine. 2007;357(1):39-51.
170. Press MF, Pike MC, Chazin VR, Hung G, Udove JA, Markowicz M, et al. Her-2/neu Expression in Node-negative Breast Cancer: Direct Tissue Quantitation by Computerized Image Analysis and Association of Overexpression with Increased Risk of Recurrent Disease1. Cancer Research. 1993;53(20):4960-70.
171. Seshadri R, Firgaira FA, Horsfall DJ, McCaul K, Setlur V, Kitchen P. Clinical significance of HER-2/neu oncogene amplification in primary breast cancer. The South Australian Breast Cancer Study Group. Journal of clinical oncology : official journal of the American Society of Clinical Oncology. 1993;11(10):1936-42.
172. Cronin KA, Harlan LC, Dodd KW, Abrams JS, Ballard-Barbash R. Population-based Estimate of the Prevalence of HER-2 Positive Breast Cancer Tumors for Early Stage Patients in the US. Cancer Investigation. 2010;28(9):963-8.
173. Li YM, Pan Y, Wei Y, Cheng X, Zhou BP, Tan M, et al. Upregulation of CXCR4 is essential for HER2-mediated tumor metastasis. Cancer Cell. 2004;6(5):459-69.
174. Borgquist S, Zhou W, Jirström K, Amini R-M, Sollie T, Sørlie T, et al. The prognostic role of HER2 expression in ductal breast carcinoma in situ (DCIS); a population-based cohort study. BMC Cancer. 2015;15(1):468.
175. Brufsky AM, Mayer M, Rugo HS, Kaufman PA, Tan-Chiu E, Tripathy D, et al. Central Nervous System Metastases in Patients with HER2-Positive Metastatic Breast Cancer: Incidence, Treatment, and Survival in Patients from registHER. Clinical Cancer Research. 2011;17(14):4834-43.
176. Dimco G, Knight RA, Latchman DS, Stephanou A. STAT1 interacts directly with cyclin D1/Cdk4 and mediates cell cycle arrest. Cell Cycle. 2010;9(23):4638-49.
177. Booth L, Roberts JL, Sander C, Lalani AS, Kirkwood JM, Hancock JF, et al. Neratinib and entinostat combine to rapidly reduce the expression of K-RAS, N-RAS, Gα(q) and Gα(11) and kill uveal melanoma cells. Cancer Biol Ther. 2019;20(5):700-10.
178. Chen J, Wang H, Wang J, Huang S, Zhang W. STAT1 inhibits human hepatocellular carcinoma cell growth through induction of p53 and Fbxw7. Cancer Cell International. 2015;15(1):111.
179. Sara P, Gabriella R, Daniela B, Francesco N, Valeria P. STAT1 and STAT3 in tumorigenesis: two sides of the same coin. Madame Curie Bioscience Database. 2000.
180. Bose R, Molina H, Patterson AS, Bitok JK, Periaswamy B, Bader JS, et al. Phosphoproteomic analysis of Her2/neu signaling and inhibition. Proceedings of the National Academy of Sciences of the United States of America. 2006;103(26):9773-8.
181. Han W, Carpenter RL, Cao X, Lo H-W. STAT1 gene expression is enhanced by nuclear EGFR and HER2 via cooperation With STAT3. Molecular Carcinogenesis. 2013;52(12):959-69.

182. Shi Y, Fan X, Meng W, Deng H, Zhang N, An Z. Engagement of immune effector cells by trastuzumab induces HER2/ERBB2 downregulation in cancer cells through STAT1 activation. Breast Cancer Research. 2014;16(2):R33.
183. Meissl K, Macho-Maschler S, Müller M, Strobl B. The good and the bad faces of STAT1 in solid tumours. Cytokine. 2017;89:12-20.
184. Press MF, Lenz H-J. EGFR, HER2 and VEGF Pathways. Drugs. 2007;67(14):2045-75.
185. Ye M, Hu D, Tu L, Zhou X, Lu F, Wen B, et al. Involvement of PI3K/Akt Signaling Pathway in Hepatocyte Growth Factor–Induced Migration of Uveal Melanoma Cells. Investigative Ophthalmology & Visual Science. 2008;49(2):497-504.
186. McCubrey JA, Steelman LS, Abrams SL, Lee JT, Chang F, Bertrand FE, et al. Roles of the RAF/MEK/ERK and PI3K/PTEN/AKT pathways in malignant transformation and drug resistance. Advances in Enzyme Regulation. 2006;46(1):249-79.
187. Steelman LS, Abrams SL, Whelan J, Bertrand FE, Ludwig DE, Bäsecke J, et al. Contributions of the Raf/MEK/ERK, PI3K/PTEN/Akt/mTOR and Jak/STAT pathways to leukemia. Leukemia. 2008;22(4):686-707.
188. Wang M, Qiu S, Qin J. Baicalein induced apoptosis and autophagy of undifferentiated thyroid cancer cells by the ERK/PI3K/Akt pathway. American journal of translational research. 2019;11(6):3341-52.
189. Gril B, Palmieri D, Bronder JL, Herring JM, Vega-Valle E, Feigenbaum L, et al. Effect of lapatinib on the outgrowth of metastatic breast cancer cells to the brain. Journal of the National Cancer Institute. 2008;100(15):1092-103.
190. Llombart-Cussac A, Cortés J, Paré L, Galván P, Bermejo B, Martínez N, et al. HER2-enriched subtype as a predictor of pathological complete response following trastuzumab and lapatinib without chemotherapy in early-stage HER2-positive breast cancer (PAMELA): an open-label, single-group, multicentre, phase 2 trial. The Lancet Oncology. 2017;18(4):545-54.
191. Xuhong JC, Qi XW, Zhang Y, Jiang J. Mechanism, safety and efficacy of three tyrosine kinase inhibitors lapatinib, neratinib and pyrotinib in HER2-positive breast cancer. American journal of cancer research. 2019;9(10):2103-19.
192. Burris HA, 3rd, Taylor CW, Jones SF, Koch KM, Versola MJ, Arya N, et al. A phase I and pharmacokinetic study of oral lapatinib administered once or twice daily in patients with solid malignancies. Clinical cancer research : an official journal of the American Association for Cancer Research. 2009;15(21):6702-8.
193. Chien AJ, Munster PN, Melisko ME, Rugo HS, Park JW, Goga A, et al. Phase I dose-escalation study of 5-day intermittent oral lapatinib therapy in patients with human epidermal growth factor receptor 2-overexpressing breast cancer. Journal of clinical oncology : official journal of the American Society of Clinical Oncology. 2014;32(14):1472-9.
194. Serra M, Rubes D, Schinelli S, Paolillo M. Small Molecules against Metastatic Tumors: Concrete Perspectives and Shattered Dreams. Cancers (Basel). 2023;15(16).
195. Ma X, Yu S, Zhao B, Bai W, Cui Y, Ni J, et al. Development and Validation of a Novel Ferroptosis-Related LncRNA Signature for Predicting Prognosis and the Immune Landscape Features in Uveal Melanoma. Frontiers in immunology. 2022;13:922315.
196. You S, Luo J, Grossniklaus HE, Gou ML, Meng K, Zhang Q. Nanomedicine in the application of uveal melanoma. Int J Ophthalmol. 2016;9(8):1215-25.
197. Wang C-W, Klionsky DJ. The Molecular Mechanism of Autophagy. Molecular Medicine. 2003;9(3):65-76.
198. Klionsky DJ. The molecular machinery of autophagy: unanswered questions. Journal of cell science. 2005;118(Pt 1):7-18.

199. Glick D, Barth S, Macleod KF. Autophagy: cellular and molecular mechanisms. The Journal of pathology. 2010;221(1):3-12.
200. Djajadikerta A, Keshri S, Pavel M, Prestil R, Ryan L, Rubinsztein DC. Autophagy Induction as a Therapeutic Strategy for Neurodegenerative Diseases. Journal of molecular biology. 2020;432(8):2799-821.
201. Mizushima N. The pleiotropic role of autophagy: from protein metabolism to bactericide. Cell Death & Differentiation. 2005;12(2):1535-41.
202. Klionsky DJ. Autophagy. Current Biology. 2005;15(8):R282-R3.
203. Ryter SW, Cloonan SM, Choi AM. Autophagy: a critical regulator of cellular metabolism and homeostasis. Molecules and cells. 2013;36(1):7-16.
204. Rodriguez-Muela N, Koga H, Garcia-Ledo L, de la Villa P, de la Rosa EJ, Cuervo AM, Boya P. Balance between autophagic pathways preserves retinal homeostasis. Aging Cell. 2013;12(3):478-88.
205. Spagnolo F, Caltabiano G, Queirolo P. Uveal melanoma. Cancer treatment reviews. 2012;38(5):549-53.
206. Eskelin S, Kivelä T. Mode of presentation and time to treatment of uveal melanoma in Finland. British Journal of Ophthalmology. 2002;86(3):333.
207. Shields CL, Kaliki S, Furuta M, Mashayekhi A, Shields JA. CLINICAL SPECTRUM AND PROGNOSIS OF UVEAL MELANOMA BASED ON AGE AT PRESENTATION IN 8,033 CASES. RETINA. 2012;32(7):1363-72.
208. Griewank KG, Murali R. Pathology and genetics of uveal melanoma. Pathology. 2013;45(1):18-27.
209. Virgili G, Gatta G, Ciccolallo L, Capocaccia R, Biggeri A, Crocetti E, et al. Incidence of Uveal Melanoma in Europe. Ophthalmology. 2007;114(12):2309-15.e2.
210. Jager MJ, Shields CL, Cebulla CM, Abdel-Rahman MH, Grossniklaus HE, Stern MH, et al. Uveal melanoma. Nature reviews Disease primers. 2020;6(1):24.
211. Damato B, Lecuona K. Conservation of eyes with choroidal melanoma by a multimodality approach to treatment: an audit of 1632 patients. Ophthalmology. 2004;111(5):977-83.
212. Jin M, Klionsky DJ. The Core Molecular Machinery of Autophagosome Formation. In: Wang H-G, editor. Autophagy and Cancer. New York, NY: Springer New York; 2013. p. 25-45.
213. Reggiori F, Komatsu M, Finley K, Simonsen A. Autophagy: more than a nonselective pathway. International journal of cell biology. 2012;2012:219625.
214. Hurley JH, Young LN. Mechanisms of Autophagy Initiation. Annual review of biochemistry. 2017;86:225-44.
215. Mizushima N. Autophagy: process and function. Genes & Development. 2007;21(22):2861-73.
216. Zaffagnini G, Martens S. Mechanisms of Selective Autophagy. Journal of molecular biology. 2016;428(9, Part A):1714-24.
217. Jin R, Zhu W, Cao S, Chen R, Jin H, Liu Y, et al. Japanese Encephalitis Virus Activates Autophagy as a Viral Immune Evasion Strategy. PLOS ONE. 2013;8(1):e52909.
218. Cooper GM, Hausman R. A molecular approach. The Cell 2nd ed Sunderland, MA: Sinauer Associates. 2000.
219. Yu L, Chen Y, Tooze SA. Autophagy pathway: Cellular and molecular mechanisms. Autophagy. 2018;14(2):207-15.
220. Backer Jonathan M. The intricate regulation and complex functions of the Class III phosphoinositide 3-kinase Vps34. Biochemical Journal. 2016;473(15):2251-71.
221. Mizushima N. The role of the Atg1/ULK1 complex in autophagy regulation. Current Opinion in Cell Biology. 2010;22(2):132-9.

222. Jiang P, Mizushima N. Autophagy and human diseases. Cell research. 2014;24(1):69-79.
223. Sridhar S, Botbol Y, Macian F, Cuervo AM. Autophagy and disease: always two sides to a problem. The Journal of pathology. 2012;226(2):255-73.
224. White E, DiPaola RS. The double-edged sword of autophagy modulation in cancer. Clinical cancer research : an official journal of the American Association for Cancer Research. 2009;15(17):5308-16.
225. Mathew R, Kongara S, Beaudoin B, Karp CM, Bray K, Degenhardt K, et al. Autophagy suppresses tumor progression by limiting chromosomal instability. Genes Dev. 2007;21(11):1367-81.
226. Degenhardt K, Mathew R, Beaudoin B, Bray K, Anderson D, Chen G, et al. Autophagy promotes tumor cell survival and restricts necrosis, inflammation, and tumorigenesis. Cancer Cell. 2006;10(1):51-64.
227. Iershov A, Nemazanyy I, Alkhoury C, Girard M, Barth E, Cagnard N, et al. The class 3 PI3K coordinates autophagy and mitochondrial lipid catabolism by controlling nuclear receptor PPARα. Nature Communications. 2019;10(1):1566.
228. Gross AS, Graef M. Mechanisms of Autophagy in Metabolic Stress Response. Journal of molecular biology. 2020;432(1):28-52.
229. White E. The role for autophagy in cancer. The Journal of Clinical Investigation. 2015;125(1):42-6.
230. Yue Z, Jin S, Yang C, Levine AJ, Heintz N. Beclin 1, an autophagy gene essential for early embryonic development, is a haploinsufficient tumor suppressor. Proceedings of the National Academy of Sciences of the United States of America. 2003;100(25):15077-82.
231. Qu X, Yu J, Bhagat G, Furuya N, Hibshoosh H, Troxel A, et al. Promotion of tumorigenesis by heterozygous disruption of the beclin 1 autophagy gene. J Clin Invest. 2003;112(12):1809-20.
232. Yang J, Nie J, Ma X, Wei Y, Peng Y, Wei X. Targeting PI3K in cancer: mechanisms and advances in clinical trials. Molecular Cancer. 2019;18(1):26.
233. Kang R, Zeh HJ, Lotze MT, Tang D. The Beclin 1 network regulates autophagy and apoptosis. Cell Death & Differentiation. 2011;18(4):571-80.
234. Liang XH, Jackson S, Seaman M, Brown K, Kempkes B, Hibshoosh H, Levine B. Induction of autophagy and inhibition of tumorigenesis by beclin 1. Nature. 1999;402(6762):672-6.
235. Takahashi Y, Coppola D, Matsushita N, Cualing HD, Sun M, Sato Y, et al. Bif-1 interacts with Beclin 1 through UVRAG and regulates autophagy and tumorigenesis. Nature Cell Biology. 2007;9(10):1142-51.
236. Mathew R, White E. Why sick cells produce tumors: the protective role of autophagy. Autophagy. 2007;3(5):502-5.
237. Wei H, Wei S, Gan B, Peng X, Zou W, Guan JL. Suppression of autophagy by FIP200 deletion inhibits mammary tumorigenesis. Genes Dev. 2011;25(14):1510-27.
238. Chuah S, Chew V. Immune implication of an autophagy-related prognostic signature in uveal melanoma. Bioscience reports. 2021;41(8).
239. Patergnani S, Danese A, Bouhamida E, Aguiari G, Previati M, Pinton P, Giorgi C. Various Aspects of Calcium Signaling in the Regulation of Apoptosis, Autophagy, Cell Proliferation, and Cancer. Int J Mol Sci. 2020;21(21).
240. Vitto VAM, Bianchin S, Zolondick AA, Pellielo G, Rimessi A, Chianese D, et al. Molecular Mechanisms of Autophagy in Cancer Development, Progression, and Therapy. Biomedicines. 2022;10(7).
241. Colella B, Faienza F, Di Bartolomeo S. EMT Regulation by Autophagy: A New Perspective in Glioblastoma Biology. Cancers. 2019;11(3):312.

242. Fuentes-Fayos AC, Pérez-Gómez JM, G-García ME, Jiménez-Vacas JM, Blanco-Acevedo C, Sánchez-Sánchez R, et al. SF3B1 inhibition disrupts malignancy and prolongs survival in glioblastoma patients through BCL2L1 splicing and mTOR/ß-catenin pathways imbalances. Journal of Experimental & Clinical Cancer Research. 2022;41(1):39.
243. Rahmati M, Ebrahim S, Hashemi S, Motamedi M, Moosavi MA. New insights on the role of autophagy in the pathogenesis and treatment of melanoma. Molecular Biology Reports. 2020;47(11):9021-32.
244. Li S, Song Y, Quach C, Guo H, Jang GB, Maazi H, et al. Transcriptional regulation of autophagy-lysosomal function in BRAF-driven melanoma progression and chemoresistance. Nat Commun. 2019;10(1):1693.
245. Zheng B, Jeong JH, Asara JM, Yuan YY, Granter SR, Chin L, Cantley LC. Oncogenic B-RAF negatively regulates the tumor suppressor LKB1 to promote melanoma cell proliferation. Mol Cell. 2009;33(2):237-47.
246. Van Raamsdonk CD, Griewank KG, Crosby MB, Garrido MC, Vemula S, Wiesner T, et al. Mutations in GNA11 in Uveal Melanoma. New England Journal of Medicine. 2010;363(23):2191-9.
247. Bakhoum MF, Esmaeli B. Molecular Characteristics of Uveal Melanoma: Insights from the Cancer Genome Atlas (TCGA) Project. Cancers. 2019;11(8):1061.
248. Truong A, Yoo JH, Scherzer MT, Sanchez JMS, Dale KJ, Kinsey CG, et al. Chloroquine Sensitizes GNAQ/11-mutated Melanoma to MEK1/2 Inhibition. Clinical Cancer Research. 2020;26(23):6374-86.
249. Booth L, Roberts JL, Sander C, Lalani AS, Kirkwood JM, Hancock JF, et al. Neratinib and entinostat combine to rapidly reduce the expression of K-RAS, N-RAS, Galpha(q) and Galpha(11) and kill uveal melanoma cells. Cancer Biol Ther. 2019;20(5):700-10.
250. Zhuang A, Chai P, Wang S, Zuo S, Yu J, Jia S, et al. Metformin promotes histone deacetylation of optineurin and suppresses tumour growth through autophagy inhibition in ocular melanoma. Clin Transl Med. 2022;12(1):e660.
251. Kang H, Ling F, Xin X, Ping L. (−)-4-O-(4-O-β-D-glucopyranosylcaffeoyl) quinic acid exerts anti-tumour effects against uveal melanoma through PI3K/AKT pathway. Cutaneous and Ocular Toxicology. 2021;40(2):119-24.
252. Zhang Y, Song H, Guo T, Zhu Y, Tang H, Qi Z, et al. Overexpression of Annexin II Receptor-Induced Autophagy Protects Against Apoptosis in Uveal Melanoma Cells. Cancer Biotherapy and Radiopharmaceuticals. 2016;31(4):145-51.
253. He J, Chen J, Shen J. Selamectin increases cisplatin sensitivity by inhibiting cisplatin-resistant genes expression and autophagy in uveal melanoma. Biochem Biophys Res Commun. 2023;661:75-81.
254. Broggi G, Ieni A, Russo D, Varricchio S, Puzzo L, Russo A, et al. The Macro-Autophagy-Related Protein Beclin-1 Immunohistochemical Expression Correlates With Tumor Cell Type and Clinical Behavior of Uveal Melanoma. Frontiers in Oncology. 2020;10.
255. Giatromanolaki AN, St Charitoudis G, Bechrakis NE, Kozobolis VP, Koukourakis MI, Foerster MH, Sivridis EL. Autophagy patterns and prognosis in uveal melanomas. Modern Pathology. 2011;24(8):1036-45.
256. Imazu T, Shimizu S, Tagami S, Matsushima M, Nakamura Y, Miki T, et al. Bcl-2/E1B 19 kDa-interacting protein 3-like protein (Bnip3L) interacts with Bcl-2/Bcl-xL and induces apoptosis by altering mitochondrial membrane permeability. Oncogene. 1999;18(32):4523-9.
257. Zhang J, Ney PA. Role of BNIP3 and NIX in cell death, autophagy, and mitophagy. Cell death and differentiation. 2009;16(7):939-46.

258. Chourasia AH, Tracy K, Frankenberger C, Boland ML, Sharifi MN, Drake LE, et al. Mitophagy defects arising from BNip3 loss promote mammary tumor progression to metastasis. EMBO reports. 2015;16(9):1145-63.
259. Daido S, Kanzawa T, Yamamoto A, Takeuchi H, Kondo Y, Kondo S. Pivotal Role of the Cell Death Factor BNIP3 in Ceramide-Induced Autophagic Cell Death in Malignant Glioma Cells. Cancer Research. 2004;64(12):4286-93.
260. Giatromanolaki A, Koukourakis MI, Sowter HM, Sivridis E, Gibson S, Gatter KC, Harris AL. BNIP3 Expression Is Linked with Hypoxia-Regulated Protein Expression and with Poor Prognosis in Non–Small Cell Lung Cancer. Clinical Cancer Research. 2004;10(16):5566-71.
261. Chen Z, Wu H, Huang S, Li W, Zhang S, Zheng P, et al. Expression of BNIP3 and its correlations to hypoxia-induced autophagy and clinicopathological features in salivary adenoid cystic carcinoma. Cancer biomarkers : section A of Disease markers. 2015;15(4):467-75.
262. Jiang Z, Yu F, Li M. Upregulation of BCL2 19 kD Protein-Interacting Protein 3 (BNIP3) is Predictive of Unfavorable Prognosis in Uveal Melanoma. Med Sci Monit. 2018;24:4711-7.
263. Li X, He S, Ma B. Autophagy and autophagy-related proteins in cancer. Molecular Cancer. 2020;19(1):12.
264. Chang H, Zou Z. Targeting autophagy to overcome drug resistance: further developments. Journal of Hematology & Oncology. 2020;13(1):159.
265. Hoesel B, Schmid JA. The complexity of NF-κB signaling in inflammation and cancer. Molecular Cancer. 2013;12(1):86.
266. Li X, Lu Y, Liang K, Hsu JM, Albarracin C, Mills GB, et al. Brk/PTK6 sustains activated EGFR signaling through inhibiting EGFR degradation and transactivating EGFR. Oncogene. 2012;31(40):4372-83.
267. Lang Y-D, Chen H-Y, Ho C-M, Shih J-H, Hsu E-C, Shen R, et al. PSPC1-interchanged interactions with PTK6 and β-catenin synergize oncogenic subcellular translocations and tumor progression. Nature Communications. 2019;10(1):5716.
268. Liu C, Pan Z, Chen Q, Chen Z, Liu W, Wu L, et al. Pharmacological targeting PTK6 inhibits the JAK2/STAT3 sustained stemness and reverses chemoresistance of colorectal cancer. Journal of Experimental & Clinical Cancer Research. 2021;40(1):297.
269. Liu B, Yao X, Zhang C, Liu Y, Wei L, Huang Q, et al. PTK6 inhibits autophagy to promote uveal melanoma tumorigenesis by binding to SOCS3 and regulating mTOR phosphorylation. Cell Death & Disease. 2023;14(1):55.
270. Davies H, Bignell GR, Cox C, Stephens P, Edkins S, Clegg S, et al. Mutations of the BRAF gene in human cancer. Nature. 2002;417(6892):949-54.
271. Zuidervaart W, van Nieuwpoort F, Stark M, Dijkman R, Packer L, Borgstein AM, et al. Activation of the MAPK pathway is a common event in uveal melanomas although it rarely occurs through mutation of BRAF or RAS. British journal of cancer. 2005;92(11):2032-8.
272. Calipel A, Mouriaux F, Glotin A-L, Malecaze F, Faussat A-M, Mascarelli F. Extracellular Signal-regulated Kinase-dependent Proliferation Is Mediated through the Protein Kinase A/B-Raf Pathway in Human Uveal Melanoma Cells *. Journal of Biological Chemistry. 2006;281(14):9238-50.
273. Calipel A, Lefevre G, Pouponnot C, Mouriaux F, Eychène A, Mascarelli F. Mutation of B-Raf in Human Choroidal Melanoma Cells Mediates Cell Proliferation and Transformation through the MEK/ERK Pathway *. Journal of Biological Chemistry. 2003;278(43):42409-18.
274. Zhao Y, Wang W, Min I, Wyrwas B, Moore M, Zarnegar R, Fahey TJ. BRAF V600E-dependent role of autophagy in uveal melanoma. Journal of Cancer Research and Clinical Oncology. 2017;143(3):447-55.

275. Wang Z, Gao L, Guo X, Feng C, Lian W, Deng K, Xing B. Development and validation of a nomogram with an autophagy-related gene signature for predicting survival in patients with glioblastoma. Aging. 2019;11(24):12246-69.
276. Du JX, Chen C, Luo YH, Cai JL, Cai CZ, Xu J, et al. Establishment and validation of a novel autophagy-related gene signature for patients with breast cancer. Gene. 2020;762:144974.
277. Mo S, Dai W, Xiang W, Li Y, Feng Y, Zhang L, et al. Prognostic and predictive value of an autophagy-related signature for early relapse in stages I-III colon cancer. Carcinogenesis. 2019;40(7):861-70.
278. Zheng Z, Zhang L, Tu Z, Deng Y, Yin X. An autophagy-related prognostic signature associated with immune microenvironment features of uveal melanoma. Bioscience reports. 2021;41(3).
279. Ponjavic J, Ponting CP, Lunter G. Functionality or transcriptional noise? Evidence for selection within long noncoding RNAs. Genome research. 2007;17(5):556-65.
280. Batista PJ, Chang HY. Long noncoding RNAs: cellular address codes in development and disease. Cell. 2013;152(6):1298-307.
281. Prensner JR, Chinnaiyan AM. The Emergence of lncRNAs in Cancer Biology. Cancer Discovery. 2011;1(5):391-407.
282. Huo X, Han S, Wu G, Latchoumanin O, Zhou G, Hebbard L, et al. Dysregulated long noncoding RNAs (lncRNAs) in hepatocellular carcinoma: implications for tumorigenesis, disease progression, and liver cancer stem cells. Molecular Cancer. 2017;16(1):165.
283. An C, Wang I, Li X, Xia R, Deng F. Long non-coding RNA in prostate cancer. American journal of clinical and experimental urology. 2022;10(3):170-9.
284. Malhotra A, Jain M, Prakash H, Vasquez KM, Jain A. The regulatory roles of long non-coding RNAs in the development of chemoresistance in breast cancer. Oncotarget. 2017;8(66):110671-84.
285. Guzel E, Okyay TM, Yalçınkaya B, Karacaoglu S, Gocmen M, Akçakuyu MH. Tumor suppressor and oncogenic role of long non-coding RNAs in cancer. North Clin Istanb. 2020;7(1):81-6.
286. Li P, He J, Yang Z, Ge S, Zhang H, Zhong Q, Fan X. ZNNT1 long noncoding RNA induces autophagy to inhibit tumorigenesis of uveal melanoma by regulating key autophagy gene expression. Autophagy. 2020;16(7):1186-99.
287. Cui Y, Zheng M, Chen J, Xu N. Autophagy-Related Long Non-coding RNA Signature as Indicators for the Prognosis of Uveal Melanoma. Frontiers in Genetics. 2021;12.
288. Chen Y, Chen L, Wang J, Tan J, Wang S. Identification of Six Autophagy-Related-lncRNA Prognostic Biomarkers in Uveal Melanoma. Disease Markers. 2021;2021:2401617.
289. Liu B, Yao X, Zhang C, Li W, Wang Y, Liao Q, et al. LINC01278 Induces Autophagy to Inhibit Tumour Progression by Suppressing the mTOR Signalling Pathway. Oxidative medicine and cellular longevity. 2023;2023:8994901.
290. Hata A, Lieberman J. Dysregulation of microRNA biogenesis and gene silencing in cancer. Science Signaling. 2015;8(368):re3-re.
291. O'Brien J, Hayder H, Zayed Y, Peng C. Overview of MicroRNA Biogenesis, Mechanisms of Actions, and Circulation. Frontiers in Endocrinology. 2018;9.
292. Yang WB, Chen PH, Hsu Ts, Fu TF, Su WC, Liaw H, et al. Sp1-mediated microRNA-182 expression regulates lung cancer progression. Oncotarget. 2014;5(3):740-53.
293. Xiong X, Ren HZ, Li MH, Mei JH, Wen JF, Zheng CL. Down-regulated miRNA-214 induces a cell cycle G1 arrest in gastric cancer cells by up-regulating the PTEN protein. Pathology oncology research : POR. 2011;17(4):931-7.
294. Wang SC, Lin XL, Li J, Zhang TT, Wang HY, Shi JW, et al. MicroRNA-122 triggers mesenchymal-epithelial transition and suppresses hepatocellular carcinoma cell motility and invasion by targeting RhoA. PLoS One. 2014;9(7):e101330.

295. Huang J, Zhang SY, Gao YM, Liu YF, Liu YB, Zhao ZG, Yang K. MicroRNAs as oncogenes or tumour suppressors in oesophageal cancer: potential biomarkers and therapeutic targets. Cell proliferation. 2014;47(4):277-86.
296. Li Z, Yu X, Shen J, Jiang Y. MicroRNA dysregulation in uveal melanoma: a new player enters the game. Oncotarget. 2015;6(7):4562-8.
297. Li YF, Dong L, Li Y, Wei WB. A Review of MicroRNA in Uveal Melanoma. OncoTargets and Therapy. 2020;13:6351-9.
298. Yang C, Wang R, Hardy P. Potential of miRNA-Based Nanotherapeutics for Uveal Melanoma. Cancers. 2021;13(20):5192.
299. Worley LA, Long MD, Onken MD, Harbour JW. Micro-RNAs associated with metastasis in uveal melanoma identified by multiplexed microarray profiling. Melanoma research. 2008;18(3).
300. Xin X, Zhang Y, Ling F, Wang L, Sheng X, Qin L, Zhao X. Identification of a nine-miRNA signature for the prognosis of Uveal Melanoma. Experimental Eye Research. 2019;180:242-9.
301. Wu S, Chen H, Zuo L, Jiang H, Yan H. Suppression of long noncoding RNA MALAT1 inhibits the development of uveal melanoma via microRNA-608-mediated inhibition of HOXC4. American Journal of Physiology-Cell Physiology. 2020;318(5):C903-C12.
302. Sun L, Sun P, Zhou QY, Gao X, Han Q. Long noncoding RNA MALAT1 promotes uveal melanoma cell growth and invasion by silencing of miR-140. American journal of translational research. 2016;8(9):3939-46.
303. Sun Q, Cong R, Yan H, Gu H, Zeng Y, Liu N, et al. Genistein inhibits growth of human uveal melanoma cells and affects microRNA-27a and target gene expression. Oncol Rep. 2009;22(3):563-7.
304. Liu Y, Du H, Wan Q, He Y, Lu W, Wang W, Lv X. A Novel Four Genes of Prognostic Signature for Uveal Melanoma. Journal of oncology. 2022;2022:8281067.
305. Damato B. Treatment of primary intraocular melanoma. Expert Review of Anticancer Therapy. 2006;6(4):493-506.
306. Group TCOMS. Assessment of Metastatic Disease Status at Death in 435 Patients With Large Choroidal Melanoma in the Collaborative Ocular Melanoma Study (COMS): COMS Report No. 15. Archives of Ophthalmology. 2001;119(5):670-6.
307. Khoja L, Atenafu EG, Suciu S, Leyvraz S, Sato T, Marshall E, et al. Meta-analysis in metastatic uveal melanoma to determine progression free and overall survival benchmarks: an international rare cancers initiative (IRCI) ocular melanoma study. Annals of Oncology. 2019;30(8):1370-80.
308. Carvajal RD, Sacco JJ, Jager MJ, Eschelman DJ, Olofsson Bagge R, Harbour JW, et al. Advances in the clinical management of uveal melanoma. Nature Reviews Clinical Oncology. 2023;20(2):99-115.
309. Sayan M, Mamidanna S, Oncel D, Jan I, Vergalasova I, Weiner J, et al. Clinical management of uveal melanoma: a comprehensive review with a treatment algorithm. Radiation oncology journal. 2020;38(3):162-9.
310. Gill VT, Norrman E, Sabazade S, Karim A, Lardner E, Stålhammar G. Multiorgan Involvement of Dormant Uveal Melanoma Micrometastases in Postmortem Tissue From Patients Without Coexisting Macrometastases. American journal of clinical pathology. 2023;160(2):164-74.
311. Carvajal RD, Schwartz GK, Tezel T, Marr B, Francis JH, Nathan PD. Metastatic disease from uveal melanoma: treatment options and future prospects. British Journal of Ophthalmology. 2017;101(1):38.
312. Li Y, Zhu X, Wang K, Zhu L, Murray M, Zhou F. Ginkgo biloba extracts (GBE) protect human RPE cells from t-BHP-induced oxidative stress and necrosis by activating the Nrf2-mediated antioxidant defence. Journal of Pharmacy and Pharmacology. 2023;75(1):105-16.

313. Li Y, Cheng Z, Wang K, Zhu X, Ali Y, Shu W, et al. Procyanidin B2 and rutin in Ginkgo biloba extracts protect human retinal pigment epithelial (RPE) cells from oxidative stress by modulating Nrf2 and Erk1/2 signalling. Experimental Eye Research. 2021;207:108586.
314. Shu W, Wang JZ, Zhu X, Wang K, Cherepanoff S, Conway RM, et al. Lapatinib dysregulates HER2 signaling and impairs the viability of human uveal melanoma cells. Journal of Cancer. 2023;14(18):3477-95.
315. Ji J, Wang K, Meng X, Zhong H, Li X, Zhao H, et al. Elaiophylin Inhibits Tumorigenesis of Human Lung Adenocarcinoma by Inhibiting Mitophagy via Suppression of SIRT1/Nrf2 Signaling. Cancers (Basel). 2022;14(23).
316. Meng X, Zhu X, Ji J, Zhong H, Li X, Zhao H, et al. Erdafitinib Inhibits Tumorigenesis of Human Lung Adenocarcinoma A549 by Inducing S-Phase Cell-Cycle Arrest as a CDK2 Inhibitor. Molecules (Basel, Switzerland). 2022;27(19).
317. Alvarez PB, Laskaris A, Goyeneche AA, Chen Y, Telleria CM, Burnier JV. Anticancer effects of mifepristone on human uveal melanoma cells. Cancer Cell International. 2021;21(1):607.
318. Anbunathan H, Verstraten R, Singh AD, Harbour JW, Bowcock AM. Integrative Copy Number Analysis of Uveal Melanoma Reveals Novel Candidate Genes Involved in Tumorigenesis Including a Tumor Suppressor Role for PHF10/BAF45a. Clinical Cancer Research. 2019;25(16):5156-66.
319. Kalirai H, Damato BE, Coupland SE. Uveal Melanoma Cell Lines Contain Stem-Like Cells That Self-Renew, Produce Differentiated Progeny, and Survive Chemotherapy. Investigative Ophthalmology & Visual Science. 2011;52(11):8458-66.
320. Jinhai Y, Yunxiu C, Qi J, Jiancheng G, Zhida P, Sha W, et al. Three-dimensional cell spheroid culture and cell viability study of uveal melanoma cell line C918 with luteolin treatment. International Ophthalmology. 2024;44(1):385.
321. Towers CG, Wodetzki D, Thorburn A. Autophagy and cancer: Modulation of cell death pathways and cancer cell adaptations. Journal of Cell Biology. 2019;219(1):e201909033.
322. Liu B, Yao X, Shang Y, Dai J. The multiple roles of autophagy in uveal melanoma and the microenvironment. Journal of Cancer Research and Clinical Oncology. 2024;150(3):121.
323. Xu S, Gierisch ME, Barchi E, Poser I, Alberti S, Salomons FA, Dantuma NP. Chemical inhibition of the integrated stress response impairs the ubiquitin-proteasome system. Communications Biology. 2024;7(1):1282.
324. Corazzari M, Gagliardi M, Fimia GM, Piacentini M. Endoplasmic Reticulum Stress, Unfolded Protein Response, and Cancer Cell Fate. Frontiers in Oncology. 2017;7.
325. Gething M-J. Role and regulation of the ER chaperone BiP. Seminars in Cell & Developmental Biology. 1999;10(5):465-72.
326. Lusby R, Demirdizen E, Inayatullah M, Kundu P, Maiques O, Zhang Z, et al. Pan-cancer drivers of metastasis. Molecular Cancer. 2025;24(1):2.
327. Krantz BA, Dave N, Komatsubara KM, Marr BP, Carvajal RD. Uveal melanoma: epidemiology, etiology, and treatment of primary disease. Clinical ophthalmology (Auckland, NZ). 2017;11:279-89.
328. Kapałczyńska M, Kolenda T, Przybyła W, Zajączkowska M, Teresiak A, Filas V, et al. 2D and 3D cell cultures - a comparison of different types of cancer cell cultures. Archives of medical science : AMS. 2018;14(4):910-9.
329. Yuan Z, Li Y, Zhang S, Wang X, Dou H, Yu X, et al. Extracellular matrix remodeling in tumor progression and immune escape: from mechanisms to treatments. Molecular Cancer. 2023;22(1):48.
330. Henke E, Nandigama R, Ergün S. Extracellular Matrix in the Tumor Microenvironment and Its Impact on Cancer Therapy. Frontiers in Molecular Biosciences. 2020;6.
331. Ozbolat IT, Peng W, Ozbolat V. Application areas of 3D bioprinting. Drug Discovery Today. 2016;21(8):1257-71.

332. Rübben A, Araujo A. Cancer heterogeneity: converting a limitation into a source of biologic information. Journal of Translational Medicine. 2017;15(1):190.
333. Welch DR. Tumor Heterogeneity—A 'Contemporary Concept' Founded on Historical Insights and Predictions. Cancer Research. 2016;76(1):4-6.
334. Chen F, Xue Y, Zhang W, Zhou H, Zhou Z, Chen T, et al. The role of mitochondria in tumor metastasis and advances in mitochondria-targeted cancer therapy. Cancer and Metastasis Reviews. 2024;43(4):1419-43.
335. Chen YR, Tsou B, Hu S, Ma H, Liu X, Yen Y, Ann DK. Autophagy induction causes a synthetic lethal sensitization to ribonucleotide reductase inhibition in breast cancer cells. Oncotarget. 2016;7(2):1984-99.
336. Fiorini C, Cordani M, Gotte G, Picone D, Donadelli M. Onconase induces autophagy sensitizing pancreatic cancer cells to gemcitabine and activates Akt/mTOR pathway in a ROS-dependent manner. Biochimica et biophysica acta. 2015;1853(3):549-60.
337. Amaravadi RK, Thompson CB. The Roles of Therapy-Induced Autophagy and Necrosis in Cancer Treatment. Clinical Cancer Research. 2007;13(24):7271-9.
338. Zhang L, Cui T, Wang X. The Interplay Between Autophagy and Regulated Necrosis. Antioxidants & redox signaling. 2023;38(7-9):550-80.
339. Chen Q, Kang J, Fu C. The independence of and associations among apoptosis, autophagy, and necrosis. Signal Transduction and Targeted Therapy. 2018;3(1):18.
340. Singh L, Atilano SR, Jager MJ, Kenney MC. Mitochondrial DNA polymorphisms and biogenesis genes in primary and metastatic uveal melanoma cell lines. Cancer Genetics. 2021;256-257:91-9.
341. van der Ent W, Burrello C, Teunisse AFAS, Ksander BR, van der Velden PA, Jager MJ, et al. Modeling of Human Uveal Melanoma in Zebrafish Xenograft Embryos. Investigative Ophthalmology & Visual Science. 2014;55(10):6612-22.
342. Oakes SA. Endoplasmic Reticulum Stress Signaling in Cancer Cells. The American journal of pathology. 2020;190(5):934-46.
343. Schubert U, Antón LC, Gibbs J, Norbury CC, Yewdell JW, Bennink JR. Rapid degradation of a large fraction of newly synthesized proteins by proteasomes. Nature. 2000;404(6779):770-4.
344. Qi Z, Chen L. Endoplasmic Reticulum Stress and Autophagy. In: Qin Z-H, editor. Autophagy: Biology and Diseases: Basic Science. Singapore: Springer Singapore; 2019. p. 167-77.
345. Hsieh C-L, Huang H-S, Chen K-C, Saka T, Chiang C-Y, Chung LWK, Sung S-Y. A Novel Salicylanilide Derivative Induces Autophagy Cell Death in Castration-Resistant Prostate Cancer via ER Stress-Activated PERK Signaling Pathway. Molecular Cancer Therapeutics. 2020;19(1):101-11.
346. Xu D, Liu Z, Liang M-X, Fei Y-J, Zhang W, Wu Y, Tang J-H. Endoplasmic reticulum stress targeted therapy for breast cancer. Cell Communication and Signaling. 2022;20(1):174.
347. Høyer-Hansen M, Jäättelä M. Connecting endoplasmic reticulum stress to autophagy by unfolded protein response and calcium. Cell Death & Differentiation. 2007;14(9):1576-82.
348. Yorimitsu T, Nair U, Yang Z, Klionsky DJ. Endoplasmic reticulum stress triggers autophagy. The Journal of biological chemistry. 2006;281(40):30299-304.
349. Beilankouhi EAV, Sajadi MA, Alipourfard I, Hassani P, Valilo M, Safaralizadeh R. Role of the ER-induced UPR pathway, apoptosis, and autophagy in colorectal cancer. Pathology, research and practice. 2023;248:154706.
350. Liao H, Liu S, Ma Q, Huang H, Goel A, Torabian P, et al. Endoplasmic reticulum stress induced autophagy in cancer and its potential interactions with apoptosis and ferroptosis. Biochimica et Biophysica Acta (BBA) - Molecular Cell Research. 2025;1872(1):119869.

351. Lin Y, Jiang M, Chen W, Zhao T, Wei Y. Cancer and ER stress: Mutual crosstalk between autophagy, oxidative stress and inflammatory response. Biomedicine & pharmacotherapy = Biomedecine & pharmacotherapie. 2019;118:109249.
352. Vermeulen K, Van Bockstaele DR, Berneman ZN. The cell cycle: a review of regulation, deregulation and therapeutic targets in cancer. Cell proliferation. 2003;36(3):131-49.
353. Khan MGM, Wang Y. Cell Cycle-Related Clinical Applications. In: Wang Z, editor. Cell-Cycle Synchronization: Methods and Protocols. New York, NY: Springer US; 2022. p. 35-46.
354. Mills CC, Kolb EA, Sampson VB. Development of Chemotherapy with Cell-Cycle Inhibitors for Adult and Pediatric Cancer Therapy. Cancer Research. 2018;78(2):320-5.
355. Vihinen P, Kähäri V-M. Matrix metalloproteinases in cancer: Prognostic markers and therapeutic targets. International Journal of Cancer. 2002;99(2):157-66.
356. Thiery JP. Epithelial–mesenchymal transitions in tumour progression. Nature Reviews Cancer. 2002;2(6):442-54.
357. Chen H-T, Liu H, Mao M-J, Tan Y, Mo X-Q, Meng X-J, et al. Crosstalk between autophagy and epithelial-mesenchymal transition and its application in cancer therapy. Molecular Cancer. 2019;18(1):101.
358. Wettersten HI, Hee Hwang S, Li C, Shiu EY, Wecksler AT, Hammock BD, Weiss RH. A novel p21 attenuator which is structurally related to sorafenib. Cancer Biol Ther. 2013;14(3):278-85.
359. Sánchez López de Nava A, Raja A. Physiology, Metabolism. StatPearls. Treasure Island (FL) relationships with ineligible companies. Disclosure: Avais Raja declares no relevant financial relationships with ineligible companies.: StatPearls Publishing

360. Dashty M. A quick look at biochemistry: Carbohydrate metabolism. Clinical Biochemistry. 2013;46(15):1339-52.
361. Finn PF, Dice JF. Proteolytic and lipolytic responses to starvation. Nutrition. 2006;22(7):830-44.
362. Abumrad NA, Davidson NO. Role of the gut in lipid homeostasis. Physiological reviews. 2012;92(3):1061-85.
363. Hanahan D, Weinberg Robert A. Hallmarks of Cancer: The Next Generation. Cell. 2011;144(5):646-74.
364. Stratton MR, Campbell PJ, Futreal PA. The cancer genome. Nature. 2009;458(7239):719-24.
365. Newsholme EA, Crabtree B, Ardawi MSM. The role of high rates of glycolysis and glutamine utilization in rapidly dividing cells. Bioscience reports. 1985;5(5):393-400.
366. Cantor JR, Sabatini DM. Cancer cell metabolism: one hallmark, many faces. Cancer Discov. 2012;2(10):881-98.
367. Pfeiffer T, Schuster S, Bonhoeffer S. Cooperation and Competition in the Evolution of ATP-Producing Pathways. Science. 2001;292(5516):504-7.
368. House SW, Warburg O, Burk D, Schade AL. On Respiratory Impairment in Cancer Cells. Science. 1956;124(3215):267-72.
369. Eagle H, Oyama VI, Levy M, Horton CL, Fleischman R. The growth response of mammalian cells in tissue culture to L-glutamine and L-glutamic acid. The Journal of biological chemistry. 1956;218(2):607-16.
370. Mazurek S, Boschek CB, Hugo F, Eigenbrodt E. Pyruvate kinase type M2 and its role in tumor growth and spreading. Seminars in Cancer Biology. 2005;15(4):300-8.
371. Ramapriyan R, Caetano MS, Barsoumian HB, Mafra ACP, Zambalde EP, Menon H, et al. Altered cancer metabolism in mechanisms of immunotherapy resistance. Pharmacology & Therapeutics. 2019;195:162-71.

372. Bian X, Liu R, Meng Y, Xing D, Xu D, Lu Z. Lipid metabolism and cancer. The Journal of experimental medicine. 2021;218(1).
373. Röhrig F, Schulze A. The multifaceted roles of fatty acid synthesis in cancer. Nature Reviews Cancer. 2016;16(11):732-49.
374. Walther TC, Farese RV, Jr. The life of lipid droplets. Biochimica et biophysica acta. 2009;1791(6):459-66.
375. McLaughlin CC, Wu XC, Jemal A, Martin HJ, Roche LM, Chen VW. Incidence of noncutaneous melanomas in the U.S. Cancer. 2005;103(5):1000-7.
376. Andreoli MT, Mieler WF, Leiderman YI. Epidemiological trends in uveal melanoma. British Journal of Ophthalmology. 2015;99(11):1550.
377. Helgadottir H, Höiom V. The genetics of uveal melanoma: current insights. The application of clinical genetics. 2016;9:147-55.
378. Vaquero-Garcia J, Lalonde E, Ewens KG, Ebrahimzadeh J, Richard-Yutz J, Shields CL, et al. PRiMeUM: A Model for Predicting Risk of Metastasis in Uveal Melanoma. Investigative Ophthalmology & Visual Science. 2017;58(10):4096-105.
379. Koch EAT, Heppt MV, Berking C. The Current State of Systemic Therapy of Metastatic Uveal Melanoma. American Journal of Clinical Dermatology. 2024;25(5):691-700.
380. Cioanca AV, McCluskey PJ, Eamegdool SS, Madigan MC. Human choroidal melanocytes express functional Toll-like receptors (TLRs). Exp Eye Res. 2018;173:73-84.
381. Childers G, Harry GJ. Mitochondrial Stress Assay and Glycolytic Rate Assay in Microglia Using Agilent Seahorse Extracellular Flux Analyzers. In: Llorens J, Barenys M, editors. Experimental Neurotoxicology Methods. New York, NY: Springer US; 2021. p. 305-24.
382. Faubert B, Solmonson A, DeBerardinis RJ. Metabolic reprogramming and cancer progression. Science. 2020;368(6487).
383. Harris AL. Hypoxia — a key regulatory factor in tumour growth. Nature Reviews Cancer. 2002;2(1):38-47.
384. Smolle E, Leko P, Stacher-Priehse E, Brcic L, El-Heliebi A, Hofmann L, et al. Distribution and prognostic significance of gluconeogenesis and glycolysis in lung cancer. Molecular Oncology. 2020;14(11):2853-67.
385. Sullivan MR, Danai LV, Lewis CA, Chan SH, Gui DY, Kunchok T, et al. Quantification of microenvironmental metabolites in murine cancers reveals determinants of tumor nutrient availability. eLife. 2019;8:e44235.
386. Rocha CM, Barros AS, Gil AM, Goodfellow BJ, Humpfer E, Spraul M, et al. Metabolic Profiling of Human Lung Cancer Tissue by 1H High Resolution Magic Angle Spinning (HRMAS) NMR Spectroscopy. Journal of Proteome Research. 2010;9(1):319-32.
387. Grasmann G, Mondal A, Leithner K. Flexibility and Adaptation of Cancer Cells in a Heterogenous Metabolic Microenvironment. International Journal of Molecular Sciences. 2021;22(3):1476.
388. DeBerardinis RJ, Chandel NS. We need to talk about the Warburg effect. Nature Metabolism. 2020;2(2):127-9.
389. Phan LM, Yeung SC, Lee MH. Cancer metabolic reprogramming: importance, main features, and potentials for precise targeted anti-cancer therapies. Cancer biology & medicine. 2014;11(1):1-19.
390. Jones RG, Thompson CB. Tumor suppressors and cell metabolism: a recipe for cancer growth. Genes Dev. 2009;23(5):537-48.
391. Semenza GL. Tumor metabolism: cancer cells give and take lactate. J Clin Invest. 2008;118(12):3835-7.

392. Vander Heiden MG, Cantley LC, Thompson CB. Understanding the Warburg effect: the metabolic requirements of cell proliferation. Science. 2009;324(5930):1029-33.
393. Bonuccelli G, Tsirigos A, Whitaker-Menezes D, Pavlides S, Pestell RG, Chiavarina B, et al. Ketones and lactate "fuel" tumor growth and metastasis: Evidence that epithelial cancer cells use oxidative mitochondrial metabolism. Cell Cycle. 2010;9(17):3506-14.
394. Locasale JW, Cantley LC. Metabolic flux and the regulation of mammalian cell growth. Cell metabolism. 2011;14(4):443-51.
395. Gill KS, Fernandes P, O'Donovan TR, McKenna SL, Doddakula KK, Power DG, et al. Glycolysis inhibition as a cancer treatment and its role in an anti-tumour immune response. Biochimica et Biophysica Acta (BBA) - Reviews on Cancer. 2016;1866(1):87-105.
396. del Carpio LP, Algarra MA, Sabaté-Llobera A, Rodriguez-Vida A, Rossi-Seoane S, Ruiz S, et al. Differences in glucose metabolic activity in liver metastasis separates two groups of metastatic uveal melanoma patients with different prognosis. Cancer Medicine. 2023;12(13):14062-71.
397. Maaßen T, Vardanyan S, Brosig A, Merz H, Ranjbar M, Kakkassery V, et al. Monosomy-3 Alters the Expression Profile of the Glucose Transporters GLUT1-3 in Uveal Melanoma. International Journal of Molecular Sciences. 2020;21(24):9345.
398. Tura A, Herfs V, Maaßen T, Zuo H, Vardanyan S, Prasuhn M, et al. Quercetin Impairs the Growth of Uveal Melanoma Cells by Interfering with Glucose Uptake and Metabolism. International Journal of Molecular Sciences. 2024;25(8):4292.
399. Menendez JA, Lupu R. Fatty acid synthase and the lipogenic phenotype in cancer pathogenesis. Nature Reviews Cancer. 2007;7(10):763-77.
400. Tufail M, Jiang C-H, Li N. Altered metabolism in cancer: insights into energy pathways and therapeutic targets. Molecular Cancer. 2024;23(1):203.
401. Abramson HN. The Lipogenesis Pathway as a Cancer Target. Journal of Medicinal Chemistry. 2011;54(16):5615-38.
402. Kamphorst JJ, Cross JR, Fan J, de Stanchina E, Mathew R, White EP, et al. Hypoxic and Ras-transformed cells support growth by scavenging unsaturated fatty acids from lysophospholipids. Proceedings of the National Academy of Sciences. 2013;110(22):8882-7.
403. Ventura R, Mordec K, Waszczuk J, Wang Z, Lai J, Fridlib M, et al. Inhibition of de novo Palmitate Synthesis by Fatty Acid Synthase Induces Apoptosis in Tumor Cells by Remodeling Cell Membranes, Inhibiting Signaling Pathways, and Reprogramming Gene Expression. eBioMedicine. 2015;2(8):808-24.
404. Chua V, Han A, Bechtel N, Purwin TJ, Hunter E, Liao C, et al. The AMP-dependent kinase pathway is upregulated in BAP1 mutant uveal melanoma. Pigment Cell & Melanoma Research. 2022;35(1):78-87.
405. Matareed M, Maranou E, Koskela SA, Mehmood A, Kalirai H, Coupland SE, Figueiredo CR. Novel prognostication biomarker adipophilin reveals a metabolic shift in uveal melanoma and new therapeutic opportunities. The Journal of pathology. 2023;260(2):203-21.
406. Fiorentzis M, Kalirai H, Katopodis P, Coupland SE. Adipophilin expression in primary and metastatic uveal melanoma: a pilot study. Graefe's Archive for Clinical and Experimental Ophthalmology. 2017;255(5):1049-51.
407. Han A, Mukha D, Chua V, Purwin TJ, Tiago M, Modasia B, et al. Co-Targeting FASN and mTOR Suppresses Uveal Melanoma Growth. Cancers. 2023;15(13):3451.

Supplementary data

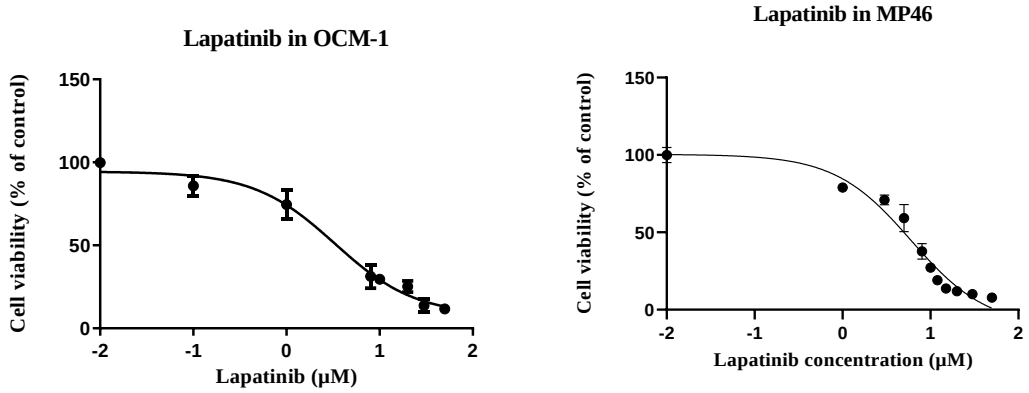

IC_{50}= 3.29 ± 0.87 µM IC_{50}=6.01 ± 1.52 µM

Supplementary Figure 1. Anti-cancer activity of lapatinib in OCM-1 and MP46 UM cell lines. OCM-1 and MP46 cells were treated with lapatinib (0-50 µM) at 37°C for 24 h. Cell viability was assessed using MTT reduction assays. IC_{50}s of lapatinib in UM cell lines were estimated by non-linear regression (GraphPad Prism 7.0; San Diego, CA).

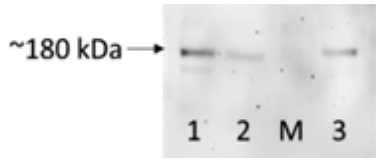

Supplementary Figure 2. Protein expression of Her2 in the patient tumour-derived UM primary cell lines.

The total cell lysate of the three-patient tumour-derived UM primary cell lines was subject to western blot analysis. The blots were probed with anti-Her2 antibody.

Lanes: 1: cell line 1; 2: cell line 2; 3: cell line 3; M: protein marker.

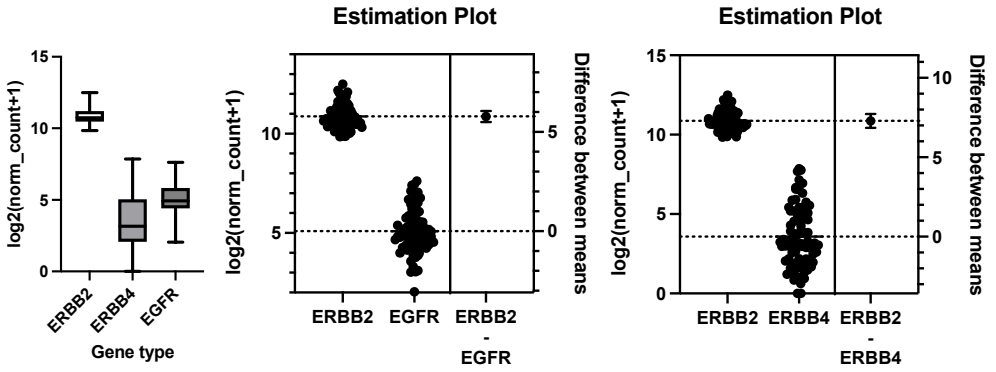

Supplementary Figure 3. The expression of HER2 (ERBB2), EGFR and HER4 (ERBB4) in UM from the TCGA database.

The expression of EGFR and HER4 was compared with that of HER2 via the unpaired t-test (the middle and right panels).

HER2 *vs* EGFR: p<0.0001, t=41.00, df=158, mean of HER2=10.87, mean of EGFR=5.089

HER2 *vs* HER4: p<0.0001, t=32.89, df=158, mean of HER2=10.87, mean of HER4=3.578

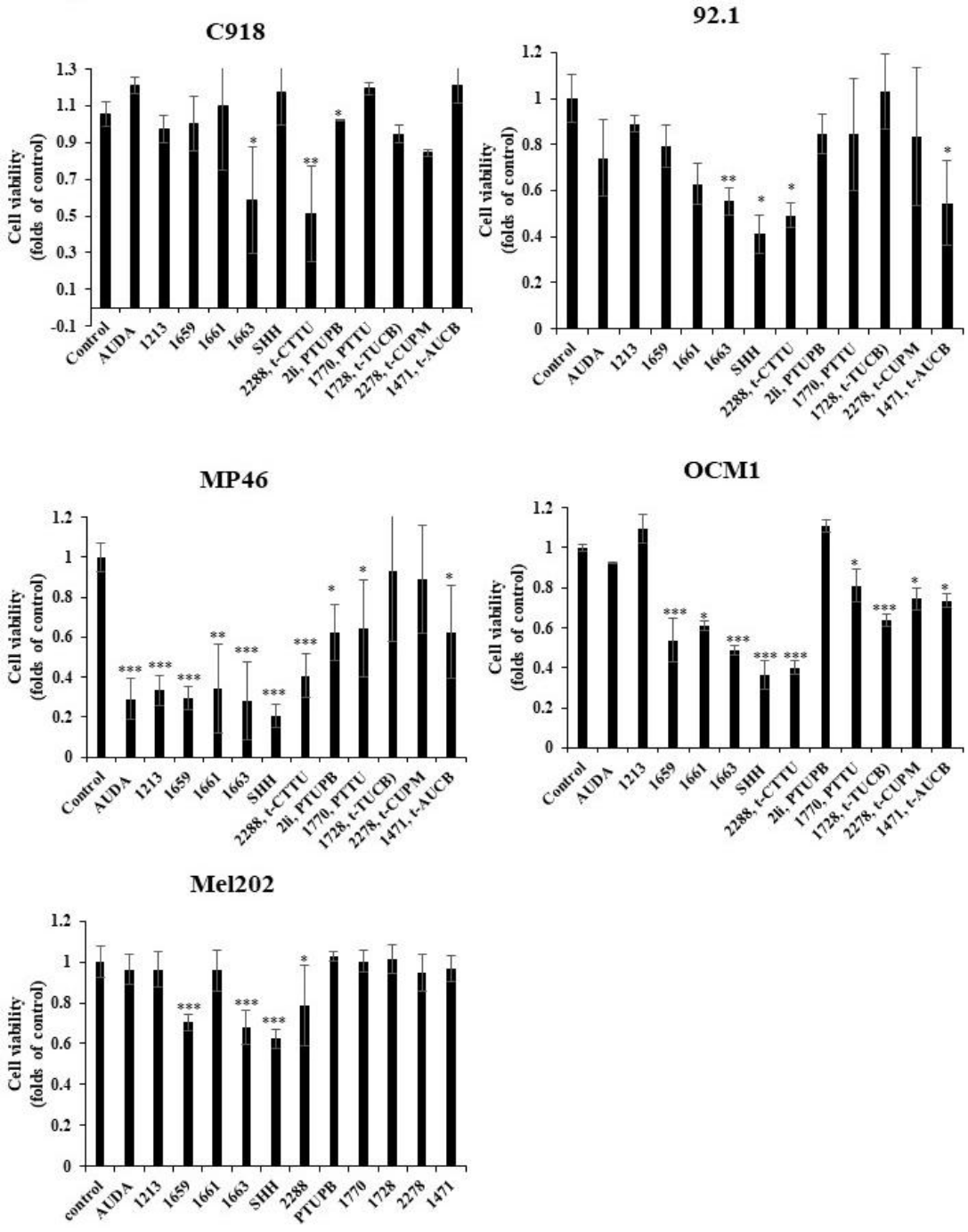

Supplementary figure 4. Drug screening of novel sEH and P21 inhibitors on UM cell lines. C918, 92.1, Mel202 and MP46 were primary UM cell lines and OCM1 was a cutaneous melanoma cell line. All drugs were treated at 1µM of respective drugs with DMSO in culture medium as negative control. MTT assay was conducted 24 hours post addition of drug and data

is represented as folds compared to negative control (mean ± SD). Experiments were repeated on one to two occasions with 6 replicated in each experiment. * $P \leq 0.05$, ** $P \leq 0.01$, *** $P \leq 0.001$.

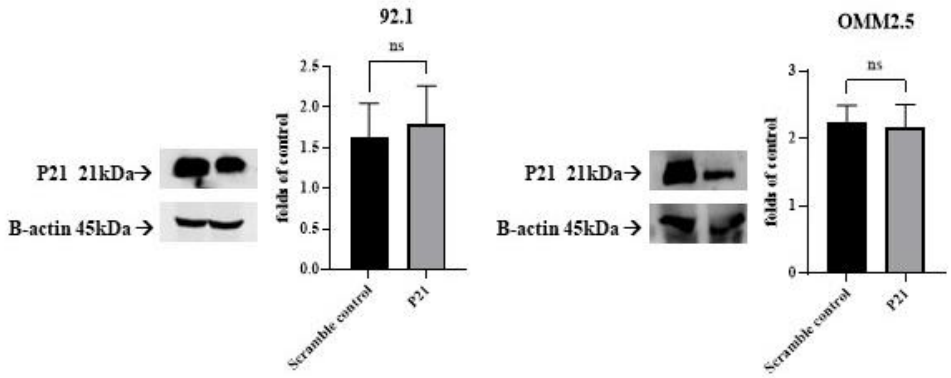

Supplementary figure 5. of P21 SiRNA silencing on cell viability of UM cell lines. The effect of P21 inhibition in UM cell lines was confirmed with SiRNA silencing. Cells were incubated with P21 SiRNA as recommended by the manufacturer. Cell were incubated for 48 hours before sacrificed to conduct western blot for inhibition confirmation and MTT for cell viability confirmation. Successful silencing of P21 did not affect cell viability in 92.1 cell lines.